Article (refereed) - postprint

He, Hailong; Aogu, Kailin; Li, Min; Xu, Jinghui; Sheng, Wenyi; Jones, Scott B.;
González-Teruel, Juan D.; Robinson, David A.; Horton, Robert; Bristow, Keith; Dyck,
Miles; Filipović, Vilim; Noborio, Kosuke; Wu, Qingbai; Jin, Huijun; Feng, Hao; Si,
Bingcheng; Lv, Jialong. 2021. **A review of time domain reflectometry (TDR)
applications in porous media.**

A Review of Time Domain Reflectometry (TDR) Applications in Porous Media

Hailong He[1], Gukailin Ao[1,2,3], Min Li[2], Jinghui Xu[2], Wenyi Sheng[4], Scott B. Jones[5],

Juan D. González Teruel[6], David A. Robinson[7], Robert Horton[8], Keith Bristow[9],

Miles Dyck[10], Vilim Filipović[11], Kosuke Noborio[12], Qingbai Wu[13], Huijun Jin[13], Hao

Feng[2,14], Bingcheng Si[15], Jialong Lv[1,3*]

[1] College of Natural Resources and Environment, Northwest A&F University, Yangling 712100, China (aogu2455@163.com; ljlll@nwsuaf.edu.cn; hailong.he@hotmail.com)

[2] Key Laboratory of Agricultural Soil and Water Engineering in Arid and Semiarid Areas (Ministry of Education), Northwest A&F University, Yangling, Shaanxi, 712100 China (x36936@163.com; nercwsi@vip.sina.com; limin2016@nwafu.edu.cn)

[3] Key Laboratory of Plant Nutrition and Agri-Environment in Northwest China (Ministry of Agriculture), Northwest A&F University, Yangling 712100, China

[4] College of Information and Electrical Engineering, China Agriculture University, Beijing 100083, China (wenyi.sheng@cau.edu.cn)

[5] Department of Plants, Soils and Climate, Utah State University, Logan, UT 84322, United States (scott.jones@usu.edu)

[6] Dept. of Automatics, Electrical Engineering and Electronic Technology, Technical University of Cartagena, Murcia, Spain 30202

[7] UK Centre for Ecology and Hydrology, Environment Centre Wales, Deiniol Road, Bangor, Gwynedd LL57 2UW, UK (juando.gonzalez.teruel@gmail.com; davi2@ceh.ac.uk)

[8] Department of Agronomy, Iowa State University, Ames, Iowa, USA (rhorton@iastate.edu)

[9] CSIRO Agriculture & Food, PMB Aitkenvale, Townsville, QLD, Australia (Keith.Bristow@csiro.au)

[10] Department of Renewable Resources, University of Alberta, Edmonton, Alberta T6G2H1 Canada (miles.dyck@ualberta.ca)

[11] University of Zagreb, Faculty of Agriculture, Zagreb, Croatia (vfilipovic@agr.hr)

[12] School of Agriculture, Meiji University, Kawasaki, Kanagawa 214-8571, Japan (noboriok@meiji.ac.jp)

[13] State Key Laboratory of Frozen Soil Engineering, Northwest Institute of Eco-Environment and Resources, Chinese Academy of Sciences, Lanzhou, Gansu, PR China (hjjin@lzb.ac.cn; qbwu@lzb.ac.cn)

[14] The State Key Laboratory of Soil Erosion and Dryland Farming on the Loess Plateau, Institute of Soil and Water Conservation, CAS&MWR, Northwest A&F University, Yangling, China

[15] Department of Soil Science, University of Saskatchewan, Saskatoon, SK S7N5A8 Canada (bing.Si@usask.ca)

*Hailong He and Gukailin Ao contributed equally

**Correspondence to: JL (ljlll@nwsuaf.edu.cn)

Highlights:

- A comprehensive TDR application review for soil, plant, food, and concrete

- Principles of TDR, commercially available TDR units, selected designs of TDR probes and programs for waveform analysis

- Spatial profile of soil water content, measurement of electric conductivity, tree trunk water content/storage, hydraulic conductivity, and matric potential

- Detection of water depth, snow depth, drying/wetting front, freezing/thawing front, rock/soil deformation, and groundwater table and piezometric pressure

- Combination of TDR with other methods to detect a wide variety of physical properties

- Limitations of TDR application and future perspectives

Abstract:

Time domain reflectometry (TDR) is the most widely used non-destructive method to determine the water content of soils and other porous media. TDR equipment can be automated and multiplexed to acquire accurate and rapid waveforms (return signal) without safety concerns associated with radioactive methods (e.g., neutron probe and Gamma-ray probe). Two key steps are required for TDR applications: (1) Obtain and analyze TDR waveforms using travel-time and signal attenuation analysis to determine dielectric permittivity and electrical conductivity, respectively. (2) Calibrate to determine a new- or apply an existing (e.g., Topp et al., 1980) relationship between the derived soil dielectric permittivity and the volumetric water content of the porous medium of interest. A majority of researchers and practitioners focus on step two and additionally develop new mathematical models to get better estimates of water content. Although there are reviews of TDR principles and applications in soil science, there is a lack of information on how TDR can disclose critical information in porous media beyond average soil water content. Therefore, we present a newly expanded review of TDR applications in porous media including soils, plants, snow, food stuffs, and concrete. We begin by reviewing TDR basics, including principles, probe design, commercially available equipment, and graphical and numerical methods as well as available software for waveform analysis. Applications of TDR to estimate volumetric water content in various types of porous media, the latest techniques available to derive spatial variability of soil water distributions along a single TDR probe are included, followed by TDR waveform based analyses to estimate electrical conductivity (EC), wetting/drying and freezing/thawing fronts, and snow depth. The combination of TDR measurements coupled with other methods (e.g., gypsum/ceramics and heat pulse method) to determine a wide range of soil physical properties (e.g., soil water retention curve, thermal properties, and hydraulic conductivity) and fluxes (e.g., soil heat flux, liquid water flux, and vapor flux) are also included. The study concludes with a discussion of limitations and future perspectives on various TDR applications.

Keywords: TDR, soil water content; electric conductivity; tree stem water content; snow depth and wetness, wetting/drying interface; freezing/thawing interface; dielectric

Table of Contents

List of Abbreviation

EC	Electrical conductivity
EM	Electromagnetic
SWRC	Soil water retention characteristics
TDR	Time domain reflectometry

List of Symbols

L	length of TDR probe (m)
L_a	distance between reflections at the beginning and the end of the probe (apparent length) (m)
L_{s_frozen}	depth of the frozen soil (m)
L_{soil}	depth of the soil (m)
R	Reflection coefficient
V_p	ratio of the velocity of propagation in a coaxial cable to that in free space
c	velocity of the electromagnetic wave in free space (3×10^8 m s^{-1})
t	Travel time of the EM wave (s).
f	The frequency readings
f_{eff}	Effective frequency
χ	The period of signal oscillation (μs).
ρ	Density
λ	Thermal conductivity
r	Rod spacing (mm)
d	Rod diameter (mm)
V_T	Excitation voltage (V)
V_R	Reflected voltage (V)
K_a	dielectric permittivity of porous media such as soil (unitless)
$K_{a,stem}$	apparent dielectric permittivity of the plant stem (unitless)
ε_{air}	dielectric permittivity of air (unitless)
ε_{ice}	dielectric permittivity of ice (unitless)
ε_w	dielectric permittivity of liquid water(unitless)
ε_{sm}	dielectric permittivity of soil matrix (unitless)
ε_{snow}	dielectric permittivity of snow (unitless)
θ_{lw}	Unfrozen/liquid water content (cm^3 cm^{-3} or m^3 m^{-3})
θ_v	volumetric water content (cm^3 cm^{-3} or m^3 m^{-3})
σ	electrical conductivity of the bulk soil (dS m^{-1})
σ_w	electrical conductivity of the soil solution (dS m^{-1})
σ_s	soil apparent electrical conductivity (dS m^{-1})
θ_{stem}	volume of water/total volume of stem (cm^3/cm^3 or m^3 m^{-3})
$\theta_{storage}$	stem water storage (cm^3/cm^3 or m^3 m^{-3})
θ_{snow}	snow wetness (cm^3/cm^3 or m^3 m^{-3})
ρ_{snow}	snow density (cm^3/cm^3 or m^3 m^{-3})
ψ_m	soil matric potential (m or kPa)

1. Introduction

The time domain reflectometry (TDR) cable tester is an instrument originally used to locate discontinuities or faults along coaxial, paired or multi-conductor metallic cables from the 1960's (Fellner-Feldegg, 1969; Payne, 1968). Fellner-Feldegg (1969) was the first to determine dielectric properties of materials in a coaxial cell based on the response of a fast rise time ($\sim 10^{-12}$ s) voltage step or pulse voltage transmitted through or reflected from the material (Friel and Or, 1999; Topp and Davis, 1981). Discontinuities at known locations along a transmission line (i.e., open-ended TDR waveguides or probe rods) resulted in an electrical signal reflection that could be used to determine the dielectric constant or relative permittivity as it is now known. Davis (1975) was among the pioneers to apply the TDR technique to estimate the volumetric water content (θ_v) of a porous medium (e.g., soil). The θ_v was estimated from the apparent permittivity (K_a), where K_a is used to denote a measurement by an instrument and ε_{eff} is the effective permittivity of a material. K_a and ε_{eff} should be the same for lossless dielectrics in the vicinity of a transmission line inserted a material under test (Černý, 2009; Noborio, 2001; O'Connor and O'Connor, 1999; Robinson et al., 2003b; Siddiqui et al., 2000; Topp et al., 2003; Whalley, 1993). The permittivity is a measure of the ability of a material to polarize when an electrical field is applied. Topp et al. (1980) performed laboratory measurements on soils of varying texture to determine empirically the dependence of K_a on θ_v at electromagnetic frequencies between 1 MHz and 1 GHz. They presented a third-degree polynomial equation that

related on the θ_v to K_a. The equation is commonly referred to as the Topp et al. (1980) equation. The Topp et al. (1980) equation is the most widely used model to estimate θ_v from the TDR-determined K_a, because it is assumed to be somewhat independent of soil characteristics including soil type, soil density, soil temperature, and soluble salt content. It is able to effectively estimate soil water contents from air dry to water saturation with a standard error of 0.013 cm^3 cm^{-3}, although later studies showed that the Topp et al. (1980) equation is not really universal and soil specific calibration is required. Patterson and Smith (1980) were among the first to use TDR to measure unfrozen/liquid water content ($\theta_{lw,} \leq \theta_v$) in frozen/freezing soils (He et al., 2016). This discovery significantly boosted the applications of TDR in soil science and opened a new era for soil water measurements. Many subsequent investigations, including TDR cable testers, TDR probe designs (Zegelin et al., 1989), TDR waveform recording or analysis tools (Wang et al., 2016), and TDR calibration curves (Dirksen and Dasberg, 1993; Dyck et al., 2019; Friedman, 1998; He and Dyck, 2013; He et al., 2016; Malicki et al., 1996; Ponizovsky et al., 1999; Robinson et al., 2005a; Roth et al., 1990) led to improvements in TDR capabilities. Detailed history of TDR developments in soil science studies is reported by Topp et al. (2003).

The application of the TDR methods to determine θ_v is based on the measurement of the travel time of an electromagnetic wave pulse (usually < 1.5 GHz) generated by a TDR cable tester through a wave guide (also called a probe or sensor) inserted into a porous medium (e.g., soil, food, concrete, snow or plant), at normal or frozen

conditions. The travel time of the wave through the probe is a function of the apparent or effective permittivity of bulk soil (here after K_a), which in turn is a function of the permittivity of the individual constituents in the soil (i.e., air, water, solids and ice), their volumetric fractions and geometric arrangements. The key to TDR's success is its ability to accurately determine the permittivity of a material and the strong relationship between K_a and its θ_v, as demonstrated in the pioneering works of Hoekstra and Delaney (1974) and Topp et al. (1980). Another unique advantage of TDR is its ability to make rapid and continuous measurements of both electric conductivity (EC) and θ_v with a single probe and in the same sampling volume (Castiglione and Shouse, 2003; Wraith et al., 2005). In addition, TDR probes can be installed in any orientation (e.g., vertically to obtain near-surface soil profile water content or horizontally to obtain better information at a particular depth) (Wraith et al., 2005), are easily multiplexed (e.g., up to 512 probes for a single TDR device) and data acquisition can be automated (Baker and Allmaras, 1990; Heimovaara and Bouten, 1990; Herkelrath et al., 1991; Spaans and Baker, 1995). Moreover, TDR methods are safe, unlike the neutron probe and gamma ray methods that release hazardous radiations. These characteristics make electromagnetic and more specifically, TDR the most widely used non-destructive method for soil water content measurement in field and laboratory studies (He and Dyck, 2013; He et al., 2015a; He et al., 2015b). The readers, if interested, may consult previous studies for more information on TDR principles and applications for measuring electrical conductivity

and soil water content (Benson and Bosscher, 1998; Clarke Topp, 1998; Ferre and Topp, 2002; Hendrickx et al., 2002; Jones et al., 2002; Noborio, 2001; Pettinelli et al., 2002; Robinson et al., 2008; Robinson and Friedman, 2003; Robinson et al., 2003b; Stein and Kane, 1983; Stein et al., 1997; Topp et al., 2003; Whalley, 1993; Wraith, 2003; Wraith et al., 2005; Zegelin et al., 1989).

There are two key steps in the application of the TDR method: (1) TDR waveform analysis and (2) the mathematical relationships/models between material permittivity and other predicted properties (e.g., water content). The most common application of TDR is to estimate water content from K_a measurements for unfrozen Topp et al. (1980) and frozen soils (Spaans and Baker, 1995). Applications are focused to agriculture which include irrigation scheduling (Topp and Davis, 1985) and plant water uptake estimation (Holbrook and Sinclair, 1992; Irvine and Grace, 1997; Kobayashi and Tanaka, 2001; Nadler, 2004; Wullschleger et al., 1996) and applications in science and engineering (Yadav et al., 2019). Advances in TDR waveform interpretation were associated with the emergence of new techniques and tools and to enable the detection of various properties and processes in a variety of porous media, including soil, snow, plant, food and concrete (Baker et al., 1982; Dalton et al., 1984; Dalton and Van Genuchten, 1986; Greco, 2006; Hayhoe et al., 1983; Laloy et al., 2014; Marchand et al., 2001; Roberson and Siekmeier, 2000; Topp et al., 1982a). In addition, TDR methods have been combined with other sensing techniques to determine a wide variety of soil physical properties and processes

(Lungal and Si, 2008; Noborio et al., 1999; Ren et al., 1999; Ren et al., 2003; Vaz and Hopmans, 2001; Wraith and Or, 2001). Although TDR is widely used, to our knowledge no study has synthesized and critically reviewed the versatile applications of TDR.

The objectives of this review, therefore, are to review the many applications of TDR focused on waveform interpretation in addition to for a variety of porous media, including soil, snow, plant, food and concrete. The review focuses on:

(1) TDR principles including TDR basics, probe designs, commercially available TDR units and associated waveform analysis tools;

(2) The applications of TDR are categorized according to determination of physical properties (e.g., profile distribution of water content, tree trunk water content, liquid water content of snow or snow wetness, frost detection and other properties pertaining to food science, concrete engineering and geophysics) and characteristic processes (e.g., solute transport, wetting/drying front, water flux across soil horizon, freezing/thawing front, snow depth, water depth and rock movement) in porous media;

(3) The combination of TDR with other sensing technologies for determining a wide variety of soil physical properties and processes;

(4) Limitations of the TDR method and perspectives on future studies.

2. TDR Basics

2.1. Principles of TDR

The TDR method is based on the measurement of the travel time of an electromagnetic (EM) wave generated by a TDR cable tester along a wave guide (commonly referred to as a probe) inserted into a porous medium. A TDR cable tester consists of an EM wave generator and a sampling oscilloscope. The electromagnetic wave generator creates a high frequency, broadband (0.001~1.5 GHz) EM wave that travels through the open-ended probes that are inserted into the porous media of interest. As the EM wave travels through the probe, its voltage or amplitude is sampled at every point along the probe by the oscilloscope and displayed on the screen of the cable tester as a function of distance (or time). The travel time of the EM wave through the probe depends on the K_a of the porous medium surrounding the probe. The K_a in turn depends on the permittivity of the individual constituents (e.g., air, water, solid matrix, and ice), their volumetric fractions and geometric arrangement. The permittivity of water (ε_w) is a function of temperature (i.e., ε_w varying from 96 at -20 °C to 88 at 0 °C to 80 at 20 °C) (Kaatze, 1989). Because ε_w is much greater than the permittivity of solids (e.g., ε_s varying from 5 to 10 for soil matrix (Robinson, 2004; Robinson and Friedman, 2003), and from 50 to 70 for meat (at temperatures between 15 °C and 65 °C at a frequency of 2.45GHz) (Nelson and Trabelsi, 2008; Sipahioglu et al., 2003; Tanaka et al., 2000), 1.3 to 4.5 for dry wood (with density between 0.1 and 1.5 g/cm^3 at a frequency of 0.1GHz) (Amato et al., 2019), 2.5 to 7 for dry concrete (McGraw Jr, 2015), air (ε_{air} =~1) and ice at high frequencies (ε_{ice} = ~3.2) (Dirksen and Dasberg, 1993; Friedman, 1998; Miyamoto et

al., 2005; Robinson and Friedman, 2003; Roth et al., 1990; Seyfried and Murdock, 1996), θ_v of a porous media can be estimated based on a calibration relationship between K_a of a porous medium and θ_v. Example waveforms and K_a values of selected materials are presented in **Fig. 1**.
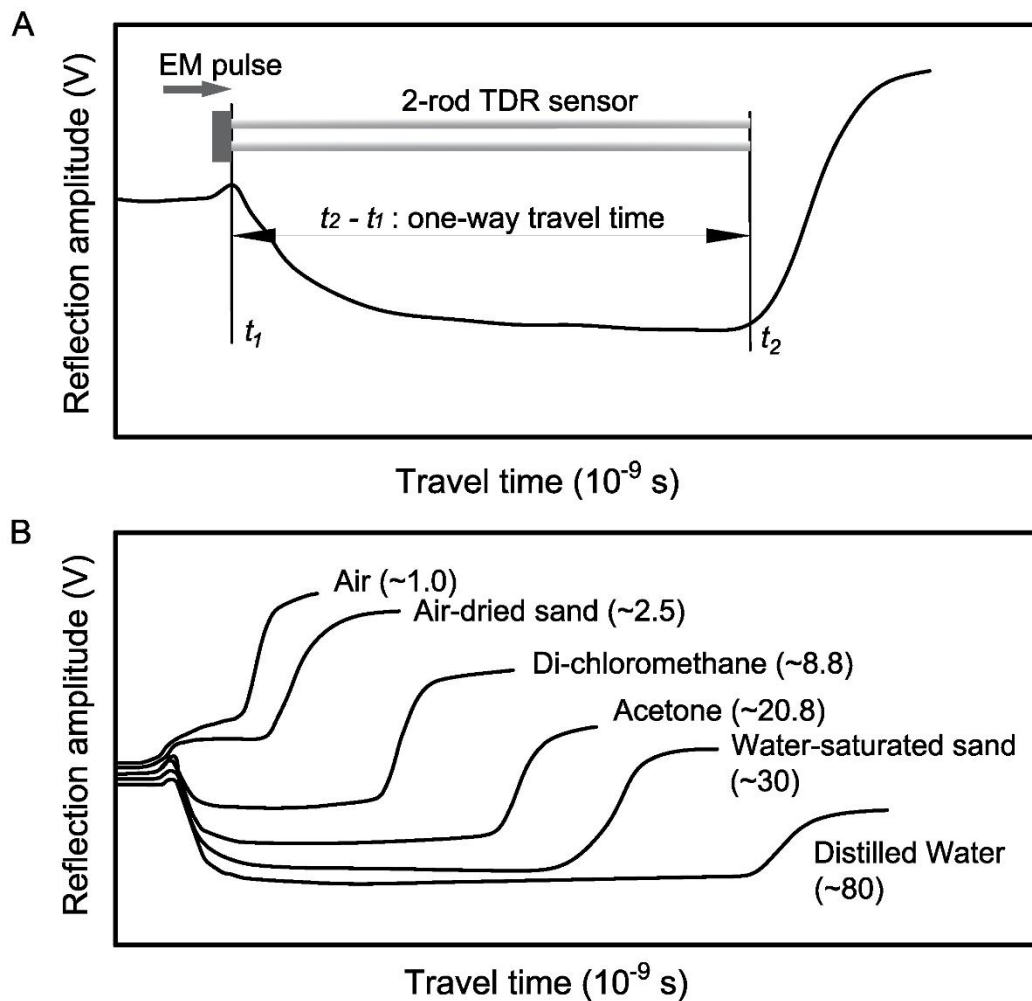
Fig. 1. Principles of TDR: (A) conversion of TDR waveform to permittivity after **Huisman et al. (2002)** and **Evett (2000a)**. Difference between t_1 and t_2 indicates time for electromagnetic waveform travel through the rod of TDR probe; (B) schematics of TDR waveforms in various materials with different permittivity after **Noborio (2001)** and **Wraith et al. (2005)**.

The K_a can be estimated by the following:

$$K_a = \left(\frac{c\Delta t}{2L}\right)^2 = \left(\frac{L_a}{V_p L}\right)^2$$

* MERGEFORMAT (1)

where c is velocity of the EM in free space (3×10^8 m s^{-1}), Δt is the two-way travel time for the wave down and back via the wave guide (s), L is the length of the wave guide or rods of a TDR probe (m), L_a is the apparent length that is the distance between reflections at the beginning and the end of the TDR rod, V_p is ratio of the velocity of EM propagation in the material under test to that in free space. Equation improves travel time determination of TDR method (Robinson et al., 2003a).

2.2.   TDR Probe Designs

A conventional TDR probe usually consists of two or three parallel rods (Greco, 2006; Zegelin et al., 1989), although TDR probes with a single rod or with four to seven rods have sometimes been used (Jones et al., 2002). The design of TDR rods varies with respect to material, length, shape, diameter, and spacing. For instance, brass was used as the rod material in early designs, while stainless steel is currently a preferred option for manufactured probes. Lengths of TDR rods generally vary from 21 mm (Amato and Ritchie, 1995) to 1500 mm (Previati et al., 2011), and rod diameters range from 1.3 mm (Hudson et al., 1996) to 12.7 mm (Topp et al., 1982a). Souza et al. (2004) developed a variable-volume TDR probe consisting of multiple single TDR probes to measure water content in large soil volumes. Some of the selected TDR probe designs are tabulated in **Table 1**. There are limited number of

real TDR probes commercially available (Vaz et al., 2013) and most of them are custom made.

Compared to two-rod TDR probes, probes with three or more rods in a coaxial configuration do not require the use of balun (i.e., balancing transformer), which was sometimes used in two-rod TDR probes to reduce signal and information losses or to match the impedance of the rods and the coaxial cable (Spaans and Baker, 1993; White et al., 1995). However, the three- or three plus-rod probes disturb the soil to a greater extent compared to the two-rod probes (Jones et al., 2002; Zegelin et al., 1989). Although a variety of TDR probes have been proposed to date, comprehensive criteria are somewhat lacking for a conventional TDR probe design. Where necessary, TDR probe design has been customized for various applications. Whalley (1993) contrasted two-rod TDR probes with a balun to three-rod probes and concluded that: (1) two-rod probe with a balun can estimate water content on a larger volume of soil; (2) probes with small diameter and closely spaced rods may result in unwanted errors in measurements; and (3) a three-rod probe is a preferred choice when a short-rod probe is required as it can produce a much clearer and more easily-interpreted reflected signal.

In order to reduce the pulse signal attenuation and facilitate accurate travel time estimation, the approximate maximum and minimum rod length of a balanced TDR probe can be estimated with (Dalton and Van Genuchten, 1986; Ren et al., 1999):

$$L_{\max} = \frac{\ln\left(\dfrac{V_T}{V_R}\right) \cdot \sqrt{\varepsilon_{\mathit{eff}}}}{12\pi\sigma} \qquad \text{\textbackslash* MERGEFORMAT (}$$

$$L_{\min} = \frac{tc}{2\sqrt{\varepsilon_{\mathit{eff}}}} \qquad \text{\textbackslash* MERGEFORMAT (3)}$$

where $L_{\max}$ and $L_{\min}$ are the maximum and minimum rod lengths (m); V_T and V_R are excitation voltage and reflected voltage (V), respectively; σ is the bulk electrical conductivity (dS m^{-1}), t is travel time (s), and c is the velocity of light in a vacuum (3×10^8 m s^{-1}). The optimized ratio of rod spacing to the rod diameter r/d is recommended to be less than 10, and the ratio should be as large as possible in order to minimize the "skin effect", while avoiding significant soil disturbance (Knight, 1992).

Table 1. Selected designs of time domain reflectometry (TDR) probes

No.	Name/Source	TDR dimension				Applications	Note
		Rod No.	Length (mm)	Dia. (mm)	Spacing (mm)		
						Commercially available TDR probes	
1	FP/MTS	2	100	2	16	Soil moisture, temperature and salinity	- Field probe, paired with FOM2/mts-handheld meter, developed by E-test, Poland (Bajno et al., 2020; Skierucha et al., 2008), https://www.e-test.eu/
2	LP/MS	2	53	0.8	5	Soil moisture and salinity	Laboratory mini Probe paired with FOM2/mts-handheld meter
3	SoilVUE 10	1	550, 1050	5.2, 5.8	NA	Soil moisture, temperature and EC profile	Profile probe distributed by Campbell Scientific, Inc., Logan, UT, USA. https://www.campbellsci.com/
4	TDR305H/310H/315H	3	50/100/150	3.5	NA/11.4/19	Soil water, permittivity, EC, and temperature measurement	Produced by Acclima, Inc., Boise, ID, USA. https://www.acclima.com/sdiproducts.html
5	Trase TDR Soilmoisture Probes	2/3	150, 200, 400			Soil water and permittivity	Soilmoisture Equipment Corp., Santa Barbara, CA, USA https://www.soilmoisture.com
6	TRIME Pico 32/64	2	110/160	3.5/6	20/40	Soil moisture (sample volume > 1250 ml) and temperature	Produced by Acclima, Inc., Boise, ID, USA. TDR probe paired with HD2 Mobile (Dettmann and Bechtold, 2018; Huza et al., 2014), https://www.imko.de/en/
7	TRIME Pico IPH T3/44 TDR probe	1	480	37	N/A	Capturing soil moisture profile to a 3 m depth (0-60 vol.%	Produced by Acclima, Inc., Boise, ID, USA (Lv et al., 2016),

No.	Name/Source	TDR dimension				Applications	Note
		Rod No.	Length (mm)	Dia. (mm)	Spacing (mm)		
						moisture), ideal for soil with high salinity	https://www.imko.de/en/
Customized TDR probes							
8	Davis (1975)	N/A	N/A	13	50	Field measurements of sandy and clay soil's relative permittivity	The original paper is unavailable, data are from (Patterson and Smith, 1981)
9	Davis and Chudobiak (1975)	N/A	> 1000	N/A	50	Field measurement of relative permittivity of soils.	The original paper is unavailable, data are from (Patterson and Smith, 1981) and Topp et al. (1980)
10	Patterson and Smith (1981)	2	100	3,10	20, 25, 50	Laboratory measurement of unfrozen water of frozen soils.	
11	Topp et al. (1982a)	2	~1000	12.7	50	Laboratory measurement of θ and wetting fronts	Also in Topp et al. (1982b); Balanced transmission lines (Patterson and Smith, 1981)).
12	Zegelin et al. (1989)	3~4	150	4.76	30	Field measurement of θ and EC	No need for balancing transformers, more precise & less noisy than traditional 2-rod probe; Wraith et al. (1993)
13	Constantz and Murphy (1990)	2	130	3.2	25	Laboratory measurement of water storage in trees	
14	Heimovaara (1993)	3	50, 100, 200, 500	2,4	18, 46	Laboratory test of the effects of different triple-wire TDR probe dimensions and cable lengths on the measurements.	Triple-wire probe ?
15	Heimovaara (1994)	7	98	2	15	Measurement of the soil's complex dielectric constant	
16	Amato and	2	21	5	50	Field measurement of θ	

No.	Name/Source	TDR dimension				Applications	Note
		Rod No.	Length (mm)	Dia. (mm)	Spacing (mm)		
	Ritchie (1995)						
17	Robinson and Friedman (2000)	2, 3	150	4	20	Field and laboratory test of comparing parallel plates with conventional rods in measuring soil moisture.	
18	Jones and Friedman (2000)	3	100	4	50	Laboratory determination of permittivity to determine particle shape and probe-particle orientation effects in mica.	
19	Nadler (2004)	2	200	3	50	Field measurement soil water content.	
20	Greco (2006)	3	99~380	3~12	8~57	Field, spatial variability of θ_v	Horizontal (H) and vertical (V) placed.
21	Greco and Guida (2008)	1	105, 150, 300, 450, 600	3	32	Field measurement of top soil water profile.	
22	Hernández-Santana and Martínez-Fernández (2010)	2	120	3	30	Laboratory measurement of water content in soil and oak stem.	
23	Cheng et al. (2010)	4	60	3	20 (radius)	Laboratory measurement of soil moisture.	
24	Previati et al. (2011)	2	150~1500	5	50	Joint use of Ground Penetrating Radar (GPR) and TDR to map dry snow depth, layering, and density.	

No.	Name/Source	TDR dimension				Applications	Note
		Rod No.	Length (mm)	Dia. (mm)	Spacing (mm)		
25	Boike and Roth (2015)	3	250	5	30	Field measurement of soil water content at a continuous permafrost site.	
26	He et al. (2015b)	3	140	1.6	10 (inter-rod spacing)	Laboratory measurement of liquid water content and ice content in partially fozen soils.	
27	Szerement et al. (2019)	7	40-45	2	7	Lab test	

*inclusion of the commercial brands does not mean promotion of them

It should be noted that the list of companies is not complete, and it does not imply any company endorsement

Table 2. Selected commercially available time domain reflectometry (TDR) cable testers for measurement of water content

No.	Name/Mode	Manufacture	TDR characteristics					Pictures	Contacts	Note
			Price (US 10^3\$)	Rising time (ps)	Dimension (L×W×H, cm)	Weight (kg)	Operating voltage			
1	FOM2/mts (Field Operated Meter of moisture, temperature and salinity of soils)	E-Test Ltd.	3	200	1.9 × 7.0 × 12.5	0.20	3.7 V dc		**Address:** E-Test Ltd. 21-030 Motycz, Stasin 90 Poland **Email:** info@e-test.eu **Tel:** +48 508 499 494 https://www.e-test.eu/field-operated-meter.html https://www.e-test.eu/laboratory-meter.html	Handheld TDR moisture meter (Skierucha et al., 2008; Skierucha et al., 2006)
2	TDR/MUX/mpts		~14-17	200	18 × 8.5 ×5.8	0.35	6-15 V dc			TDR meter with a multiplexer for soil moisture, matric pressure, temperature and EC measurement
3										
4										
5	Tektronix 1502B/C, 1503B/C	Tektronix MOHR	~2.4	200	47.5×12.7 ×31.5	8.2	115 V ac		**Address:** 815 W 1800 N, Logan, UT 84321-1784，USA **Tel:** (435) 227-9120 **Fax:** (435) 227-9001 https://www.testequipmentdepot.com/usedequipment/tektronix/tdrs/1502b-1503b.htm	Retired
6	CT100 Series		NA	NA	60-100	10.9 cm*29.2cm*17.5 cm	2.2		**Address:** MOHR Test and Measurement LLC 2105 Henderson Loop Richland, WA 99354 USA **Tel:** +1 (888) 852-0408 **Fax:** +1 (888) 278-8037 **Email:** sales@mohrandassociates.com http://www.mohr-engineering.com/tdr-cable-analyzer-time-domain-reflectometer-frequency-do	CT100B enables FDR analysis

No.	Name/Mode	Manufacture	TDR characteristics					Pictures	Contacts	Note
			Price (US 10³$)	Rising time (ps)	Dimension (L×W×H, cm)	Weight (kg)	Operating voltage			
									main-analyzer-CT100B.php	
7	TDR100/200	Campbell Scientific	~4.5	≤ 85	21.6 ×10.7 ×5.1	0.79	12 V dc		https://www.campbellsci.com/tdr200	
8	Trase SystemI6050X1	Soilmoisture Equipment Corporation	~15	120	53.3 cm*43.18 cm *38.1 cm	11.92	18 V dc		**Address:** 801 South Kellogg Ave., Goleta, CA 93117, USA **Tel:** +1 (805) 964-3525 **Email:** sales@soilmoisture.com https://www.soilmoisture.com/HT/	0- 100 % Soil Moisture Sensing, irrigation management, Mining
9	Handi-TRASE TDR Soilmoisture Meter		~13	< 130	12.0×10.0×4.0	2.27	3.7 V			Perform well in high salinity & high EC soils.
10	HD2 Mobile TDR meter	IMKO Micromodultechnik GmbH	~2.9	NA	15×6.4 ×3.6	0.437	4-8 V dc		**Address:** Am Reutgraben 2 76275 Ettlingen Germany **Tel:** +49 (0) 7243 / 59210 **Emal:** info@imko.de https://www.imko.de/en/hd2-mobile/	The mobile reading device for TRIME-PICO Series soil moisture probes, showing moisture, temperature and EC.

It should be noted that the list of companies is not complete, and it does not imply any company endorsement

2.3. Commercially Available TDR Cable Testers

The Tektronix series TDR cable testers (i.e., Tektronix 1502, 1502B/C, 1503) were often used in the laboratory and field to measure soil water content since the 1980s. As this method has become more widely accepted by researchers and practitioners, a variety of TDR cable testers were developed to share the ~$200 million market for soil water measurement (https://www.grandviewresearch.com/industry-analysis/soil-moisture-sensors-market; https://www.marketsandmarkets.com/Market-Reports/soil-moisture-sensor-market-14 0653896.html). Some of the companies producing TDR instruments for soil applications are Acclima, Inc., Ltd., Campbell Scientific, Inc., MOHR Test and Measurement LLC, Soil Moisture Equipment Corporation (Fatás et al., 2013). These TDR cable testers vary in measurement accuracy and precision, cost, design, dimension, durability and portability. The size of instruments has also come down so that now, TDR sensors are available with the TDR embedded in the head of the instrument (e.g. Acclima TDR sensors). Some commonly used and commercially available TDR cable testers are described in **Table 2.** Some of the TDR cable testers (e.g., TDR from Campbell Scientific and Soil Moisture Equipment Corporation) provide software to collect and analyze TDR waveforms. Third-party programs developed for data acquisition and analysis are described in the next section.

2.4. Analysis of TDR waveforms

2.4.1. Graphical Interpretation Methods for Water Content

Graphical interpretations of TDR waveforms can be used to determine properties of and processes in porous media. For instance, the determination of water content requires the t_1 and t_2 values (**Fig. 1**) in order to calculate L_a with Eq. . The detection of a wetting/drying or a freezing/thawing interface requires the reflection points on a TDR waveform between t_1 and t_2 to be determined. The measurement of electrical conductivity (EC) requires the reflection amplitude of the long-time EM waveforms

(Giese and Tiemann, 1975; Lin et al., 2008). TDR waveform can be processed automatically with software, sometimes built into the assembled TDR units that directly output properties like water content and EC. However, manual analysis of the EM waveforms using specific analysis methods can provide quite accurate estimates of soil water profile, wetting and freezing front or interface, snow depth and water level. Topp et al. (1980) analyzed TDR waveforms from the screenshot of the oscilloscope display to derive K_a based on the method proposed by Loeb et al. (1971). Many graphical interpretation methods (e.g., tangent waveform analysis, double-tangent waveform analysis) to increase the accuracy or efficiency of TDR waveform interpretations were developed (Baker and Allmaras, 1990; Heimovaara, 1993; Heimovaara and Bouten, 1990; Herkelrath et al., 1991; Wang et al., 2016). These graphic methods are generally based on the determination of three points including t_0, t_1 and t_2 (**Fig. 1**). Many methods are available to determine these three parameters. For example, methods to determine t_1 include: (1) time corresponding to the minimum of the first derivative; (2) based on $t_0 + a$, a is the distance between t_0 and t_1 that can be obtained by the short circuiting the TDR probe. t_0 can be determined from the cross of tangent lines of l_1 for the flat limb and l_2 for the rising limb; (3) cross of the tangent lines of l_3 for the rising limb and l_5 for the declining limb; and (4) cross of the tangent lines of l_4 and either the l_3 or l_5. Methods to determine t_2: (1) the minimum point after t_1; (2) cross of the tangent line of the minimum point after t_1 and the tangent line of l_7 for the rising limb; and (3) cross of tangent lines of l_6 for the

baseline and l_7 for the rising limb. Evett (2000b) incorporated some of the EM waveform interpretation methods in TACQ software.
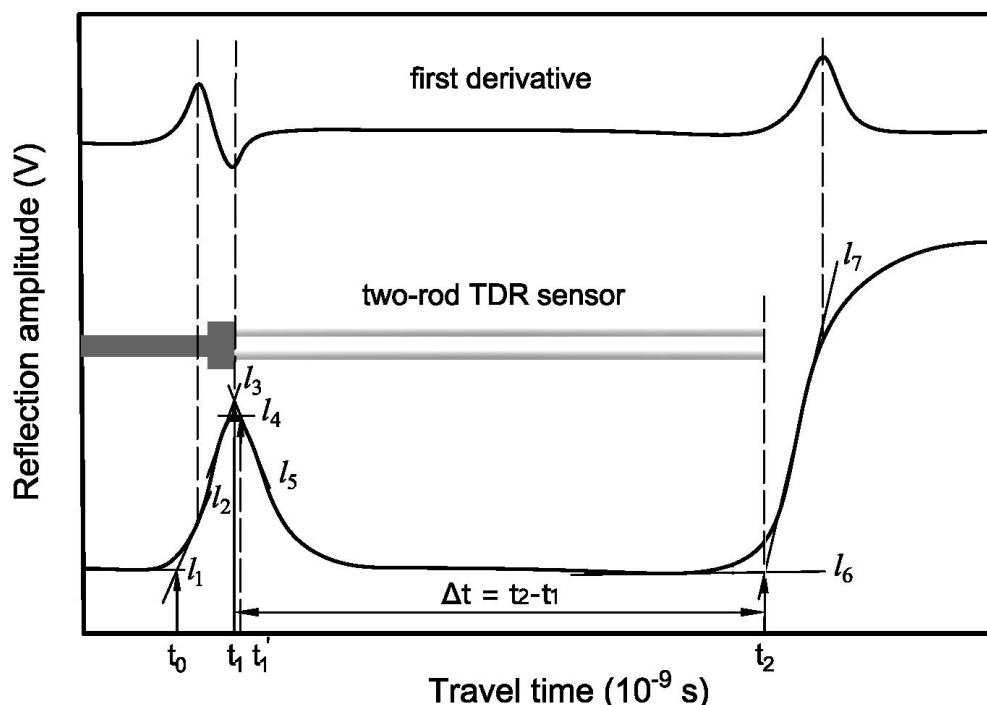
Fig. 2. Illustration of graphical interpretation methods of TDR waveforms, t_0 indicates the point where the electromagnetic waveform transitions from the coaxial cable to the TDR probe handle, t_1 indicates the first reflection peak where electromagnetic waveforms enters the porous medium via the TDR probe rod from the probe handle, and t_2 indicates the second reflection from the end of the TDR probe rod. The values of t_1 and t_2 have to be determined in order to find their difference and subsequently calculate K_a using Eq.. After **Huisman et al. (2002)** and **Evett (2000a).**

2.4.2. *Graphical Interpretation Methods for EC*

TDR waveforms contain information about electromagnetic energy attenuation besides travel time of an EM pulse (Dalton et al., 1984; Dalton and Van Genuchten, 1986; Giese and Tiemann, 1975; Heimovaara et al., 1995). Because the attenuation or reflection amplitude is positively correlated to electrical conductivity (EC, σ), TDR can be used to calculate soil bulk EC and infer soil water salinity (Nadler, 2005) (**Fig. 3**).
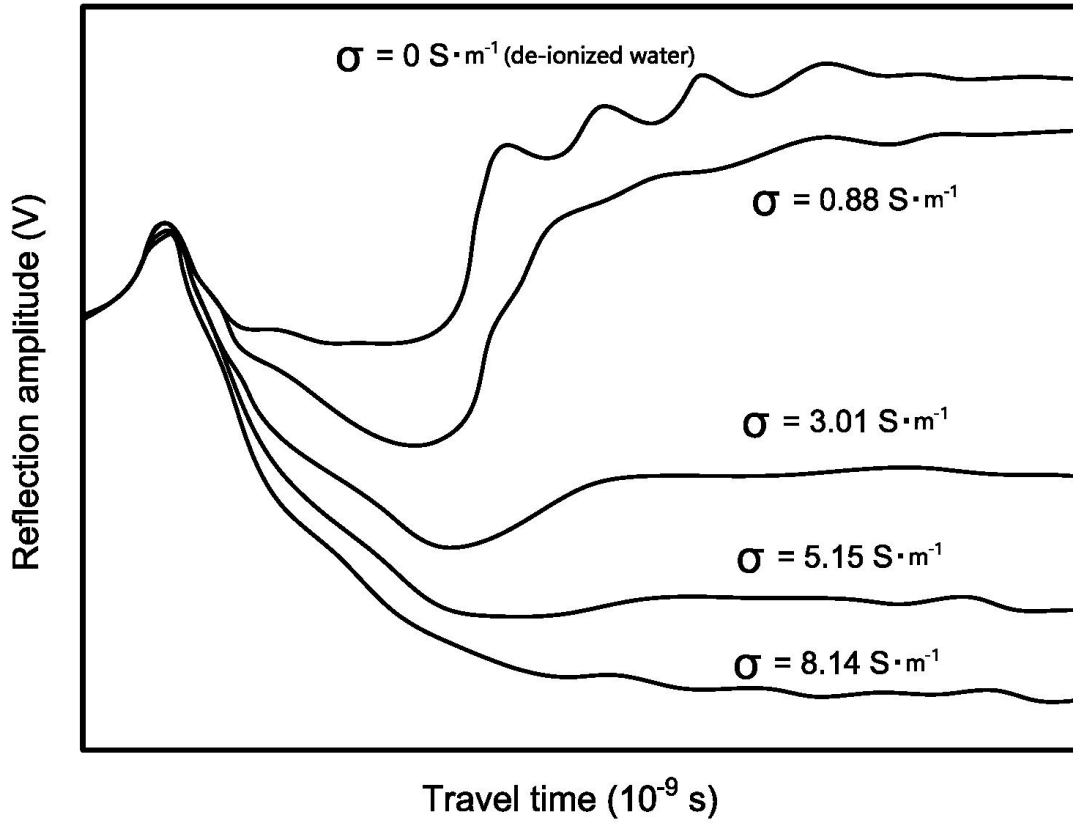
Fig. 3. Schematics of TDR waveforms in deionized water (σ=0 S m^{-1}) and soils of different bulk electrical conductivities (σ=0.88, 3.01, 5.15, 8.14 S m^{-1}), after **Patterson and Smith (1985)** and **Cristi et al. (2016)**.

Giese and Tiemann (1975) estimated σ from a TDR waveform as follows:

$$\sigma = \frac{K_p}{Z_r}\left(\frac{1-\rho_{\infty,scale}}{1+\rho_{\infty,scale}}\right) \quad \backslash^* \text{ MERGEFORMAT (4)}$$

where Zr is the output impedance of the TDR cable tester (50 Ω); Kp is the probe-geometry-dependent cell constant value (m^{-1}), and $\rho_{\infty,scale}$ is the scaled steady-state reflection coefficient for ideal condition calculated from (Lin et al., 2008; Lin et al., 2007):

$$\rho_{\infty,scale} = 2\frac{(\rho_{air}-\rho_{sc})(\rho-\rho_{air})}{(1+\rho_{sc})(\rho-\rho_{air})+(\rho_{air}-\rho_{sc})(1+\rho_{air})}+1 \backslash^* \text{ MERGEFORMAT (5)}$$

where ρ, ρ_{air} and ρ_{SC} are the long-time reflection coefficient measured in the studied porous medium, in air and of a short-circuited TDR probe, respectively.
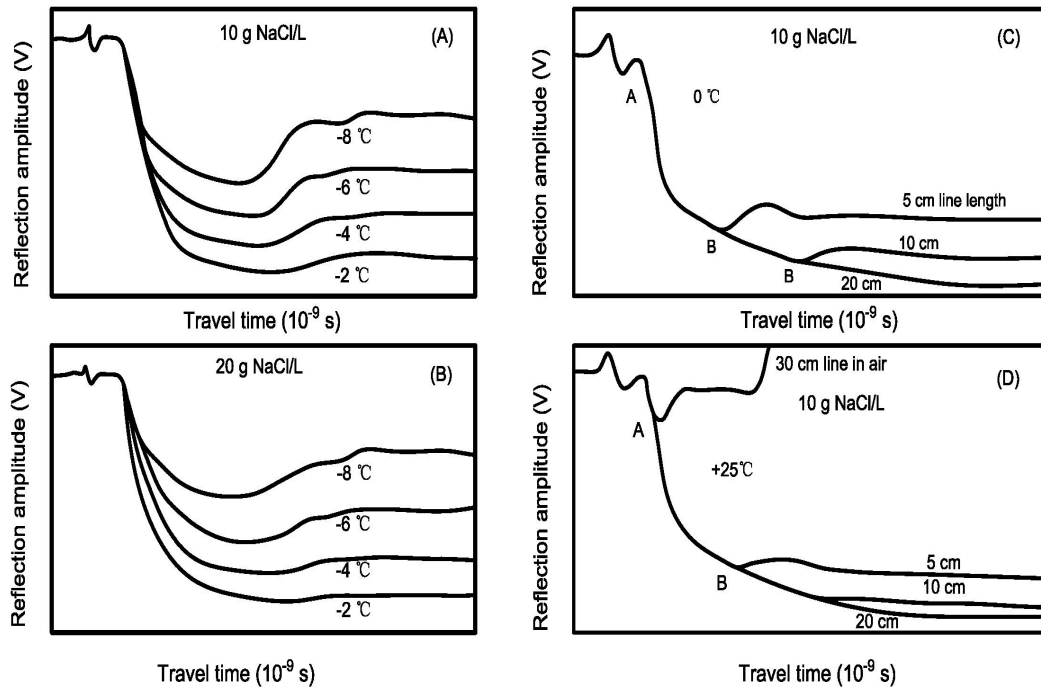
Fig. 4. Schematics of TDR waveforms in response to soils at different salinities and temperatures (A and B) and with different length in a saline sand at 0ºC (C) and 25 ºC (D), after **Patterson and Smith (1985)**.

The shapes of TDR waveforms obtained in saline soils are affected by the combined effects of pore water salinity, water content, temperature and the length of the TDR probe (see **Fig. 4)** (Patterson and Smith, 1985). Zegelin et al. (1989) reported that coaxial emulating sensors with 3 or 4 rods without a balun overcame the impedance mismatch problem associated with conventional parallel-rod probes, and produced more accurate measurements of EC. More studies pertaining to the principles, the waveform analysis method and measurement of soil EC have been well documented (Robinson et al., 2003b; Wraith et al., 2005).

The TDR measurement results in a single bulk permittivity value that corresponds to a particular, but unknown "effective" frequency (f_{eff}). It is important to estimating f_{eff} because accounting of measurement frequency enables us to compare the accuracy and performance of TDR probes with other techniques (i.e., 0.001 to 1.5 GHz), such

as impedance or capacitance probes (e.g., 20~300 MHz (Vaz et al., 2013)), or microwave remote sensing devices (e.g., L band: 0.5 to 1.5 GHz, S band: 2 to 4 GHz, and C band: 4 to 8 GHz, L, S and C are abbreviation for long, short and compromise, respectively). Soils with high clay and organic matter content show large dielectric dispersion and the real and imaginary permittivity change as a function of frequency. Robinson et al. (2005b) used a transmission line model to investigated the effects of dielectric dispersion on the TDR signal. They found $0.7 < f_{eff} < 1$ GHz for most nonconductive TDR measurements, while $f_{eff} < 0.6$ GHz in dispersive media.

2.4.3. Time-to frequency-domain transformation

The Fourier transformation method has been used to extract information on frequency-dependent dielectric properties contained in TDR waveforms (Chen and Or, 2006; Jones and Or, 2004). This method can be used to transform TDR (time domain) EM waveforms to the frequency domain (Fatás et al., 2013). Frequency-dependent dielectric properties can be used for a variety of purposes: (1) to identify and quantify the influence of various sources of errors on TDR applications; (2) to improve the accuracy of estimates as well as to provide valuable information on interactions between the solid and liquid phases and on possible dielectric relaxation phenomena(Friel and Or, 1999; Hoekstra and Delaney, 1974); (3) to estimate both water content and soil bulk electrical conductivity (Fatás et al., 2013; Greco, 2006; Heimovaara et al., 2004; Huisman et al., 2002; Moret-Fernández et al., 2012); and (4) TDR waveform transformation from the time- to frequency-domain was shown to

facilitate permittivity estimation using shorter TDR probes, down to 2 cm length under increasingly higher electrical conductivity solutions beyond which travel-time analysis failed (Jones and Or, 2004).

Heimovaara (1994) presented the theory for the frequency domain analysis of TDR waveforms. Friel and Or (1999) extended this work by focusing on scatter functions. The frequency domain analysis of TDR waveforms can be considered as an interpretation of complex interactions between the input TDR-induced EM field and the tested porous medium around TDR probes or in a coaxial cell (e.g., geometry and termination). Fourier transformation can be applied to the reflected or output TDR signal to simulate the porous medium's dielectric response. It can be expressed as a convolution integral of the input TDR signal as (Gemert, 1974)

$$r(t) = \int_{-\infty}^{+\infty} v_0(t - \tau) s(\tau) d(\tau) \quad \text{* MERGEFORMAT (6)}$$

where $r(t)$ is the response function expressed as the convolution of the input signal, $v_0(t)$; $s(t)$ is the system function; t is time and τ is the integration variable. By applying the convolution theorem (Lathi, 1992), Eq. in the frequency domain can be reduced to

$$R(f) = V_0(f) S(f) \quad \text{* MERGEFORMAT (7)}$$

where response function $R(f)$, input signal $V_0(f)$, and scatter function or S-parameter $S(f)$ are the Fourier transforms of $r(t)$, $v_0(t)$, and $s(t)$, respectively, and f is the frequency (Hz). The $S(f)$ describes how the $V_0(f)$ is modified by the porous medium-TDR probe system. The porous medium dielectric properties are largely

determined by the accuracy of S(f) estimation from the measured TDR waveforms (**Fig. 5**).
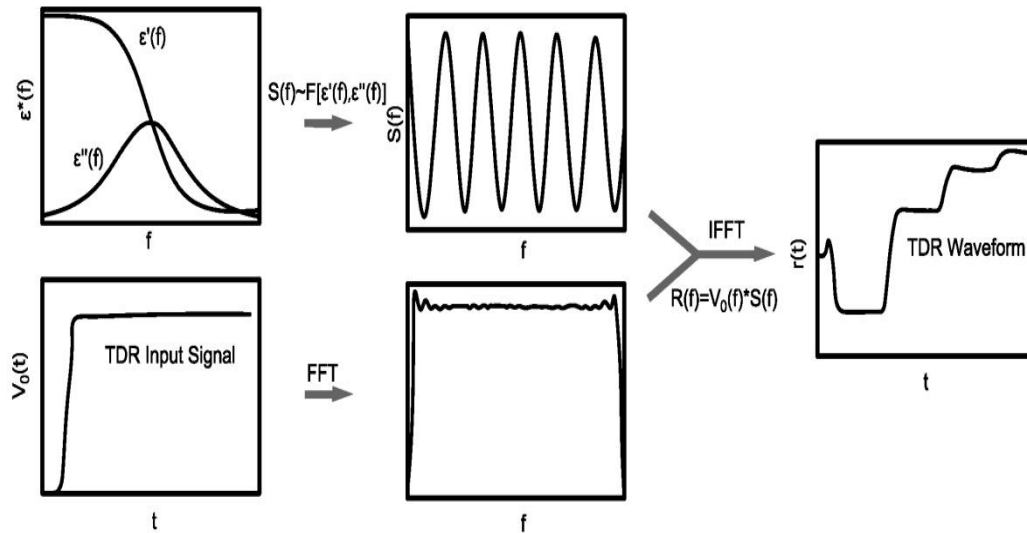
Fig. 5. Schematics for TDR waveform simulation using permittivity, system function, and FFT/IFFT techniques (Chen and Or, 2006).

An assessment of TDR-based estimates of S(f) and the potential information losses/errors in making such time-to-frequency transformations is important for practical applications. The S(f) consists of S_{11} and S_{21} parameters that represent scatter function for an open-ended probe and the scatter function for transmission of the TDR wave where the probe is terminated with a load matching the input impedance (time domain transmission (Friel and Or, 1999). This method was used by de Winter et al. (1996) and Huisman et al. (2002) to calculate the Debye model parameters of a dielectric medium. Huisman et al. (2002) proposed a simplified method to calculate a frequency independent K_a based on the fact that the commonly used TDR frequency bandwidth was not affected by the relaxation phenomena in most porous media. The TDR-Lab software (Fatás et al., 2013) puts K_a calculated from the Topp et al. (1980) equation, Eq. below, in a model that accounts for the cable-probe-soil impedance to

simulate a TDR signal using the Fourier analysis proposed by Heimovaara et al. (2004) and Huebner and Kupfer (2007). The resulting θ_v is derived by minimizing the root mean square error (RMSE) between the measured and the simulated TDR signals.

2.4.4. *Software Programs for TDR Waveform Analysis*

Several waveform analysis software tools (TACQ by Steve. R. Evett (Evett, 2000a, b), TDRANA by Timo J. Heimovaara, TDRAPP by Hailong He, TDR-LAB by David Moret-Fernández and E. Fatás, TDR_SPS by Jean-Paul Laurent, WinTDR by Dani Or (Or et al., 2004), and PC-TDR by Campbell Scientific) are available for automatic or manual waveform analysis. TDR-LAB 2.0 includes numerical methods for analyzing TDR waveforms. TACQ provides a number of graphical interpretation methods. TDRAPP includes all of the graphical methods used by TACQ and has a drag-and-move function to determine the $t_{1.bis}$, t_1 and t_2. The latest version of PC-TDR includes the Second-Order Bounded Mean Oscillation (BMO) algorithm developed by Wang et al. (2016) for analyzing TDR waveforms of short TDR probes. **Table 3** lists some of the major software available for EM waveform analysis and serves as a reference guide for users to select the appropriate software for their application. More details on these software programs are provided in their respective manuals. It should be noted that all the non-profit software programs face the same limitation: once they were developed using a given operating system (OS), there is diminishing opportunity to keep the software running on newer OS without funding and programmers that continue to be available.

Table 3 Features of selected software for TDR waveform recording and analysis (ordered by name of software programs).

Software	Features
AutoTDR	• Developed by Thomsen (1994) and Thomsen and Thomsen (1994), from (Thomsen et al., 2000)
PC-TDR	• Compatible with TDR100/200 from the Campbell Scientific cable testers (available at https://www.campbellsci.com/pc-tdr) • Acquisition and analysis of TDR EM waveforms • The sampling points of waveforms can be customized • Support manual or automated analysis of TDR EM waveforms
TACQ/TAC Qbeta	• Run under Disk Operation System (DOS) or system not newer than Windows XP (Evett, 2000a, b) (available at http://www.cprl.ars.usda.gov/programs/) • Support automated acquisition of TDR EM waveforms • Support multiplexed systems with up to 256 probes • Support manual or automated analysis of TDR EM waveforms • Various graphical interpretation methods were provided for analysis of bulk electric conductivity and soil water content
TDRANA	• Compatible with Tektronix 1502B and IBM PC/XT/AT computer/laptop (8255), developed by (Heimovaara and Bouten, 1990) • Support automated acquisition of TDR EM waveforms • Support multiplexer up to 36-channel coaxial relay • Support manual or automated analysis of TDR EM waveforms • A new graphical interpretation method was developed
TDR APP (by the authors)	• Written with Matlab graphical user interface (GUI) program • Data analysis for water content only, not compatible with TDR cable tester • Manual and automated Waveform analysis • Various waveform analysis methods are provided (derivative and tangent methods are used as reference)

Software	Features
TDR-LAB 1.0	• Compatible with two different TDR cable testers (i.e., Tektronics 1502C and TDR100) (Moret-Fernández et al., 2010) (available at http://digital.csic.es/handle/10261/35790) • Does not support multiplexers (Fatás et al., 2013) • Included a user-friendly and dynamic file format to show and save the TDR waveforms • Able to determine θ and σ • Two TDR waveform analysis methods(graphical and inverse modelling methods) (Moret-Fernández et al., 2012) • Unsuitable for low capacity computers, work with SQL database engine
TDR-LAB 2.0	• Updated version of TDR-LAB 1.0 written in C# with Microsoft®.Net Framework® 3.5 (only new features will be listed here) • Compatible with three different TDR cable testers (Tektronix 1502C, TDR-100, TRASE Soil-moisture Equipment) and support multiplexer system SDMX50 (Fatás et al., 2013) (available at http://digital.csic.es/handle/10261/35790.) • Can be used to analyze bulk electrical conductivity, water level, matric potential, and soil solution electrical conductivity in addition to soil water content
TDR-LAB 2.0 Lite	• Simplified version of TDR-LAB 2.0 with fewer features for field tests and measurements (Fatás et al., 2013) (available at http://digital.csic.es/handle/10261/35790.) • Fits low-end ultraportable devices, works with XML-files
TDR_SPS	• Mentioned in (Fatás et al., 2013), no further information was found
WINTDR (final version 6.1)	• Compatible with operating systems Windows 9x, ME, NT, 2000, or XP, fit for 32 bit machines only (available at http://psc.usu.edu/soilphysics/win-tdr) • Support Tektronix 1502/3 B/C TDR units, via the Tektronix SP232 module • Support multiplexers • Automated readings for automatic data capturing and analysis • Can be used to determine volumetric water content, electrical conductivity, and permittivity of soils or solutions • The coefficients in Topp et al. (1980) equation can be customized

Software	Features
WinTrase 2.07	• Compatible with TDR products from Soil Moisture Equipment Corp. (available at https://www.soilmoisture.com/downloads/WINTRASE.zip) • Run under 32-bit (for any operating system) or 64-bi (only XP operating system or PCs with XP emulator)

3. Applications of TDR

3.1. Physical properties of porous media

3.1.1. Soil Water Content Measurement with Traditional TDR Methods

Soil water content is estimated based on the calibration relationship (i.e., mathematical model) between the TDR-measured K_a value and θ_v of the porous media. Numerous mathematical models have been proposed to describe the relationship between K_a and θ_v. They can generally be divided into four categories:

(1) Empirical model. Empirical models relate measured K_a to θ_v via least squares regression. The original development of TDR for soil water content is the third-order polynomial calibration curve given by Topp et al. (1980).

$$\theta_v = -5.3 \times 10^{-2} + 2.92 \times 10^{-2} K_a - 5.5 \times 10^{-4} K_a^2 + 4.3 \times 10^{-6} K_a^3 \quad \text{\\* MERGEFORMAT (8)}$$

The Topp et al. (1980) equation related θ_v to K_a in unsaturated soils, and it was found to be almost unaffected by change in soil bulk density, texture, salinity and temperature in the soils tested. The standard error of the estimation was very low (1.3%) and could be calibrated to a lower level (1%) for a specific soil type. However, this equation was found to be restricted to unfrozen soils and soils with low specific surface areas (Dirksen and Dasberg, 1993; Dobson et al., 1985; Dyck et al., 2019). A special calibration was required for partially frozen soil (Stein and Kane, 1983).

Patterson and Smith (1981) were the first to measure unfrozen or liquid water content with TDR, and Smith and Tice (1988), Spaans and Baker (1995), and Watanabe and Wake (2009) attempted to calibrate TDR in partially frozen soils by relating TDR-measured water permittivity, ε_w, to independently measured liquid water content, θ_{lw}.
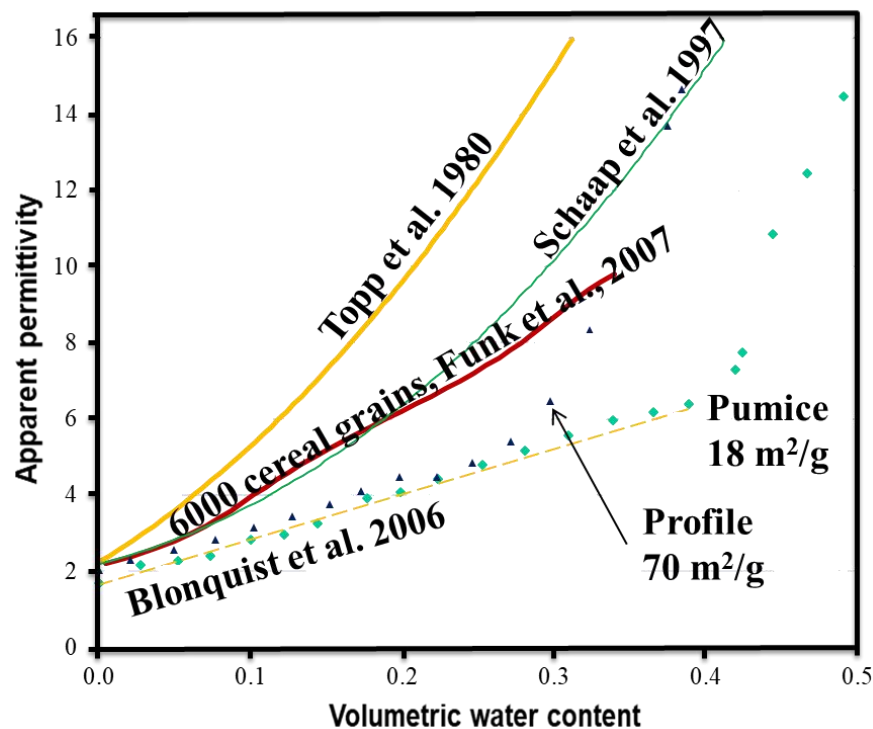
Fig. 6. Illustration of different volumetric water content-apparent permittivity relationships among different porous media. The calibration equations of Topp et al. (1980), Schaap et al. (1997) ,Funk et al. (2007) and Blonquist et al. (2006) were compared.

Therefore, it should be noted that TDR calibration curves vary with different porous media as shown in **Fig. 6**. The Topp et al. (1980) (Eq. (8)) represents a wide variety of soils, while Schaap et al. (1997) represents forest litter and Funk et al. (2007) is an empirical relation describing over 6000 cereal grain samples, all corrected for density and other factors. Considering bound water effects, Blonquist et al. (2006) demonstrated similar relations between high surface area clay aggregates

(Profile) compared to pumice of a much lower surface area, suggesting constituent phase configuration may dominate as a factor causing reduced permittivity relative to Topp et al. (1980).

(2) Semi-empirical model. Models that are partly theoretical models and partly empirical models (Ansoult et al., 1985; Heimovaara, 1994; Robinson et al., 2005a; Roth et al., 1990; Whalley, 1993).

(3) Physical models. This type of model can be described as mixture equations which account for the constituent components of a porous medium such as soil. Birchak et al. (1974) employed a two phase mixture equation to describe soil moisture and Dobson et al., (1985) expanded on this concept to include the air phase as well as to divide the water phase into free and bound water, written

$$K_a^{\alpha} = \theta_s \varepsilon_s^{\alpha} + \theta_a \varepsilon_a^{\alpha} + \theta_{fw} \varepsilon_{fw}^{\alpha} + \theta_{bw} \varepsilon_{bw}^{\alpha}$$

* MERGEFORMAT (9)

where θ_s, θ_a, $\theta_{fw,}$ and θ_{bw} are volumetric fractions of solid-, air-, free-water- and bound-water-constituents, respectively. The permittivity of each constituent uses similar notation and α is a constant, which when $\alpha = 0.5$, yields a refractive mixing formula. Ignoring the bound water phase, one may also introduce the spectral properties of the free water phase dielectric permittivity, which consist of real and imaginary components, where the spectral signature of water accounts for frequency-dependent dielectric dispersion and imaginary losses (Dobson et al., 1985; Mironov et al., 2004).

Another category of physical models includes the use of simplified geometrical arrangement of soil constituents with varied assumptions (He and Dyck, 2013; He et al., 2016). Some of the widely used models are discrete ellipsoid models (de Loor, 1968; Sihvola, 2000), confocal models (Jones and Friedman, 2000; Sihvola and Lindell, 1990) and spherical models (Friedman, 1998; Miyamoto et al., 2005). The applicability of these models in frozen soil has been evaluated by He et al. (2015b). Note that specific knowledge of soil physical properties and volumetric fractions of soil components are required to use this type of calibration model (He et al., 2017).

3.1.2. TDR for Soil Moisture Profile Distributions

Spatial distribution of soil water content within the sampling volume is important for applications such as soil water management (Fares and Polyakov, 2006; Hatfield et al., 2017; Rousseva et al., 2017), irrigation scheduling and runoff/erosion/flood forecasting. The spatial distribution of soil water content can be obtained by three approaches:

(1) multiple vertical TDR probes of varying lengths or multiple horizontal TDR probes at different depths (**Fig. 7A**). For the vertical deployment, the rod length of the TDR probe should be equal to the targeted soil depth investigated. Average soil water contents of specific soil layers with defined depths can be determined by measurements each probe directly and by the using length-weighted differences of water contents determined by the TDR probes. TDR probes can be horizontally inserted at various depths to estimate water content at each depth;

(2) a single TDR probe with a special discontinuity designed (Topp and Davis, 1981), which functions in a similar way to multiple horizontally inserted TDR probes (**Fig. 7B**); and

(3) numerical inversion methods to reconstruct a soil water profile along a single TDR probe (**Fig. 7C**). The first two approaches are generally based on the average soil water content of the sampling volume and the mathematical models in **section 3.1.1** have to be used. The third approach is based on the extraction of information from the TDR signal that varies along the TDR probes. TDR waveform inversion methods have been proposed to estimate the soil moisture profile distribution along the TDR probe (Greco, 2006; Greco and Guida, 2008; Laloy et al., 2014; Oswald et al., 2003).
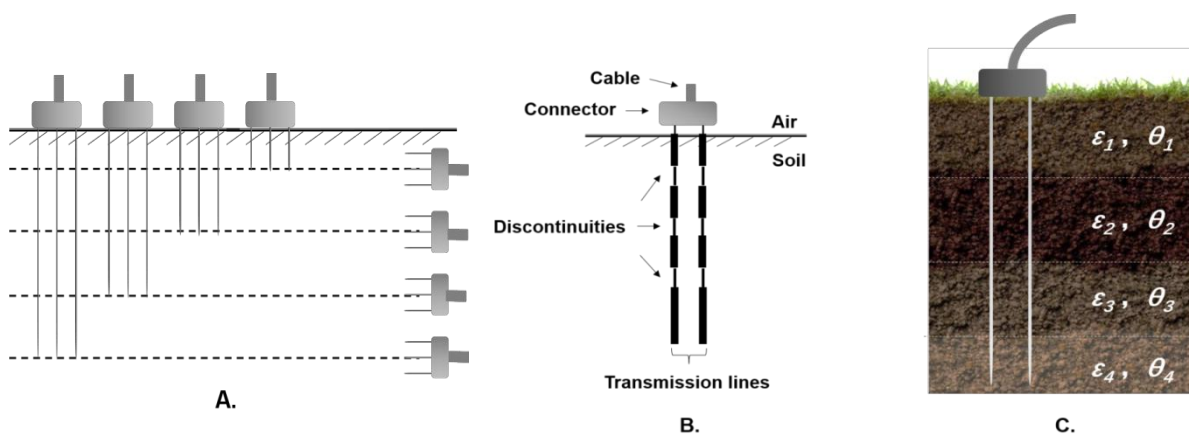

Fig. 7. Spatial profile of soil water content measurement with TDR: (A) multiple TDR probes for different depths; (B) segmented TDR/TDT (time domain reflectometry/transmission with discontinuities), after **Topp and Davis (1981), Persson and Dahlin (2010), Adelakun and Sri Ranjan (2013) and Kafarski et al. (2019)**; (C) spatial TDR with inverse modeling method.

Oswald et al. (2003) investigated the use of a single TDR probe to estimate the spatial variation of soil water content along the soil profile using an inverse profiling technique. Heimovaara et al. (2004) presented a different inversion approach, which integrated a multi-section scatter function model for the TDR system with the shuffled complex evolution Metropolis algorithm to estimate the soil water content profile. Later, Greco (2006) presented an inversion method based on the telegraph equation for estimating soil water content profiles under laboratory conditions, which was tested by Greco and Guida (2008) in the field:

$$\frac{\partial_i}{\partial_t} + \frac{1}{H(x)} \cdot \frac{\partial_V}{\partial_x} + \frac{R(x)}{H(x)} i = 0 \qquad \text{* MERGEFORMAT (10)}$$

$$\frac{\partial_V}{\partial_t} + \frac{1}{C(x)} \cdot \frac{\partial_i}{\partial_x} + \frac{G(x)}{C(x)} \cdot V = \delta(x - \tilde{x})(1 - e^{-\beta t}) \qquad \text{* MERGEFORMAT (11)}$$

The method by Greco (2006) illustrates an electromagnetic pulse propagation along a uni-dimensional TDR transmission rod in terms of electrical current $I(x,t)$ and electrical voltage $V_{(x,t)}$ that are associated with resistance (R), inductance (H), transverse conductance (G) and capacitance (C) of the transmission rod unit length. In the equation, both R and H are constant for a given probe, while $C_{(x)}$ and $G_{(x)}$ depend on the relative permittivity $K_{a(x)}$ and the bulk electrical conductivity $\sigma_{(x)}$, and both of the parameters are in turn related to the water content profile $\theta_{v(x)}$. The proposed inverse profiling technique produces good estimations of water content profiles, but accuracy is reduced by the presence of heterogeneous soil layers.

The inversion profiling techniques were further improved with innovative mathematical methods that enabled estimations of soil water profiles at a

higher-resolution (Laloy et al., 2014; Mboh et al., 2011; Oswald et al., 2003). The inverse methods face several challenges, such as the accuracy of the wave propagation model, the non-uniqueness of the inverse solution, the temperature dependence of the cable properties, while both water content and salinity influences on the TDR waveform as discussed in **section 2.4** (Laloy et al., 2014; Persson et al., 2000).

3.1.3. *Liquid Water Content and Density of Snow*

Liquid water content (also usually referred as snow wetness) and density of snow are essential information for many snow hydrological applications, such as avalanche warning, flood prediction, optimization of hydro- power generation and investigations of glacier melting due to global warming. Techniques used to determine liquid water content of snow include destructive methods (e.g., centrifugal separation, melting calorimetry, freezing calorimetry and dilution method) and non-destructive methods (e.g., capacitance technique and snow pillow) that are time-consuming and laborious (Stein and Kane, 1983; Stein et al., 1997). Stein et al. (1997) calibrated the TDR method for an in-situ measurement of snow liquid water content by relating snow liquid water content to permittivity and snow density. They proposed an equation to determine the density of dry snow, ρ_{snow} (g cm^{-3}), from TDR measured permittivity of snow, $K_{a,\,snow}$

$$\rho_{snow} = 0.61(K_{a,snow} - 1) \text{ \textbackslash* MERGEFORMAT (12)}$$

Similarly, an empirical relationship was established between snow wetness, θ_{snow} and $K_{a,\,snow}$

$$\theta_{snow} = 1.1 K_{a,snow}{}^2 \qquad \text{\textbackslash* MERGEFORMAT (13)}$$

Lundberg (1997) compared the TDR method with the dilution method, and their results demonstrated that the TDR method estimate θ_{snow} with 1-2 vol.% error when changes in snow density were small. However, they also pointed out that determination of density was required when ρ_{snow} changed greatly.

3.1.4. Tree Trunk Water Content

Gibbs (1930) demonstrated a seasonal variation in tree stem water content (θ_{stem} = volume of water/total volume of stem), also referred to as stem relative water content (Malavasi et al., 2016). θ_{stem} varied with xylem water potential, and different environmental factors including soil water status, climatic conditions or present tree disease. Reynolds (1965) showed that stem water storage ($\theta_{storage}$) of large Douglas firs contributed significantly to daily transpiration during high evaporative demand periods. Calculations of Waring and Running (1978) indicated that an equivalent of about 22 mm water was stored in the sapwood of older Douglas fir trees. Stem water changes in various tree species, including maple, pine, birch, oak, and gum under different growing and climate conditions, were also reported (Clark and Gibbs, 1957; Jackson et al., 1995; Waring et al., 1979; Wullschleger et al., 1996). In addition, stem water content could help to characterize plant water relationships, schedule irrigation, help with watershed management, and forest ecology (Constantz and Murphy, 1990; Fernández, 2017). These pioneering studies indicated the importance of quantifying stem water content/storage.

Methods, including the dendrometer (Turcotte et al., 2011), coring and gravimetric analysis (Clark and Gibbs, 1957; Waring and Running, 1978; Waring et al., 1979), gamma-ray attenuation (Brough et al., 1986; Edwards and Jarvis, 1983), MRI-nuclear magnetic resonance imaging (Choat et al., 2010; De Schepper et al., 2012; Reinders et al., 1988a; Reinders et al., 1988b; Windt et al., 2009), X-ray computer tomography (Raschi et al., 1995), stem diameter transduction (Cuevas Sánchez and Fernández Luque, 2010), ultrasonic echo detection (Lyu et al., 2016), TDR (Dahlen et al., 2015; Hernández-Santana and Martínez-Fernández, 2010; Irvine and Grace, 1997; Nadler et al., 2003; Wullschleger et al., 1996), FDR-frequency domain reflectometry (Beedlow et al., 2017; Holbrook et al., 1992; Kumagai et al., 2009; Zhou et al., 2018), and heat tracer methods (Trcala et al., 2015), were demonstrated to determine stem water content/storage. More details about the pros and cons of the approaches to the measurement can be found in Malavasi et al. (2016).

Among the methods mentioned, TDR provides a rapid, automated, in situ and low impact approach for measuring stem water content in living trees. Theoretically, TDR can be applied to moisture measurement in any porous material that contains water, including plant stems or tree trunk, because the permittivity of water is much larger than most other natural materials including tree stems. Measurements show that TDR is capable of estimating stem water content (at different time scales) across a range of tree water status.

Constantz and Murphy (1990) were among the first to apply TDR to measure daily and seasonal changes in stem water content of living trees. They developed an empirical calibration relationship equation between stem water content and permittivity determined by TDR for a range of tree species (i.e., an English walnut trees (*Juglans regia*) and ten evergreen and deciduous trees). Based on the study of Constantz and Murphy (1990), Wullschleger et al. (1996) produced a calibration relationship equation based on a larger data pool:

$$\theta_{stem} = 0.251 + 4.66 \times 10^{-2} K_{a,stem} - 4.93 \times 10^{-4} K_{a,stem}^2 \quad \backslash^* \text{ MERGEFORMAT (13)}$$

There is no universal calibration curve available to estimate stem water content of all tree species (Hernández-Santana and Martínez-Fernández, 2010). Accordingly, numerous studies were conducted on varying tree species, proposing species-specific calibrations to accurately measure the stem water content of a specific tree (Hernández-Santana and Martínez-Fernández, 2010; Irvine and Grace, 1997; Sparks et al., 2001; Topp et al., 1980). In addition, trees may be subject to freezing stress during winter with phase change of tree trunk water to ice, which may impede tree growth. Knowledge of both liquid water content and total water content are needed to calculate the ice fraction to assess the ice formation in stem during winter season and to develop anti-freezing strategies (Sparks et al., 2001; Sun et al., 2019).

3.1.5. *TDR Applications in Food Science, Engineering and Geophysics*

Water content significantly affects the storability and the quality of agri-food products, and TDR has been used widely to determine water content of various agri-food products (Kraszewski and Nelson, 2004), including meat (Fulladosa et al.,

2013; Rubio et al., 2013), fruit (Nelson and Trabelsi, 2008), honey (Puranik et al., 1991), liquids/oil (Ragni et al., 2012), grain seeds or flour (Cataldo et al., 2017; Cataldo et al., 2010; Yasunaga et al., 2009). The following equations have been proposed for a conventional two-rod probe in corn flour (Cataldo et al., 2010)

$$\theta_v = -0.158 + 0.0962K_a - 0.0089K_a^2 + 0.0004K_a^3 \ , R^2 = 0.964 \text{* MERGEFORMAT (14}$$

in corn (Cataldo et al., 2010)

$$\theta_v = -0.4694 + 0.393K_a - 0.0916K_a^2 + 0.0079K_a^3 , R^2 = 0.971 \text{ * MERGEFORMAT (15}$$

in bran (Cataldo et al., 2010)

$$\theta_v = -0.0509 + 0.0116K_a + 0.0224K_a^2 - 0.0028K_a^3 , R^2 = 0.981 \text{ * MERGEFORMAT (16}$$

in rough rice (Cataldo et al., 2010; Yasunaga et al., 2009)

$$\theta_v = 0.2780 \ln K_a - 0.1969 , R^2 = 0.983 \text{* MERGEFORMAT (17)}$$

Fiala et al. (2014) used the Malicki et al. (1996) model to measure water profiles in cellular concrete. Pavlik et al. (2008) and Cataldo et al. (2018) applied TDR to measure water content of construction materials and proposed the following calibration equations for sand

$$\theta_v = -0.06116 + 0.02504K_a , R^2 = 0.989 \text{* MERGEFORMAT (18)}$$

grey cement,

$$\theta_v = -0.43724 + 0.18850K_a - 0.02090K_a^2 + 0.00086K_a^3 , R^2 = 0.976 \text{* MERGEFORMAT (}$$

and for white cement

$$\theta_v = -0.28450 + 0.11403K_a - 0.01036K_a^2 + 0.00034K_a^3 , R^2 = 0.980 \text{* MERGEFORMAT}$$

Similarly, Suchorab et al. (2018) used a non-invasive surface TDR probe to detect aerated autoclaved concrete, and proposed the following expression for rigid building material (e.g., $2 < K_a < 12$)

$$\theta_v = -0.1956 + 0.0691 K_a - 0.0017 K_a^2 \quad , R^2 = 0.986 \backslash* \text{ MERGEFORMAT (21)}$$

Equations ~ were slightly different from the original equation of (Yasunaga et al., 2009), because the unit has been converted from % to cm^3 cm^{-3}. A comparison of these eight equations (**Fig. 8**) shows considerable differences among different materials, which indicates material specific calibration may be required.
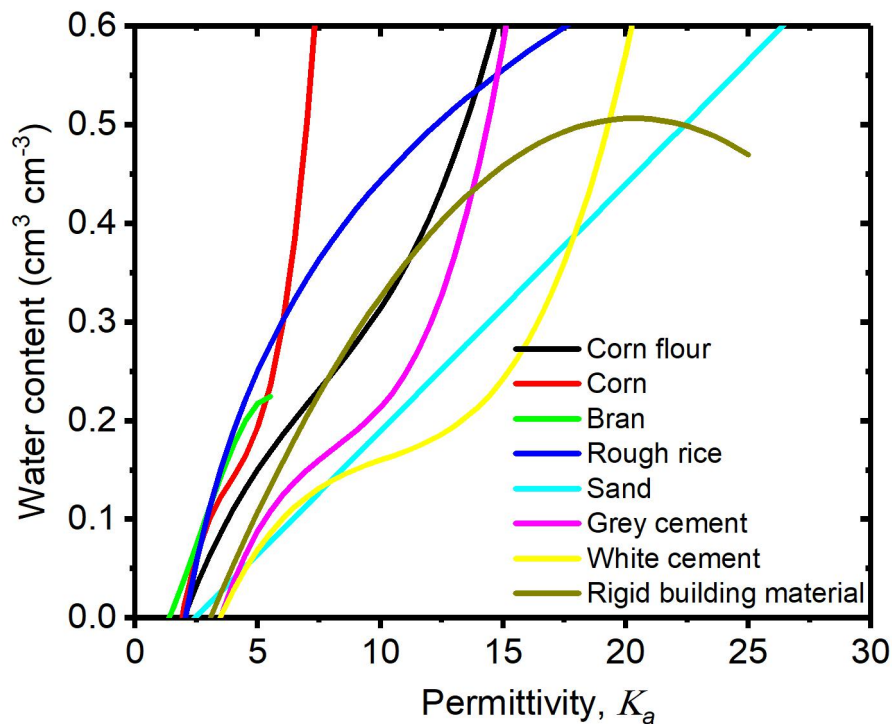
Fig. 8. A comparison of TDR calibration curves for agri-foods and construction materials with Eqs. ~.

3.2. Waveform analysis to determine porous media processes

3.2.1. Electrical Conductivity (EC) and Solute Transport

Estimation of EC can be obtained by either graphical method s or modelling methods. Graphical methods are based on interpretations of the TDR waveform (see section 2.4.2), while modelling methods are based on an inverse analysis of a TDR waveform using physically-based models as stated in **Section 3.1.1**. In the modelling method, the TDR signal is the transient response of the cable-probe-soil set to the

cable tester excitation signal. The estimation of EC from a TDR signal relies on a numerical inversion method that searches for the EC values that minimize the root mean square error obtained from the comparison of the measured and calculated TDR signals.

The TDR's applicability to simultaneously measure soil water content (θ_v) and soil apparent electrical conductivity, σ_s, of the same soil sample contributes to its usefulness to study solute transport in soils (Kargas et al., 2017; Persson et al., 2000). Kachanoski et al. (1992) proposed a TDR method to measure the solute travel-time density functions, $F_L(T)$ to characterize solute transport. Their findings showed that the TDR estimated σ was related to the total specific mass of the added solute tracer between the TDR transmission lines at constant soil volumetric water content, and that there was a linear relationship between the σ_s variation with time and the mass flux of the solute past the rod ends of the TDR probe. Noborio et al. (2006) extended the method of Kachanoski et al. (1992) to measure the solute travel time probability density function, in-situ under transient field conditions using a vertical TDR probe of length. Several studies were performed (Mallants et al., 1996; Nissen et al., 2000; Persson et al., 2000; Stahli and Stadler, 1997; Wraith, 2003; Wraith et al., 1993) to investigate solute transport in soils, or to determine solute transport properties in laboratory soil columns and in field soil.

3.2.2. Locating Wetting/Drying Fronts

Topp et al. (1982a) tested the use of TDR to locate a wetting front, namely, the interface between a wet and a dry soil layer. The underlying reasoning is that the

sudden change of soil water content along the TDR probe results in an amplitude or voltage change in the TDR waveform as illustrated in **Fig. 9** (Topp et al., 1982b). The amplitude change can be quantified as the reflection coefficient R:

$$R = \frac{\sqrt{\varepsilon_{dry}} - \sqrt{\varepsilon_{wet}}}{\sqrt{\varepsilon_{dry}} + \sqrt{\varepsilon_{wet}}} = \frac{\sqrt{f(\theta_{dry})} - \sqrt{f(\theta_{wet})}}{\sqrt{f(\theta_{dry})} + \sqrt{f(\theta_{wet})}}$$

* MERGEFORMAT (22)

where ε_{wet} and ε_{dry} denote the permittivity in the wet and dry soil layers, respectively; θ_{wet} and θ_{dry} denote the water content of the wet and dry soil layer, respectively.
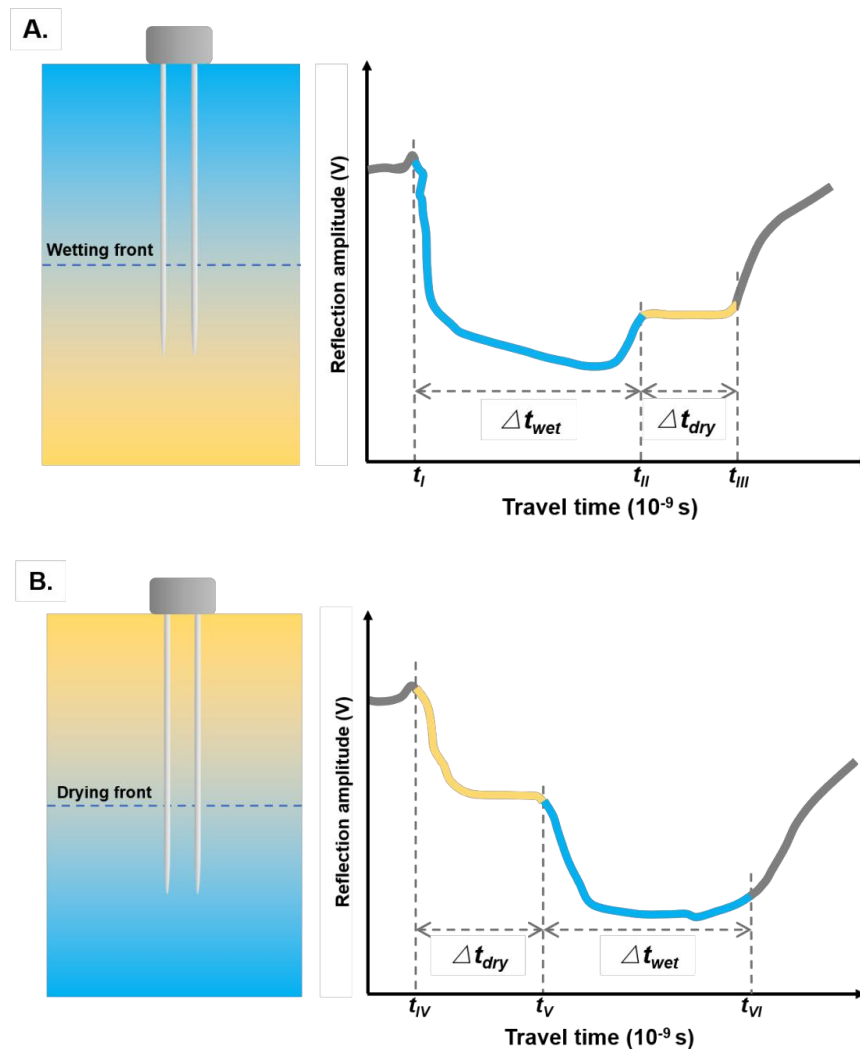

Fig. 9. Examples of TDR waveforms that indicate (A) a wetting/drying front or (B) wet/dry layers, adapted from Topp et al. (1982a).

During a soil wetting process, the wetting front can be easily located by estimating the depth of the wet layer from the transmission time of the EM pulse (see **Fig. 9A**):

$$L_{wet} = L - L_{dry} = L - \frac{ct_{dry}}{2\sqrt{\varepsilon_{dry}}} \text{ \textbackslash* MERGEFORMAT (23)}$$

where L_{wet}, L_{dry} and L denote the thickness of the wet layer, dryer layer and length of the transmission line, respectively; t_{dry} represents the two-way transmission time of the EM pulse in the dryer layer.

Topp et al. (1982a) demonstrated that TDR-measured average water content along a TDR probe was the sum of the depth weighted water content of each layer.

$$\bar{\theta} = \sum_{i=1}^{n} z_i \theta_i \bigg/ \sum_{i=1}^{n} z_i \quad \text{\textbackslash* MERGEFORMAT (24)}$$

where n is the number of soil layers; Z_i is the thickness of the ith layer, and θ_i is the volumetric water content of the ith layer.

Topp et al. (1982b) demonstrated that TDR was able to profile soil water content in the 0-1.2 m layer. Dasberg and Hopmans (1992) showed that Eq.   could be used to estimate water contents in a layered soil. However, difficulties in interpreting the TDR waveform were found when a very wet layer was overlying a very dry soil layer. Several researchers used TDR to measure wetting fronts (Germann, 2017; Noborio et al., 1996a; Overduin et al., 2006; Robinson et al., 2005a; Robinson et al., 2003b).

3.2.3.   *Measurement of Local-Scale Soil Water Flux with Vertical TDR Probes*

3.2.3.1. *One-dimensional, Transient Vertical Soil Water Flux*

Parkin et al. (1995) and Si and Kachanoski (2003) developed at TDR method to measure transient soil water flux under quasi-steady surface water applications. TDR probes of length, L (m), were installed vertically at the soil surface (z = 0) such that the TDR probe spanned a depth from soil from the surface (z = 0), to a depth of L m below the surface. A quasi-steady water flux was applied to the soil surface. As the wetting front moved through the depth of soil spanned by the TDR rods, the average water content ($\widehat{\theta}_L$; m^3 m^{-3}) measurements from the vertical TDR probes can be used to determine water storage along the length of the probe with time (Si and Kachanoski, 2000a):

$$W_L(t) = \widehat{\theta}_L(t)L \qquad \backslash\text{* MERGEFORMAT (25)}$$

where W_L (t) (m^3 m^{-2}) is the soil water storage in the depth interval, [0, L] as a function of time (s).

The TDR-measured W_L (t) was linked to local, transient soil water flux through the one-dimensional continuity equation for conservation of mass:

$$\frac{d\theta}{dt} = -\frac{dq_w}{dz} \qquad \backslash\text{* MERGEFORMAT (26)}$$

where q_w is the local, vertical soil water flux (m^3 m^{-2} s^{-1}). Integrating both sides of the continuity equation with respect to depth, z, between the depths spanned by the TDR probe (z = 0, z = L), yields:

$$\frac{d}{dt}\int_0^L \theta\, dz = -\int_0^L \frac{-dq_w}{dz} dz \rightarrow \frac{dW_L(t)}{dt} = q_w(0) - q_w(L) \backslash\text{* MERGEFORMAT (27)}$$

where $q_w(0)$ and $q_w(L)$ are the vertical soil water flux at depths z = 0 and z = L, respectively.

Under the field conditions described in Parkin et al. (1995) and Si and Kachanoski (2000a), root water uptake, and surface evaporation were reasonably

assumed to be negligible. Further at early times, when the wetting front is between depths z = 0 and z = L, it was reasonably assumed that $q_w(L) = 0$. Finally, it was assumed that, even though soil pores are tortuous and water from outside of the sampling volume of the TDR probe may enter and leave the sampling volume during infiltration, the change in TDR-measured soil water storage with respect to time represents the average (effective) vertical soil water flux through the soil from the soil surface to the depth of the wetting front:

$$q_{w|0} = \frac{dW_L(t)}{dt} \qquad \backslash* \text{ MERGEFORMAT (28)}$$

This method was later extended by Dyck and Kachanoski (2009a) to measure the vertical transient soil water flux within two depth intervals ($[0,L_A]$ and $[L_A,L_B]$) representing the A and B soil horizons.

The abovementioned TDR methods for transient soil water flux measurement were coupled with analytical solutions to the 1D and 2D, Richards Equation for constant flux surface boundary conditions as a means of in-situ soil hydraulic property estimation and further understand the physics of water flow under transient conditions in the field.

Parkin et al. (1992), Parkin et al. (1995), Si et al. (1999) and Si and Kachanoski (2000a) demonstrated that TDR-measured $W_L(t)$, as described above. were consistent with predictions of the 1D analytical solutions of White and Broadbridge (1988), Parkin et al. (1992) and Si and Kachanoski (2000b). Further, through inverse procedures, soil hydraulic properties for the soil spanned by each individual TDR probe could be estimated as the optimized analytical solutions parameters that

provided the best fit of the analytical solutions to the TDR-measured $W_L(t)$. Implementation of field experiments with many vertical TDR probes along transects allowed for further contributions to quantification and understanding the spatial variability and scale-dependence of soil hydraulic properties and transient soil water flux (Si et al., 1999) and hysteresis (Si and Kachanoski, 2003).

The extension of the methodology to the measurement of soil water flux within 2 overlying horizons at the same spatial location by Dyck and Kachanoski (2009a) provided insight into the complex physics of wetting fronts as they cross soil horizon interfaces. In Dyck and Kachanoski (2010), spatial patterns of A and B horizon transient stream tube soil water flux were measured under four different quasi-steady surface water application rates. The scale-dependent vertical continuity of soil water flux across the A–B horizon interface was quantified with Fourier-domain coherency spectra. Comparison of the A and B horizon fluxes across and within different water application rates revealed a loss of coherency between A and B horizon water flux with increasing flow rate between spatial scales of 1.0 to 6.75 and 0.38 to 0.50 m. The flux- and scale-dependent behavior of the horizon interface is probably the outcome of: (1) convergence of the pattern of preferred flow domains in the A horizon to the spatial pattern of the saturated hydraulic conductivity of the A horizon with increasing water application rate; and (2) increased modification of the A horizon soil water flux pattern as the wetting front moves across the soil horizon interface. The results of this study indicate that the pedon, like the representative elementary volume (REV), is hydrologically significant.

3.2.3.2.. Steady-state Vertical Soil Water Flux and Solute Transport

Continuing with the case of vertical TDR probes spanning the surface depth interval, [0, L], Si and Kachanoski (2003) assumed steady-state flow commenced once the wetting front moved past the end of the TDR probe and the TDR-measured $W_L(t)$ maintained a constant value. Following establishment of steady-state flow conditions, the EC of the water applied at the soil surface was changed through application of water spike with a conservative solute (step application of Cl- or Br-). Under steady water flow and water content ($\hat{\theta}_L$), Si and Kachanoski (2003) demonstrated a linear relationship between TDR-measured apparent electrical conductivity (ECa) and the conservative solute mass within the measurement volume of the TDR probe as a function of time as the solute front travels vertically through the soil:

$$q_{s|0} = \frac{dS_L(t)}{dt} = \hat{\theta} L \frac{dECa(t)}{dt} \text{ \\* MERGEFORMAT (29)}$$

where $q_{s|0}$ is the surface convective solute flux (kg m^{-2} s^{-1}), and S_L(t) is the solute mass (kg m^{-2}) in the depth interval, [0, L] which is equal to $\hat{\theta}_L \cdot ECa$ under the assumption of a linear relationship between applied conservative solute concentration and TDR-measured ECa.

Given the following relationship between soil water flux and convective solute flux,

$$q_{w|0} = \frac{q_{s|0}}{C_0} \text{ \\* MERGEFORMAT (30)}$$

where C_0 is the concentration (kg m^{-3}) of the conservative solute in the step application of solute, the following expression for TDR-measured, steady-state soil water flux was derived:

$$q_{w|0} = \frac{\hat{\theta} L}{EC_{a|L}(t_F) - EC_{a|L}(t_i)} \frac{dEC_{a|L}(t)}{dt} \text{ \\* MERGEFORMAT (31)}$$

where $EC_{a|L}(t_F)$ and $EC_{a|L}(t_i)$ are the TDR-measured EC_a after the solute front has passed the end of the TDR probes (t_F), and prior to solute application (t_i), respectively, and $\frac{dEC_{a|L}(t)}{dt}$ is the changed in EC_a with respect to time between times t_i and t_F.

An implicit assumption associated with Eq.   is that the distribution of the tracer within the measurement volume of the TDR probe (i.e., mobile or immobile water), does not significantly influence ECa. Another assumption is that the contribution of diffusive/dispersive solute flux is negligible compared to convective flux.

Although the above theory is for 1D, vertical flow, Zhang et al. (2000a) and Zhang et al. (2000b) used vertical TDR probes to measure the vertical component of two-dimensional, steady-sate soil water flux directly beneath a quasi-steady line source. Further Dyck and Kachanoski (2009b) extended the method for measurement of 1D, vertical steady state soil water flux within two depth intervals ([0, L_A] and [L_A, L_B]) representing the A and B soil horizons.

Like the transient flux method (**section *3.2.3.1***), under steady-state conditions, the steady-state soil water flux is equal to the soil hydraulic conductivity at the TDR-measured water content. If many vertical TDR probes and multiple water application rates are deployed, it was demonstrated that the field-average soil hydraulic conductivity curve can be measured *in-situ* (Si and Kachanoski, 2003). Further, Zhang et al. (2000a) and Zhang et al. (2000b) demonstrated consistency of TDR-measured vertical, steady-state soil water flux with the vertical component of 2D, steady-state soil water flux predicted by 2D solutions to the steady-state version of the Richards equation with a line source surface boundary condition.

Implementation of inverse procedures, allowed the best fit parameters of 2D solutions to the steady-state Richards Equation and soil hydraulic properties to be estimated (Zhang et al., 2000b).

The extension of the method for measurement of steady-state soil water flux within 2 overlying horizons at the same spatial location provided insights into the factors affecting the spatial variability and patters of steady state soil water flux at increasing soil depths. Through estimation of the multiple coherency spectra in the Fourier domain, Dyck (2008) showed that the spatial patter of the B horizon steady-state soil water flux was highly, significantly dependent on the spatial pattern of steady state water flux in the overlying A horizon and the spatial pattern of the curvature and depth of the A/B horizon interface. This result demonstrates the complex nature of the correlation between water flow and solute flux within local soil flow domains (i.e., stream tubes or REVs) not typically accounted for in numerical simulation models.

3.2.4. *Locating a Freezing/Thawing Front and Detecting Frost*

TDR can be used to demonstrate whether soil frost is present or not (i.e., some of the pore water in soils is frozen or not), because there exists a large difference in permittivity of ice at microwave frequencies (~3.2) and water (~80) (He and Dyck, 2013; Noborio, 2001). The change of permittivity at the interface of frozen (ice) and unfrozen layers (water) results in an electrical discontinuity that produces a distinct reflection in the TDR waveform (**Fig. 10**). Based on the principle for locating the wetting front as stated in **Section 3.2.2**, Baker et al. (1982) examined the use of TDR

to locate the interface between frozen and unfrozen soil layers (i.e., the freezing front). However, differing from the wetting-drying process, soil freezes from the top down in the field (**Fig. 10**A), but it thaws from top (ground surface) and bottom (deep unfrozen soils) (**Fig. 10**B), which leaves a frozen layer in the middle sandwiched between unfrozen layers (Christensen et al., 2013; He et al., 2015a).
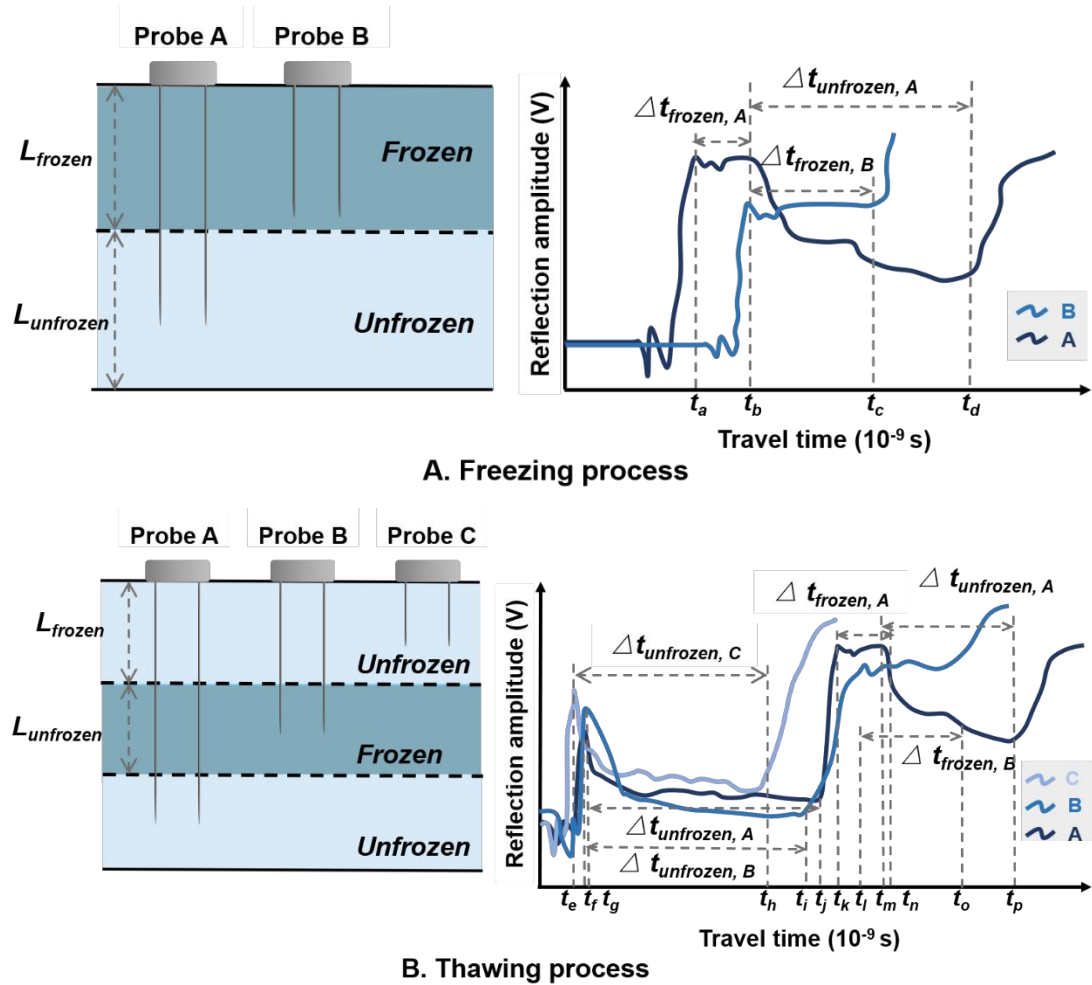

Fig. 10. Experimental layout used in freezing/thawing fronts detection: (A): freezing process and (B) thawing process, after Baker et al. (1982) and Chen and Horino (1998).

The frozen and unfrozen depths can be determined by (Chen and Horino, 1998)

$$L_{frozen} = \frac{ct_{frozen}}{2\sqrt{\varepsilon_{frozen}}} \qquad \text{* MERGEFORMAT (32)}$$

$$L_{unfrozen} = \frac{ct_{unfrozen}}{2\sqrt{\varepsilon_{unfrozen}}} \quad \text{* MERGEFORMAT (33)}$$

where L_{frozen} and $L_{unfrozen}$ indicate the thickness of the frozen and unfrozen layer, respectively; t_{frozen} and $t_{unfrozen}$ represent the return time of the EM pulse in the frozen and unfrozen layer, respectively. TDR has been used in several studies to determine frost depth (Baker et al., 1982; Chen and Horino, 1998; Hayhoe et al., 1983; Hirota et al., 2006; Kennedy and Sharratt, 1998; Overduin et al., 2006; Pilon et al., 1985; Rajaei and Baladi, 2015; Roberson and Siekmeier, 2000; Yami et al., 2012; Yanai et al., 2017). In general, results of these researches verified the reliability of TDR to locate the freezing front or to determine freezing depth. However, it should be noted that TDR probes inserted vertically from the surface may lead to preferential freezing of the surrounding soil due to the greater thermal conductivity of the stainless steel rods.

3.2.5. Hoarfrost and Dew Detection

Although frost damage on crops is attributed to hoarfrost formed on the surface of crops, hoarfrost or dew is usually observed by naked eyes. Thus, temporal monitoring hoarfrost or dew formation has not been available. Kato et al. (2020) reported that TDR successfully detected differences between dew and frozen dew with an etched-print-circuit-board probe in the controlled environment (**Fig. 11**). Dew and frozen dew are composed of the combination of liquid water and air, or that of ice and air, respectively that has distinct permittivity (Noborio, 2001). Later year in the field, Shibuya et al. (2020) detected dew, frozen dew, and hoarfrost under different weather conditions using TDR techniques. With time-series data on environmental factors and

TDR-measured hoarfrost, Ding et al. (2019) reported that machine learning techniques enabled hoarfrost forecast three-hour in advance.

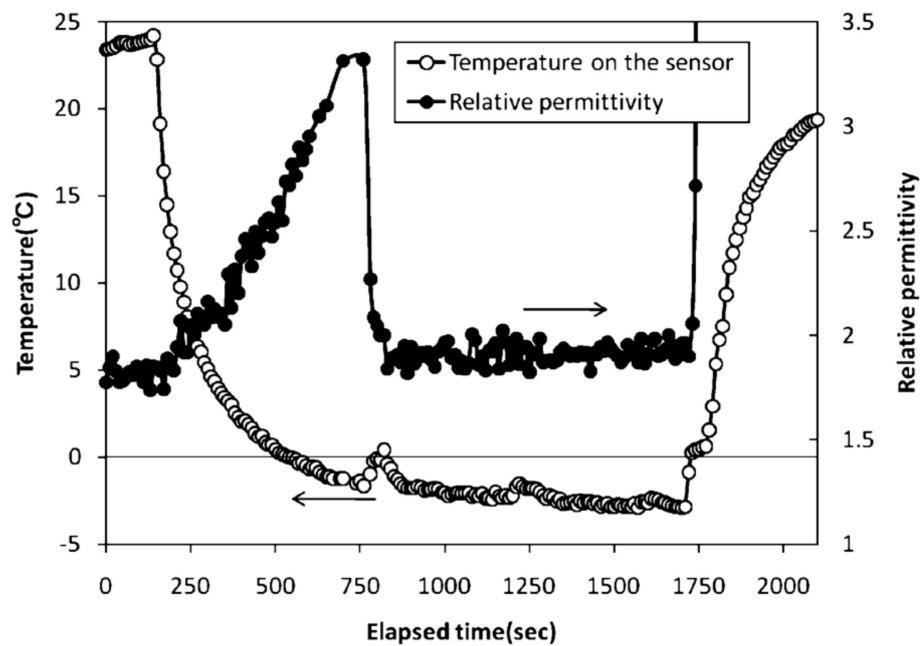**Fig. 11.** Temporal changes in dielectric constant detecting formation of dew and frozen dew as temperature at the TDR probe decreases to subzero (**Kato et al., 2020**).

3.2.6. *Determination of Snow Depth*

Knowledge of snow wetness or the liquid water content of snow (θ_{snow}), snow density (ρ_{snow}) and snow depth (L_{snow}) is of great importance for avalanche control, snowmelt simulation, runoff modeling and flooding forecast. The most commonly used snow survey is laborious, time-consuming and destructive. Many techniques have been developed (Sturm and Holmgren, 2018), but few methods are available to make continuous, multiple-point, rapid, accurate and non-destructive measurements at low cost. Similar to methods used to locate wetting/drying and freezing/thawing fronts, the TDR can theoretically be applied to measure snow depth, because of the difference in permittivity between air and ice- water-air mixtures. However, TDR has not yet been used to detect snow depth. There are studies that use ground penetrating

radar (GPR) to estimate snow depth (Marchand et al., 2001). Measurements of snow depth with GPR are based on the travel time characteristics of EM waveforms, which is similar to TDR.

Snow depth measurement with the GPR technique is based on the determination of the two-way travel time, t, of the electromagnetic (EM) propagating speed, V_{GPR}, in snow. $L_{snow} = t\ V_{GPR}$ However, this method is limited to snow with uniform density. Unreasonable snow depth measurement may be encountered in layered snowpack because of the less sensitivity of the GPR (Paolo et al., 2015; Previati et al., 2011). Recent studies combined GPR techniques and TDR measurements to obtain more accurate snow depth and density at a greater scale (Paolo et al., 2015). The TDR measurements were performed to estimate the speed of the EM wave (V_{TDR}). This is more accurate than the V_{GPR} (Paolo et al., 2015). The calibrated snow depth is therefore calculated by $L_{snow} = t\ V_{TDR}$.

3.2.7. Determination of Water Depth or Water Level

Moret et al. (2004) evaluated the use of a vertical coated TDR probe of length L immersed in a water column to estimate the water depth or water level (L-x) in a Mariotte tube. The water level is calculated according to (Fatás et al., 2013)

$$x = L\frac{\sqrt{\varepsilon_{eff}} - \sqrt{\varepsilon_w}}{\sqrt{\varepsilon_{air}} - \sqrt{\varepsilon_w}} \quad \backslash* \text{ MERGEFORMAT (34)}$$

where x is the probe length in air above the water level, K_a is the apparent permittivity measured by the TDR cable tester, and ε_{air} and ε_w are the relative dielectric permittivity values of air and water previously measured with the same probe,

respectively. From this perspective, TDR has the potential to measure water levels in rivers, channels, or from surface runoffs, and more studies on the influencing factors and their applicability are required. Cataldo et al. (2008b) and Cataldo et al. (2008a) used a similar approach to measure the level or depth of various liquids (e.g., de-ionized water, acetone, diesel oil and fuel) with 2~3% errors.

Yazaki et al. (2008) independently proposed the following equation to measure water depth, L-x, using a TDR probe installed upside down:

$$L - x = \left(\frac{L_a}{L}\right)\frac{L}{\sqrt{\varepsilon_w}} \qquad \backslash* \text{ MERGEFORMAT (35)}$$

where L_a is the apparent length between the entering location of the probe and the 1st reflection point. Equation   was valid for TDR probes with L between 10 and 20 cm. They showed a good agreement in water depths measured with a pressure transducer and TDR in a rice paddy field for about 60 d, as shown in **Fig. 12**
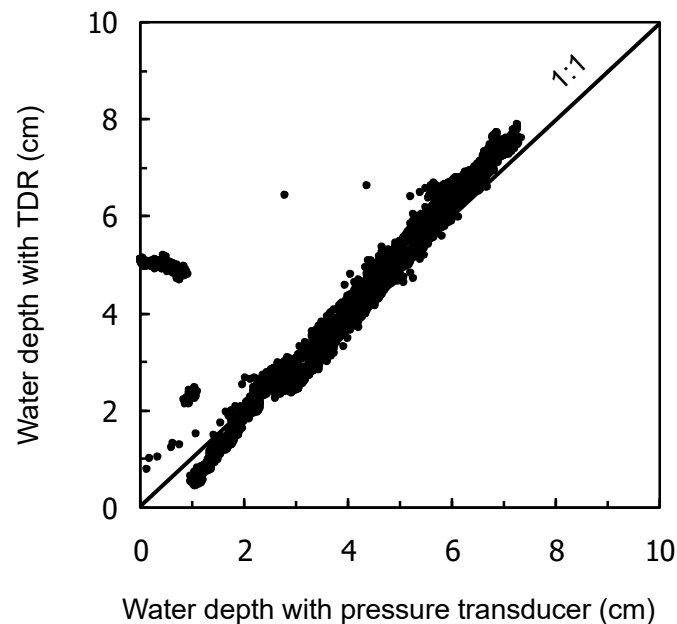

Fig. 12. Water depth measured with a pressure transduce and a 20cm-long 3-wire TDR probe in a rice paddy filed, after Yazaki et al. (2008).

Unlike the use of an open-ended TDR probes for water level measurements, Thomsen et al. (2000) developed a time domain transmission (TDT) probe to measure water depth and found it to provide comparable results to a commercial ultrasonic liquid level probe. Their new probe is actually similar to the TDT probe described by Blonquist et al. (2005) to measure soil water content, but it only has a single loop of transmission line. Similarly, an insulated coaxial cable can be used to measure water level and other characteristics (e.g., shear strength and pressure), as will be described in the next section.

3.2.8. *Detection of Rock or Soil Mass Deformation, Ground Water Level and Piezometric Pressure*

Instead of using several individual TDR probes, some geotechnical engineering applications use coaxial cable TDR systems with known crimp locations. The crimps provide permanent distance markers (e.g., rubber-insulated conductors) that allow the TDR system to be self-calibrating. The coaxial cable buried/grouted/submerged in a piezometer/borehole can be used to monitor the change of strength or pressure of its surroundings (**Fig. 13**). For instance, mechanical forces change the distance between distance markers of transmission lines, which in turn affect the spatial distribution of capacitance and inductance. These spatial variations result in partial reflections of an incident electrical step pulse from which physical parameter distributions along the inhomogeneous transmission line can be reconstructed. Therefore, TDR can be used to measure ground deformation (e.g., displacement along rock joints) (Dowding et al., 1989) and/or landslides (Drusa et al., 2013; Farrington and Sargand, 2006) at multiple

distinct locations along the coaxial cables grouted in a rock or soil mass. Coaxial cable based TDR and fiber optic based distributed temperature sensing methods are techniques available for monitoring rock/soil deformations at a field scale (Chai et al., 2004; He et al., 2018a; Kogure and Okuda, 2018).
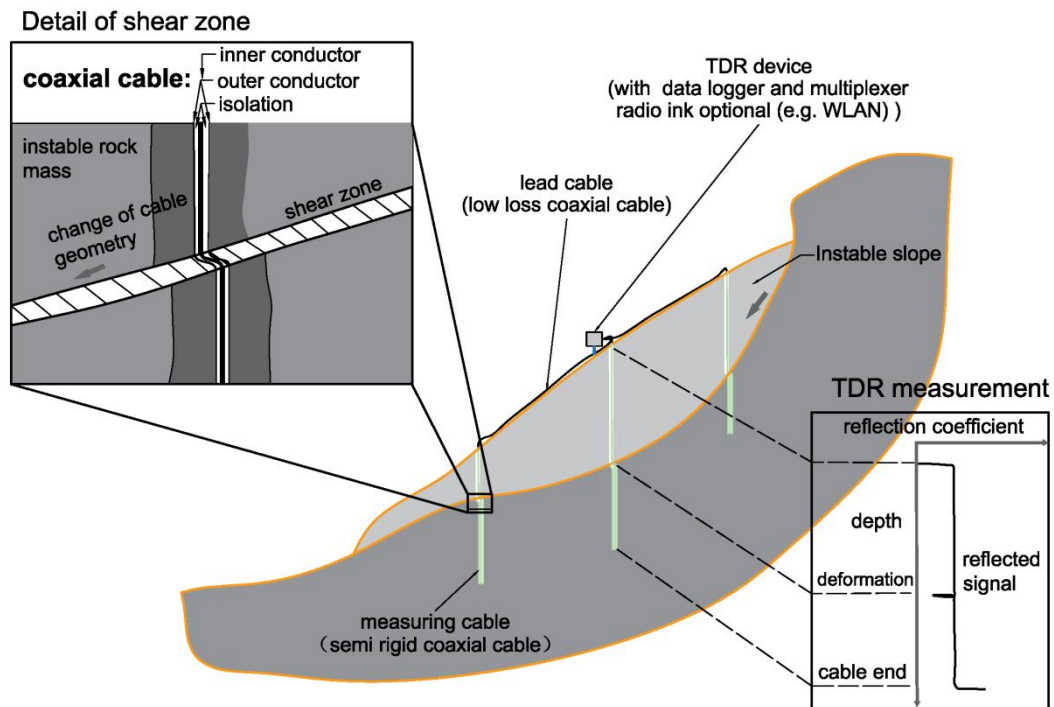
Fig. 13. Illustration of a TDR system to monitor slope movement at different locations along the slope with a closeup of the shear zone, the location of which can be identified as a signal reflection in the TDR waveform, after (Thuro et al., 2010).

The advantages of the TDR method for landslide monitoring, compared to traditional methods such as inclinometers, include being economical because of the low cost of coaxial cables and the multiplexing capability of the TDR system, in addition to the ease of installation and data collection as concluded by Sargand et al. (2004). While TDR could successfully detect the depth of shear plains, it is not able to provide direction of the movement and inferring the magnitude of the movement from the waveform is possible, though this is often a difficult task especially under field

conditions. More recommendations on coaxial cable selection and installation procedures as well as example waveform analyses for TDR slope stability monitoring can be found in the literature (Cortez et al., 2009; Kane, 2000; Sargand et al., 2004).

As an analog to the mechanical forces, a reflected voltage signal resulting from changes in impedance of the cable submerged in water can be used to measure groundwater levels and piezometric pressures (Chaney et al., 1996; Dowding and Huang, 1996). TDR is advantageous over downhole pressure transducers used in piezometers in that only small-size riser pipes (e.g., 12 mm inner diameter) are required, the installation is simple and no field calibration is required, good for long-term telemetric surveillance. Scheuermann and Hübner (2009) applied TDR to determine pressure profiles from the time-domain reflection data of transmission lines.

3.3. TDR Combined with Other Methods to Determine a Variety of Properties

In addition to the conventionally designed TDR probes, TDR has been combined with other techniques for simultaneous measurements of a wide range of soil physical properties. For instance: (1) the combination of a heat pulse probe and a TDR probe (e.g., Thermo-TDR probe) can simultaneously measure soil water content, water flux, soil temperature, electrical conductivity, thermal conductivity, thermal diffusivity, and volumetric heat capacity within the same sampling volume (He et al., 2018b; Ren et al., 1999); (2) the combination of porous material (e.g., gypsum or ceramic) and a coiled TDR probe can simultaneously measure soil matric potential and water content which comprises the soil water retention curve (Lungal and Si, 2008; Noborio et al.,

1999; Vaz et al., 2002); (3) newly designed TDR probes (e.g., hollow TDR probes combined with a tensiometer and solution extraction instruments, PVC tubes-coaxial cables based coil-type TDR, ceramic disks based three-rod TDR and apparatus combining TDR with remote switching diodes, and a TDR array with continuous rod pairs as probes) can be used for multipurpose measurements including, but not limited to, solute concentration, bedrock moisture, soil salinity, frost depth under pavements, and near-surface soil moisture profile (Baumgartner et al., 1994; Katsura et al., 2008; Moret-Fernández et al., 2012; Roberson and Siekmeier, 2000; Sheng et al., 2017); and (4) a spatial TDR based on the flat ribbon cables and inverse modeling of TDR waveforms can be used to determine water content and EC profiles along the needle of a TDR probe (Greco, 2006; Laloy et al., 2014).

3.3.1. *Thermo-TDR for Vadose Zone Measurements*

The heat pulse method, which is based on the line-heat source solution of the radial conduction heat transfer equation (Carslaw and Jaeger, 1959), is a transient method for determination of soil thermal properties and a range of other physical properties both in the laboratory and under field conditions (He et al., 2018b). A thermo-TDR device was first developed by combining a single-probe heat pulse probe with a conventional TDR probe to simultaneously determine θ_v and thermal conductivity (λ) (Baker and Goodrich, 1984; Baker and Goodrich, 1987). Noborio et al. (1996b) developed a 3-probe thermo-TDR probe (**Fig. 14**) with a central heater and two outer thermocouples, allowing for simultaneous determination of soil properties, including water content, EC, thermal conductivity, thermal diffusivity, and

heat capacity. Ren et al. (1999) re-designed the thermo-TDR probe to provide in situ, accurate and continuous measurements of θ_v, EC, thermal properties, bulk density, heat flux, liquid water flux, and vapor flux (Ren et al., 1999; Ren et al., 2003). The Thermo-TDR probe enables in-depth understanding of coupled heat and water transfer processes in the vadose zone (He et al., 2018b; Ren et al., 1999; Ren et al., 2003).
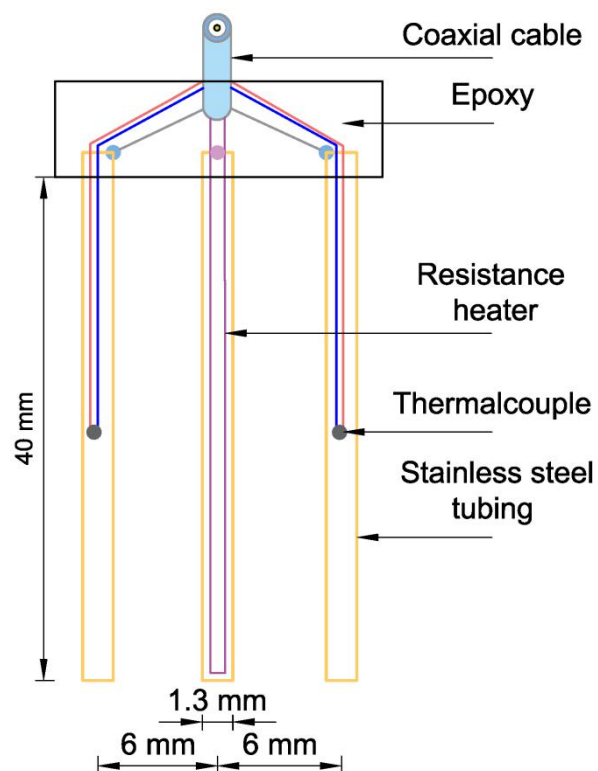
Fig. 14. Schematic of a thermo-TDR, which combines TDR and heat pulse methods. The middle needle functions as the central TDR and the heater of heat pulse method (containing a resistance heating wire); the two outer needles function as the TDR ground needles as well as the temperature sensing needles of the heat pulse method (each needle contains a thermocouple). The length of the needle ranges from 28 to 70 mm with a needle spacing of 6 - 10 mm.

3.3.2. *TDR- Matric Potential Probe to Determine Soil Water Retention Curves (SWRC)*

Soil water retention curves (SWRC), defined as soil water content as a function of soil matric potential (Ψ_m), is a critical soil hydraulic property. It is required to numerically simulate θ_v, water flow and solute transport, to schedule irrigation, and other soil and land management endeavors (Wraith and Or, 2001). A variety of direct measurement methods have been developed to measure SWRCs, including the hanging water column, pressure plate, tensiometers, centrifuge, dew point, thermal dissipation method, thermocouple psychrometer, VSA, and evaporation method (Cresswell et al., 2008; Dane and Hopmans, 2002; Klute, 1986; Romano and Santini, 2002; Scanlon et al., 2002). However, these methods vary in measurement range, accuracy, cost and portability. In situ, automatic and continuous measurement of SWRC is highly desirable, because dynamic changes in continuity of pore and pore-size distribution significantly affect the SWRC. Common ways to determine SWRC in situ requires paired water content and matric potential sensors. However, this approach suffers from errors associated with poor hydraulic coupling including unmatched spatiotemporal resolutions and incompatible measurement ranges. A probe that combines TDR with a tensiometer or with a fixed porous media (e.g., gypsum block or porous ceramics) enables the simultaneous, automatic and continuous in situ measurement of SWRC values (i.e., water content and matric potential) in the same volume.

Vaz et al. (2002) coiled copper wires around the ceramic cup of a tensiometer (for matric potential measurement) to function as TDR for θ_v measurement (**Fig. 15A**). Lungal and Si (2008) put a coiled TDR in a ceramic cup to make a coiled TDR matric potential probe (**Fig. 15B**). Whalley et al. (1994) and Baumgartner et al. (1994) used hollow stainless-steel tubes with a porous stainless-steel tip as TDR rods (**Fig. 15C**). The porous tip functioned as a tensiometer to measure soil water matric potential. The hollow TDR rod is connected with a pressure transducer system to measure the soil matric potential around the porous tip. However, Noborio et al. (1999) found that most of the TDR-matric potential methods were generally limited to the measurement range $\Psi_m > -0.085$ MPa. Therefore, Noborio et al. (1999) combined TDR with a porous ceramic block (dental plaster) to simultaneously estimate matric potential, based on the θ_v of the porous block, and θ_v of the soil (**Fig. 15D**). Their method extended the measurement range to $-1000 < \Psi_m < -10$ kPa. Or and Wraith (1999) arranged a set of commercially available porous ceramics plates along the axis of a TDR probe. More details of combined TDR with tensiometers or porous material are shown in **Table 4**.
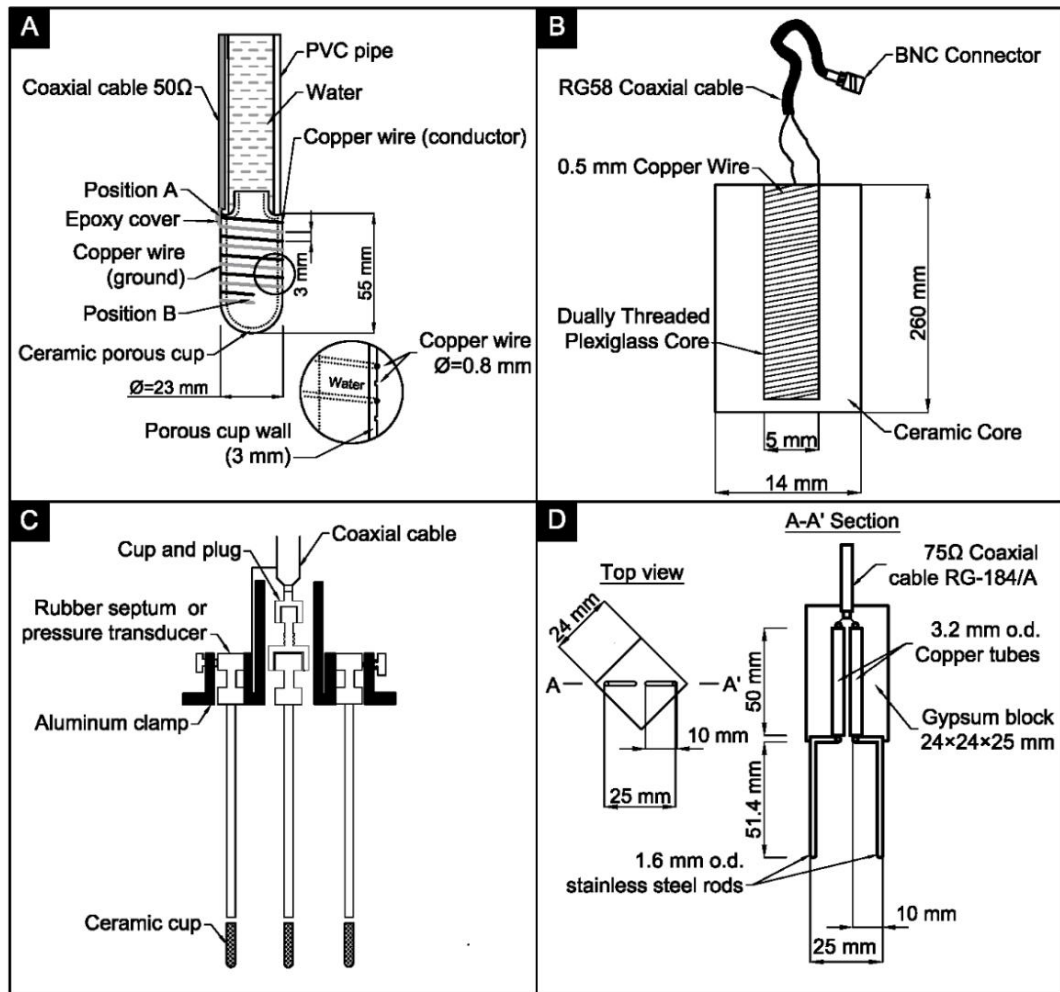
Fig. 15. Schematics of conjunct TDR with tensiometer and porous material for determination of soil water retention characteristics (A from **Vaz et al. (2002)**, B from **Lungal and Si (2008)**, C from **Whalley et al. (1994)** and D from **Noborio et al. (1999)**.

Table 4. Selected designs of time domain reflectometry (TDR) combined with matric potential probes

No.	Source	TDR design	Matric potential sensing	Notes
1	Baumgartner et al. (1994)	2 rods: hollow stainless steel tubes, 13.1 cm long, 3.9 mm i.d., 6.2 mm o.d.	Stainless steel porous cup + pressure transducer	Vacuum pump was used to sample water in the hollow tube
2	Whalley et al. (1994)	3 rods: hollow aluminum tubes,	Porous cup + rubber septum or pressure	/

| 3	Noborio et al. (1999)	2 stainless steel rods (1.6-mm diam., 25 mm apart and 51.4 mm long) soldered to 2 copper tubes (3.2-mm diam., 5 mm apart and 50 mm long)	Porous media (gypsum block)	/
4	Or and Wraith (1999)	3 rods: 150 mm long and 15 mm apart.	Porous ceramic and plastic disks	0 to -0.5 MPa
5	Wraith and Or (2001)	3 rods: 3.2-mm diam., 20 mm apart and 200 mm long	Previously characterized porous media (having similar pore-size distribution with soils under measurement)	Using paired TDR probes
6	Vaz et al. (2002)	Coiled TDR	/	/
7	Lungal and Si (2008)	Coiled TDR	Porous media (ceramics)	0 to -1.5 MPa
8	Moret-Fernández et al. (2008)	A zigzag copper rod (150-mm long, 2 mm diam.) vertically installed in a clear plastic cylinder, six vertical copper rods (60-mm long, 2 mm diam.) arranged around the inner wall of the cylinder.	Porous ceramic discs	0 to -0.5 MPa
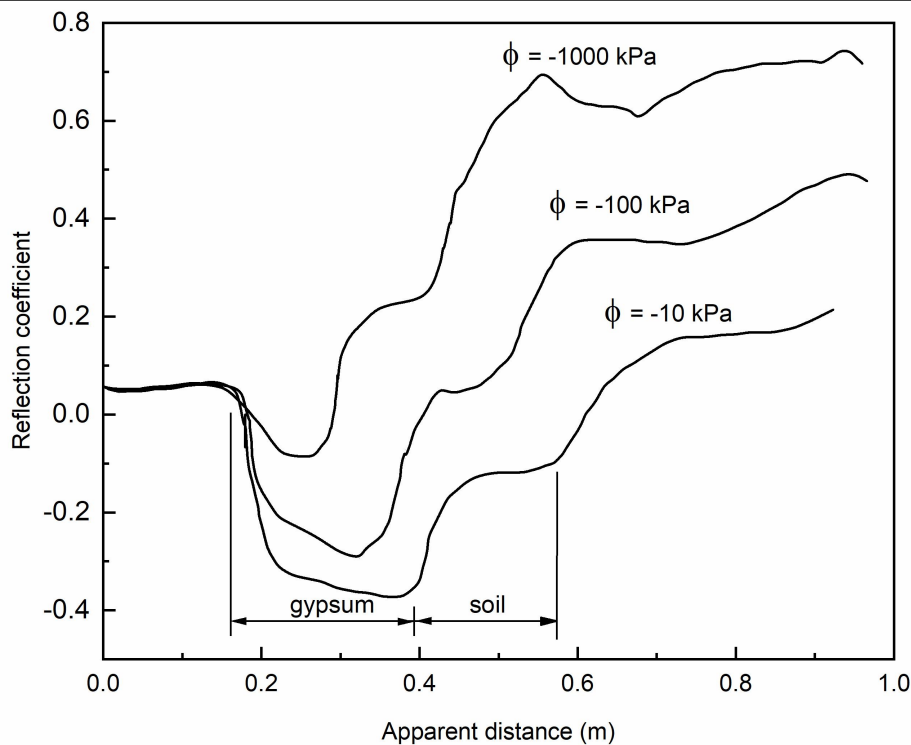
Fig. 16. TDR waveforms for the Noborio et al. (1999) probe.

The matric potential can be estimated from either permittivity or water content. Noborio et al. (1999) related TDR-measured permittivity of the gypsum to the soil water matric potential as:

$$\varepsilon_{gyp} = \varepsilon_{res} + (\varepsilon_{sat} - \varepsilon_{res}) \cdot \left[\frac{1}{(1 + |\alpha \cdot \psi_m|)^p} \right]^q$$

* MERGEFORMAT (36)

where ε_{gyp}, ε_{sat} and ε_{res} are permittivity of gypsum and permittivity at saturation and residual water contents, respectively; α, p and q are calibration constants. The dielectric constant of gypsum and soil were determined as:

$$\varepsilon_{gyp} = \left(\frac{L_a}{L} \right)^2 \quad \text{* MERGEFORMAT (37)}$$

where L_a is the apparent probe length and L is the probe length. The TDR waveforms at different matric potential values are shown in **Fig. 16**. Noborio et al. (1999) showed that the Ψ_m-θ relationship determined by the TDR probe embedded in porous ceramic was comparable to the relationship determined by traditional pressure-plate apparatus.

Or and Wraith (1999) used the van Genuchten (1980) model to establish the relationship between TDR-measured water content and ceramic-measured matric potential (Fatás et al., 2013)

$$\theta_v = \left[(\theta_{sat} - \theta_{res}) \left[\frac{1}{1 + (\alpha \psi)^n} \right]^m \right] + \theta_{res} \text{* MERGEFORMAT (38)}$$

where n is the pore-size distribution parameter, $m = 1-(1/n)$, is the scale factor related to air-entry point or bubbling pressure (kPa), and θ_{sat} and θ_{res} are the saturated and residual volumetric water contents of the ceramic plates, respectively. The

equation parameter for each TDR- matric potential probe are derived from pressure cell calibration measurements.

3.3.3. *More Combinations of TDR with other techniques*

TDR has been combined with other methods to determine a wide variety of physical properties. For instance, Roberson and Siekmeier (2000) combined type K thermocouples and a four-segment TDR probe (each TDR segment 15 cm long) to measure frost depth of pavement systems. Baumgartner et al. (1994) joined a hollow TDR probe and a pumping system for water sampling. The hydraulic conductivity can be estimated by analyzing transient soil water content and capillary pressure head profiles during a vertical drainage process (Hillel and Gardner, 1970; Kool et al., 1985). Heimovaara et al. (1993) combined TDR probes with tensiometers to simultaneously measure soil water content and pressure head profile of a soil column (**Fig. 17**A). They found that this apparatus gave more insight into the flow process through a sprinkling infiltrometer method and evaporation method. Hendrayanto et al. (1998) proposed a modified instantaneous profile method to determine the unsaturated hydraulic conductivity of forest soils in the field. Al-Jabri et al. (2006) presented a dripper-TDR field approach that enabled simultaneous measurement of a variety of hydraulic conductivity, macroscopic capillary length, immobile water fraction, mass exchange coefficient and dispersion coefficient (**Fig. 17**B).
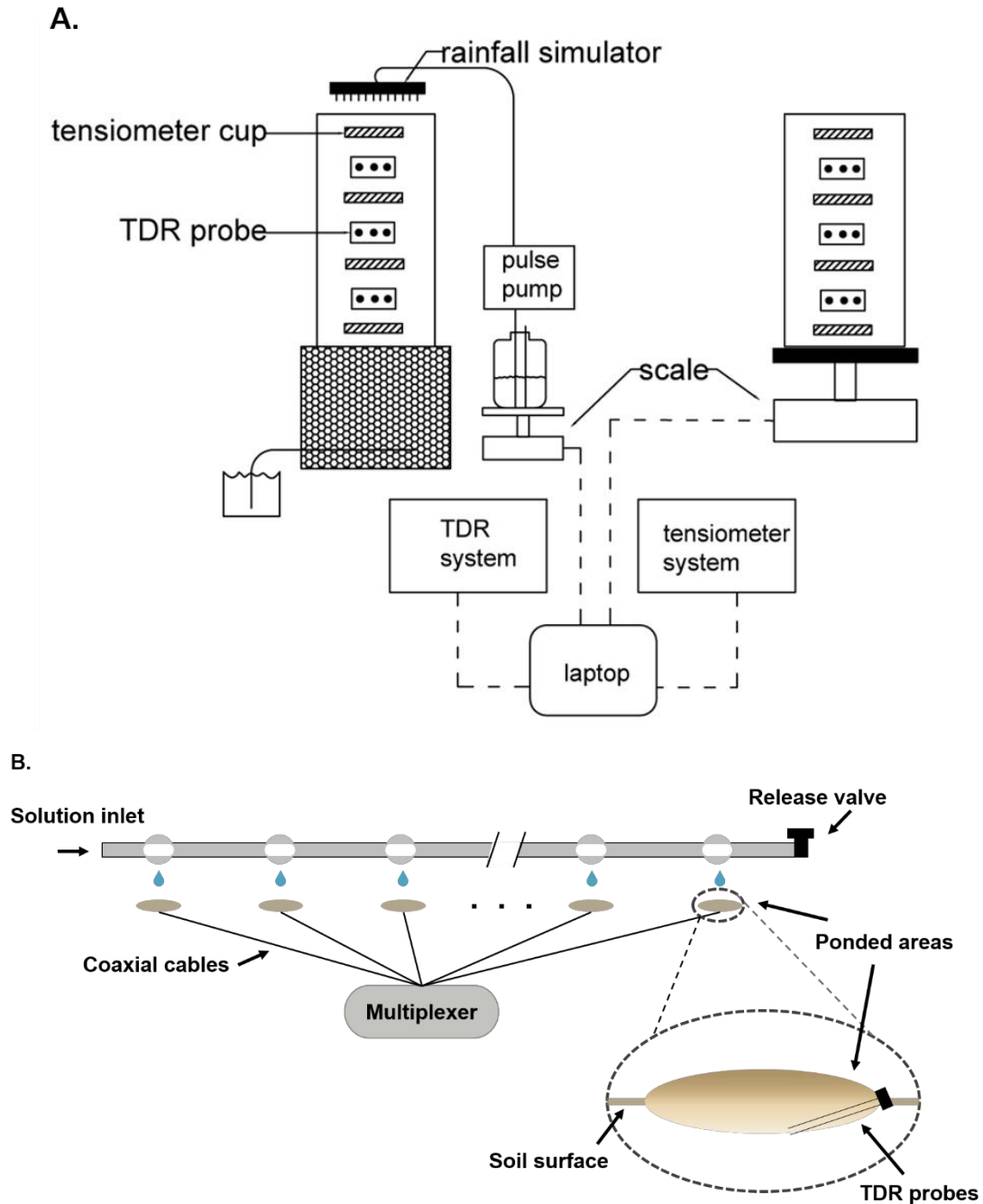
Fig. 17. TDR and tensiometer apparatus used in A. (Heimovaara et al., 1993) and B. dripper TDR apparatus applied in (Al-Jabri et al., 2006).

4. Limitations and Perspectives

4.1. Uncertainties in Graphical Interpretations

The classical graphical interpretation methods to determine travel time and reflection amplitude are easy to use, but they are subject to the setting of travel time analysis parameters (Huisman et al., 2002). Skierucha et al. (2004) argued that the

travel times of TDR waveforms must be determined at the resolution of picoseconds (ps, 10^{-12} s), because a measurement error of 10 ps lead to about a 0.2% error in soil water content (Skierucha et al., 2004). In addition, currently there is no tool available for wetting/drying and freezing/thawing interface detection in the TDR waveforms. TDR probes may be subject to the following four difficulties in practice:

(1) frost heave over winter may lift TDR rods (up to 10 cm);

(2) detrimental air voids of variable size may develop around the upper ends of vertically installed rods (Topp et al., 2003), which result in an underestimation of water content or in unrepresentative water contents when these openings function as preferential flow channels (Annan, 1977; Topp et al., 1982a);

(3) preferential freezing or thawing along the TDR rods in frozen soil may take place because the TDR rods have a larger thermal conductivity than the porous media (e.g., soil and stem) being investigated;

(4) TDR rods may lead to planes of weakness with shrinkage cracks passing between the rods in un-vegetated soils (Topp et al., 2003).

To reduce subjective interpretation and to maintain constant standards, there is a need to develop new interpretation methods or tools. Machine learning or artificial intelligence has been used for graphical interpretation or target detection in various disciplines of earth science (Arabameri et al., 2020; Nanda et al., 2020; Rizvi et al., 2019; Saha et al., 2020; Zhang and Shi, 2020; Zhou et al., 2019). The machine learning may be used to facilitate the interpretation of TDR waveforms in order to determine a variety of physical properties and processes in porous media. And

machine learning can also be used to compare the various waveform analysis for water content measurement.

Another promising alternative to the classical graphical interpretation methods is the use of numerical inverse modeling or the Fourier transformation analysis of the TDR waveforms. The advantage of this method is that it provides frequency-dependent dielectric properties contained in TDR waveforms (Cole, 1977; Friel and Or, 1999; Giese and Tiemann, 1975; Heimovaara et al., 1994). Therefore, this method can be applied to soils with high clay content or salinity that cause energy losses (e.g., dielectric dispersion and electrical conduction) in TDR EM waveforms, making them difficult to interpret graphically. In addition, it can be used to provide soil water profile along the rods of a TDR probe. It is also noteworthy that few studies were found to combine the frequency domain analysis of the TDR waveform with the numerical simulation programs.

4.2.   Uncertainty in TDR Measurements of Water Content and Water Storage

Because short TDR rods (e.g., < 10 cm) can affect the accuracy of soil water content measurements (Dalton and Van Genuchten, 1986; He et al., 2015b; He et al., 2018b; Heimovaara, 1993; Topp et al., 1984), special calibration curves (Ren et al., 2003) or special TDR waveform analysis (Wang et al., 2016) are required for soil water measurements with a short-rod TDR. This might be also true for stem water content, because the length of a TDR probe is restricted by the tree diameter and the ease of drilling/inserting the TDR needles. TDR probes used for stem water measurement have lengths of 2 cm (Irvine and Grace, 1997), 5 cm (Irvine and Grace,

1997) or 13 cm (Constantz and Murphy, 1990). Few studies have analyzed the effects of TDR dimensions on stem water measurements. TDR probe length differences (**Fig. 18**) may partially explain why the calibration curves for soil water measurements cannot be used for stem water content (i.e., less-structured soil vs well-structured stem) (Irvine and Grace, 1997). FDR has also been used for stem water measurements (Zhou et al., 2015), and FDR may be a better choice than TDR for measuring stem water contents in trees of small diameter.
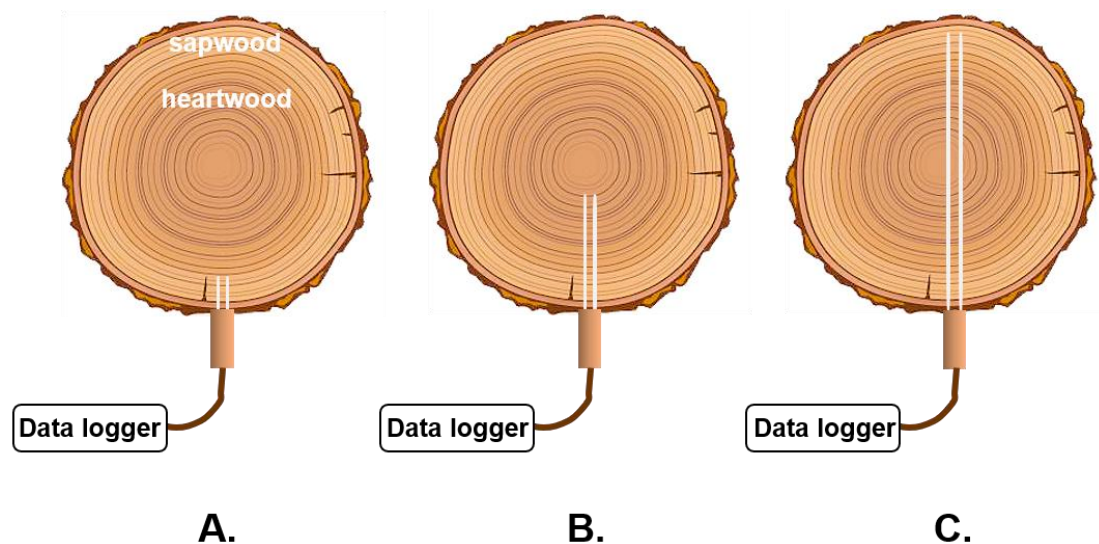
Fig. 18. Potential installation of TDR probe lengths in a tree trunk, modified from Constantz and Murphy (1990) and Sparks et al. (2001).

In addition, maximum contact between the TDR probe and the sapwood should be made, because poor installation results in air bubbles around the TDR rods (Malavasi et al., 2016). Effects of the radial variability of stem morphology (e.g., non-uniform distribution of water in the stem, different dielectric permittivity of the sapwood and heartwood) on TDR measurements should be investigated to better understand stem water content. Plant stems differ from other porous media (e.g., soil)

in that outer sapwood layers of trees tend to exhibit higher water contents compared to the inner heartwood layers (Constantz and Murphy, 1990). A study of Zhou et al. (2018) showed that the probe must sense substantial amounts of the sapwood to better account for changes in θ_{stem}. The influence of temperature on TDR coaxial cable dielectric length is another issue that should be considered (Malavasi et al., 2016).

There is no universal calibration function to estimate soil water content nor stem water content (Hernández-Santana and Martínez-Fernández, 2010). Collating and evaluating available TDR calibration curves for soil water content, stem water and liquid water/ice content should be done.

4.3.   Protocols for TDR and a New TDR Probe Design

Similar to other measurement technologies (He et al., 2018b), there is a noticeable lack of protocols or standards for TDR design and applications. Many promising combinations of TDR with other techniques (e.g., thermo-TDR and TDR-matric potential probe) have been studied but not yet commercialized. The measurement range of the TDR based SWRC method varies from probe to probe and should be fully evaluated. Because SWRC is temperature dependent (Hopmans and Dane, 1986; Liu and Dane, 1993), future studies should calibrate the effects of temperature on the measured SWRC. Hysteresis is another issue that should be solved for the TDR based SWRC instruments.

It is also noted that a combination of TDR and gypsum/ceramics has been used to measure matric potential (Lungal and Si, 2008; Noborio et al., 1999; Scanlon et al., 2002), a combination of TDR and the heat pulse method has been used to measure

thermal properties and a range of other physical properties (He et al., 2018b; Ren et al., 2003), and combination of heat pulse or thermal dissipation method and ceramics has been used to measure thermal properties and matric potential (Feng and Fredlund, 2003; Fredlund, 1992; Kojima et al., 2017; Tan et al., 2007). Theoretically, it is possible to combine the TDR, heat pulse method and gypsum/ceramics to simultaneously measure a wide range of physical properties including thermal properties, matric potential and water content on the same volume of porous media. This would facilitate the study of coupled water and heat transport in porous media.

4.4.   Development of Duty-Cycle TDR Unit

Currently, there is a lack of inexpensive but high-resolution TDR cable testers, which impede the wide application and deployment of this technique. Shibuya et al. (2021) introduced one of the good examples for the development of inexpensive but accurate TDR, a duty-cycle TDR unit, designed and manufactured by Kett Electric Laboratory Ltd. in Tokyo, as shown in **Fig. 19**. A square wave pulse generator running with 25 MHz emits a square wave with a duty cycle is 50%, as shown in **Fig. 20**A. The pulse travels through the impedance matching and the 50Ω coaxial cable to the probe. The pulse reaches the end of the probe, reflects there to return through the 50Ω coaxial cable to a comparator. The comparator compares the reflected wave voltage with the threshold voltage, E_s, which is predetermined based on the range of dielectric constant at the probe (**Fig. 20**B). The reflected wave voltage varies only depending on changes in dielectric constant at the probe throughout the signal line between the pulse generator and the probe. When the reflected wave voltage is larger

than the threshold, it would be E otherwise be zero to turn binary values, as shown in

Fig. 20. Fig. 20C. The length ratio of E to zero does not change the frequency, but

only a duty cycle. The integrator sums up E to a certain voltage corresponding to the

duty cycle induced by the comparator. The A/D part changes the analog voltage to
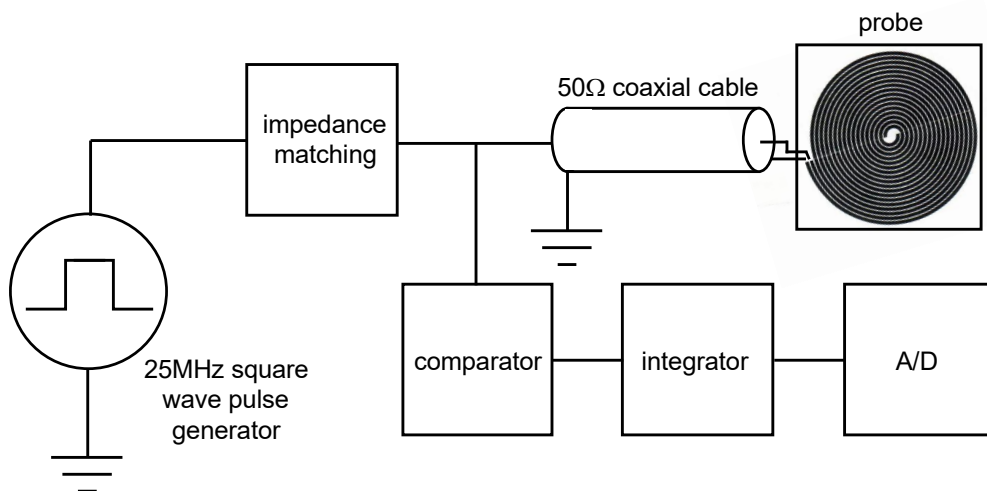
digital signals for output.

Fig. 19. A block diagram of a duty-cycle time domain reflectometry (Shibuya et al., 2021).
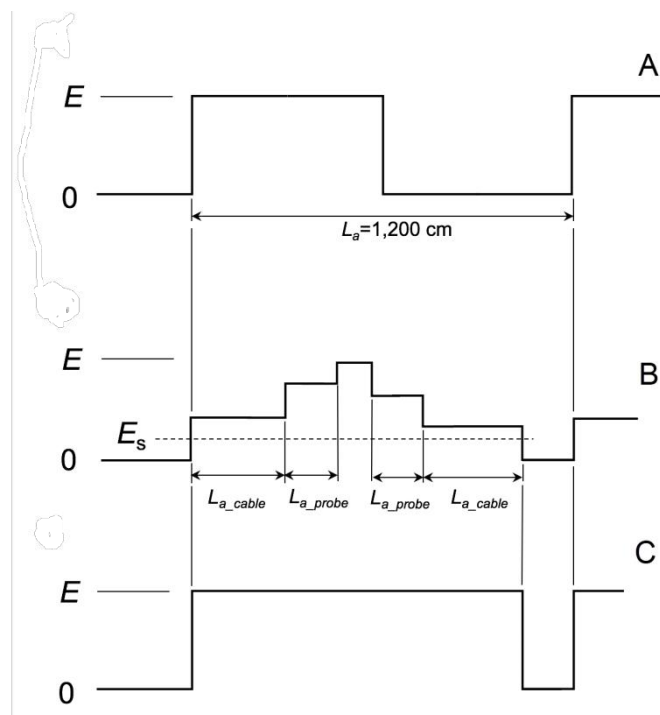
Fig. 20. (a) a square wave pulse generated at the pulse generator for sending out to a probe, (b) the wave reflected at the probe and the coaxial cable, and (c) the wave with binary values after the comparator. The E and E_s denote a circuit voltage and a threshold voltage, respectively (Shibuya et al., 2021).

5. Summary

This review shows how TDR can be used to disclose critical information in porous media beyond average soil water content. It covers basics of the TDR method including TDR principles, design of TDR probes, commercially available TDR cable testers, methods and software for TDR waveform analysis. Applications of TDR to estimate water content in various porous media, including soil, plants, snow, food and concrete are discussed. New techniques available to derive spatial variability of soil water distributions along a single TDR probe are presented, followed by TDR waveform based analyses to estimate electrical conductivity (EC), wetting/drying and freezing/thawing fronts, and snow depth. The combination of TDR measurements combined with other methods (e.g., gypsum/ceramics and heat pulse method) to determine a wide range of soil physical properties (e.g., soil water retention curve, thermal properties, and hydraulic conductivity) and fluxes (e.g., soil heat flux, liquid water flux, and vapor flux) are also presented. The study concludes with a discussion of limitations and perspectives on various TDR applications. This review provides useful information for novices and experts alike to guide them on the advantages, limitations, developments, and the applications of the TDR method in porous media.

References

Adelakun, I. A., and Sri Ranjan, R. 2013. Design of a multilevel TDR probe for measuring soil water content at different depths. *Transactions of the ASABE* **56**, 1451-1460.

Al-Jabri, S. A., Lee, J., Gaur, A., Horton, R., and Jaynes, D. B. 2006. A dripper-TDR method for in situ determination of hydraulic conductivity and chemical transport properties of surface soils. *Advances in Water Resources* **29**, 239-249.

Amato, M., and Ritchie, J. T. 1995. Small spatial scale soil water content measurement with time-domain reflectometry. *Soil Sci. Soc. Am. J.* **59**, 325-329.

Amato, M. T., Subroy, V., Giménez, D., Strom, P. F., and Krogmann, U. 2019. Dielectric permittivity-water content relationships in woodchips: Particle size and temperature effects. *J. Hydol.* **572**, 251-260.

Annan, A. P. 1977. "Time-domain reflectometry air-gap problem for parallel wire transmission lines." Department of Energy, Mines, and Resources, Geological Survey of Canada, Ottawa, ON, Canada.

Ansoult, M., De Backer, L. W., and Declercq, M. 1985. Statistical relationship between apparent dielectric constant and water content in porous media. *Soil Sci. Soc. Am. J.* **49**, 47-50.

Arabameri, A., Lee, S., Tiefenbacher, J., Thao, N., and Ngo, T. 2020. Novel ensemble of mcdm-artificial intelligence techniques for groundwater-potential mapping in arid and semi-arid regions (Iran). *Remote Sensing* **12**, 490.

Bajno, D., Bednarz, L., Matkowski, Z., and Raszczuk, K. 2020. Monitoring of thermal and moisture processes in various types of external historical walls. *Materials* **13**, 505.

Baker, J. M., and Allmaras, R. R. 1990. System for automating and multiplexing soil moisture measurement by time-domain reflectometry. *Soil Sci. Soc. Am. J.* **54**, 1-6.

Baker, T. H. W., Davis, J. L., Hayhoe, H. N., and Topp, G. C. 1982. Locating the frozen–unfrozen interface in soils using time-domain reflectometry. *Can. Geotech. J.* **19**, 511-517.

Baker, T. H. W., and Goodrich, L. 1984. A probe for measuring both thermal conductivity and water content of soils.

Baker, T. H. W., and Goodrich, L. E. 1987. Measurement of soil water content using the combined time-domain reflectometry – thermal conductivity probe. *Can. Geotech. J.* **24**, 160-163.

Baumgartner, N., Parkin, G. W., and Elrick, D. E. 1994. Soil water content and potential measured by hollow time domain reflectometry probe. *Soil Sci. Soc. Am. J.* **58**, 315-318.

Beedlow, P. A., Waschmann, R. S., Lee, E. H., and Tingey, D. T. 2017. Seasonal patterns of bole water content in old growth Douglas-fir (*Pseudotsuga menziesii* (Mirb.) Franco). *Agric For Meteorol* **242**, 109-119.

Benson, C. H., and Bosscher, P. J. 1998. Time-domain reflectometry (TDR) in geotechnics: A review. *In* "Nondestructive and Automated Testing for Soil and Rock Properties" (W. A. Marr and C. E. Fairhurst, eds.), Vol. ASTM STP 1350. American Society for Testing and Materials.

Birchak, J. R., Gardner, C. G., Hipp, J. E., and Victor, J. M. 1974. High dielectric constant microwave probes for sensing soil moisture. *Proc. IEEE* **62**, 93-98.

Blonquist, J. M., Jones, S. B., and Robinson, D. A. 2005. A time domain transmission sensor with TDR performance characteristics. *J. Hydol.* **314**, 235-245.

Blonquist, J. M. J., Jones, S. B., Lebron, I., and Robinson, D. A. 2006. Microstructural and phase configurational effects determining water content: Dielectric relationships of aggregated porous media. *Water Resour. Res.* **42**, W05424.

Boike, J., and Roth, K. 2015. Time domain reflectometry as a field method for measuring water content and soil water electrical conductivity at a continuous permafrost site. *Permafrost & Periglacial Processes* **8**, 359-370.

Brough, D. W., Jones, H. G., and Grace, J. 1986. Diurnal changes in water content of the stems of apple trees, as influenced by irrigation. *Plant, Cell Environ.* **9**, 1-7.

Carslaw, H. S., and Jaeger, J. C. 1959. "Conduction of heat in solids," 2nd/Ed. Clarendon Press, Oxford.

Castiglione, P., and Shouse, P. J. 2003. The effect of ohmic cable losses on time-domain reflectometry measurements of electrical conductivity. *Soil Sci. Soc. Am. J.* **67**, 414-424.

Cataldo, A., De Benedetto, E., Cannazza, G., Piuzzi, E., and Pittella, E. 2018. TDR-based measurements of water content in construction materials for in-the-field use and calibration. *IEEE Trans. Instrum. Meas.* **67**, 1230-1237.

Cataldo, A., De Benedetto, E., Huebner, C., and Trebbels, D. 2017. TDR application for moisture content estimation in agri-food materials. *IEEE Instrumentation & Measurement Magazine* **20**, 26-31.

Cataldo, A., Tarricone, L., Attivissimo, F., and Trotta, A. 2008a. Simultaneous measurement of dielectric properties and levels of liquids using a TDR method. *Measurement* **41**, 307-319.

Cataldo, A., Tarricone, L., Vallone, M., Cannazza, G., and Cipressa, M. 2010. TDR moisture measurements in granular materials: From the siliceous sand test case to the applications for agro-food industrial monitoring. *Computer Standards & Interfaces* **32**, 86-95.

Cataldo, A., Vallone, M., Tarricone, L., and Attivissimo, F. 2008b. An evaluation of performance limits in continuous TDR monitoring of permittivity and levels of liquid materials. *Measurement* **41**, 719-730.

Černý, R. 2009. Time-domain reflectometry method and its application for measuring moisture content in porous materials: A review. *Measurement* **42**, 329-336.

Chai, J., Wei, S. M., Chang, X. T., and Liu, J. X. 2004. Monitoring deformation and damage on rock structures with distributed fiber optical sensing. *Int. J. Rock Mech. Min. Sci.* **41**, 298-303.

Chaney, R. C., Demars, K., Dowding, C., Huang, F., and McComb, P. S. 1996. Water pressure measurement with time domain reflectometry cables. *Geotechnical Testing Journal* **19**.

Chen, X., and Horino, H. 1998. Three methods including TDR method to measure frozen or thawed depth of soil in field. pp. 104-111. Institut international du froid, Orsay, Paris, FRANCE.

Chen, Y., and Or, D. 2006. Geometrical factors and interfacial processes affecting complex dielectric permittivity of partially saturated porous media. *Water Resour. Res.* **42**.

Cheng, W., Zhao, C., Qiao, X., and Hou, R. 2010. A design of probe for measurement of moisture content using time domain reflectometry. *Sensor Lett.* **8**, 118-121.

Choat, B., Drayton, W. M., Brodersen, C., Matthews, M. A., Shackel, K. A., Wada, H., and McElrone, A. J. 2010. Measurement of vulnerability to water stress-induced cavitation in grapevine: a comparison of four techniques applied to a long-vesseled species. *Plant Cell Environ* **33**, 1502-12.

Christensen, A. F., He, H., Dyck, M., Lenore Turner, E., Chanasyk, D. S., Naeth, M. A., and Nichol, C. 2013. In situ measurement of snowmelt infiltration under various topsoil cap thicknesses on a reclaimed site. *Can. J. Soil Sci.* **93**, 497-510.

Clark, J., and Gibbs, R. 1957. Studies in tree physiology IV: Further investigations of seasonal changes in moisture content of certain Canadian forest trees. *Can. J. Bot.* **35**, 219-253.

Clarke Topp, G. 1998. Time domain reflectometry: a seminal technique for measuring mass and energy in soil. *Soil Tillage Res.* **47**, 125-132.

Cole, R. 1977. Time domain reflectometry. *Annual review of physical chemistry* **28**, 283-300.

Constantz, J., and Murphy, F. 1990. Monitoring moisture storage in trees using time domain reflectometry. *J. Hydol.* **119**, 31-42.

Cortez, E. R., Hanek, G. L., Truebe, M. A., and Kestler, M. A. 2009. Simplified user's guide to time-domain-reflectometry monitoring of slope stability.

Cresswell, H. P., Green, T. W., and McKenzie, N. J. 2008. The adequacy of pressure plate apparatus for determining soil water retention. *Soil Sci. Soc. Am. J.* **72**, 41-49.

Cristi, F., Fierro, V., Suárez, F., Muñoz, J. F., and Hausner, M. B. 2016. A TDR-waveform approach to estimate soil water content in electrically conductive soils. *Comput. Electron. Agric.* **121**, 160-168.

Cuevas Sánchez, M. V., and Fernández Luque, J. E. 2010. Irrigation scheduling from stem diameter variations: A review. *Agric. For. Meteorol.* **150**, 135-151.

Dahlen, J., Antony, F., Li, A., Love-Myers, K., Schimleck, L., and Schilling, E. B. 2015. Time-domain reflectometry for the prediction of loblolly pine and sweetgum moisture content. *Bioresources* **10**, 4947-4960.

Dalton, F. N., Herkelrath, W. N., Rawlins, D. S., and Rhoades, J. D. 1984. Time-domain reflectometry: simultaneous measurement of soil water content and electrical conductivity with a single probe. *Science* **224**, 989-990.

Dalton, F. N., and Van Genuchten, M. T. 1986. The time-domain reflectometry method for measuring soil water content and salinity. *Geoderma* **38**, 237-250.

Dane, J. H., and Hopmans, J. W. 2002. 3.3.2 Laboratory. *In* "Methods of Soil Analysis: Part 4 Physical Methods" (J. H. Dane and C. G. Topp, eds.), pp. 675-719. Soil Science Society of America, Madison, WI.

Dasberg, S., and Hopmans, J. W. 1992. Time domain reflectometry calibration for uniformly and nonuniformly wetted sandy and clayey loam soils. Vol. 56, pp. 1341-1345.

Davis, J. 1975. Relative permittivity measurements of a sand and clay soil in situ. *Geological Survey Canada, Ottawa*, 75-1C.

Davis, J., and Chudobiak, W. 1975. In situ meter for measuring relative permittivity of soils. *Geol. Surv. Can. Pap* **75**, 75-79.

de Loor, G. P. 1968. Dielectric properties of heterogenous mixtures containing water. *The Journal of Microwave Power and Electromagnetic Energy* **3**, 67-73.

De Schepper, V., van Dusschoten, D., Copini, P., Jahnke, S., and Steppe, K. 2012. MRI links stem water content to stem diameter variations in transpiring trees. *J. Exp. Bot.* **63**, 2645-53.

de Winter, E. J. G., van Loon, W. K. P., Esveld, E., and Heimovaara, T. J. 1996. Dielectric spectroscopy by inverse modelling of time domain reflectometry wave forms. *J. Food Eng.* **30**, 351-362.

Dettmann, U., and Bechtold, M. 2018. Evaluating commercial moisture probes in reference solutions covering mineral to peat soil conditions. *Vadose Zone J.* **17**.

Ding, L., Noborio, K., and Shibuya, K. 2019. Frost forecast using machine learning - from association to causality. *Procedia Computer Science* **159**, 1001-1010.

Dirksen, C., and Dasberg, S. 1993. Improved calibration of time domain reflectometry soil water content measurements. *Soil Sci. Soc. Am. J.* **57**, 660-667.

Dobson, M. C., Ulaby, F. T., Hallikainen, M. T., and El-Rayes, M. A. 1985. Microwave dielectric behavior of wet soil-part ii: Dielectric mixing models. *Geoscience and Remote Sensing, IEEE Transactions on* **GE-23**, 35-46.

Dowding, C. H., and Huang, F.-c. 1996. Ground water pressure measurement with time domain reflectometry. *In* "2nd North American Rock Mechanics Symposium".

Dowding, C. H., Su, M. B., and O'Connor, K. 1989. Measurement of rock mass deformation with grouted coaxial antenna cables. *International Journal of Rock Mechanics and Mining Sciences & Geomechanics Abstracts* **26**, A192.

Drusa, M., Cheben, V., and Proovnikova, P. 2013. Functionality of TDR piezometers and inclinometers for monitoring of slope deformations. *In* "International Multidisciplinary Scientific GeoConference Surveying Geology and Mining Ecology Management, SGEM", Vol. 2, pp. 157–164.

Dyck, M., Miyamoto, T., Iwata, Y., and Kameyama, K. 2019. Bound Water, Phase Configuration, and Dielectric Damping Effects on TDR-Measured Apparent Permittivity. *Vadose Zone J.* **18**, 1-14.

Dyck, M. F. 2008. Physics of water flow and solute transport across a soil horizon interface, University of Alberta (Canada), Canada.

Dyck, M. F., and Kachanoski, R. G. 2009a. Measurement of steady-state soil water flux across a soil horizon interface. *Soil Sci. Soc. Am. J.* **73**, 1786-1795.

Dyck, M. F., and Kachanoski, R. G. 2009b. Measurement of transient soil water flux across a soil horizon interface. *Soil Sci. Soc. Am. J.* **73**, 1604-1613.

Dyck, M. F., and Kachanoski, R. G. 2010. Spatial scale-dependence of preferred flow domains during infiltration in a layered field soil. *Vadose Zone J.* **9**, 385-396.

Edwards, W. R. N., and Jarvis, P. G. 1983. A method for measuring radial differences in water content of intact tree stems by attenuation of gamma radiation. *Plant, Cell Environ.* **6**, 255-260.

Evett, S. R. 2000a. The TACQ computer program for automatic time domain reflectometry measurements: I. Design and operating characteristics. *Trans. ASAE* **43**, 1939-1946.

Evett, S. R. 2000b. The TACQ computer program for automatic time domain reflectometry measurements: II. Waveform interpretation methods. *Trans. ASAE* **43**, 1947-1956.

Fares, A., and Polyakov, V. 2006. Advances in crop water management using capacitive water sensors. *In* "Advances in Agronomy", Vol. Volume 90, pp. 43-77. Academic Press.

Farrington, S. P., and Sargand, S. M. 2006. Advanced processing of time domain reflectometry for improved slope stability monitoring. *In* "GeoCongress 2006: Geotechnical Engineering in the Information Technology Age", pp. 1-6.

Fatás, E., Vicente, J., Latorre, B., Lera, F., Viñals, V., López, M. V., Blanco, N., Peña, C., González-Cebollada, C., and Moret-Fernández, D. 2013. TDR-LAB 2.0 Improved TDR software for soil water content and electrical conductivity measurements. *Procedia Environmental Sciences* **19**, 474-483.

Fellner-Feldegg, H. 1969. Measurement of dielectrics in the time domain. *J. Phys. Chem.* **73**, 616-623.

Feng, M., and Fredlund, D. G. 2003. Calibration of thermal conductivity sensors with consideration of hysteresis. *Can. Geotech. J.* **40**, 1048-1055.

Fernández, J. E. 2017. Plant-based methods for irrigation scheduling of woody crops. *Hortic.* **3**, 35.

Ferre, P. A., and Topp, G. C. 2002. Time domain reflectometry. *In* "Methods of Soil Analysis" (J. H. Dane and G. C. Topp, eds.), Vol. Part 4. Physical Methods, pp. 434–445. American Society of Agronomy, Madison, WI.

Fiala, L., Pavlíková, M., and Pavlík, Z. 2014. Application of TDR method for moisture profiles measurement in cellular concrete. *Advanced Materials Research* **982**, 11-15.

Fredlund, D. G. 1992. Background, theory, and research related to the use of thermal conductivity sensors for matric suction measurement. *In* "Advances in Measurement of Soil Physical Properties: Bringing Theory into Practice" (G. C. Topp, W. D. Reynolds and R. E. Green, eds.), pp. 249-261. Soil Science Society of America, Madison, WI.

Friedman, S. P. 1998. A saturation degree-dependent composite spheres model for describing the effective dielectric constant of unsaturated porous media. *Water Resour. Res.* **34**, 2949-2961.

Friel, R., and Or, D. 1999. Frequency analysis of time-domain reflectometry (TDR) with application to dielectric spectroscopy of soil constituents. *Geop* **64**, 707-718.

Fulladosa, E., Duran-Montgé, P., Serra, X., Picouet, P., Schimmer, O., and Gou, P. 2013. Estimation of dry-cured ham composition using dielectric time domain reflectometry. *Meat science* **93**, 873-879.

Funk, D. B., Gillay, Z., and Meszaros, P. 2007. Unified moisture algorithm for improved RF dielectric grain moisture measurement. *Measurement Science and Technology* **18**, 1004-1015.

Gemert, M. 1974. Evaluation of dielectric permittivity and conductivity by time domain spectroscopy. Mathematical analysis of Fellner-Feldegg's thin cell method. *The Journal of Chemical Physics* **60**, 3963-3974.

Germann, P. F. 2017. Shape of time domain reflectometry signals during the passing of wetting fronts. *Vadose Zone J.* **16**.

Gibbs, R. D. 1930. Sinkage studies. II. The seasonal distribution of water and gas in trees. *Can. J. Res.* **2**, 425-439.

Giese, K., and Tiemann, R. 1975. Determination of the complex permittivity from thin-sample time domain reflectometry improved analysis of the step response waveform. *Advances in Molecular Relaxation Processes* **7**, 45-59.

Greco, R. 2006. Soil water content inverse profiling from single TDR waveforms. *J. Hydol.* **317**, 325-339.

Greco, R., and Guida, A. 2008. Field measurements of topsoil moisture profiles by vertical TDR probes. *J. Hydol.* **348**, 442-451.

Hatfield, J. L., Sauer, T. J., and Cruse, R. M. 2017. Soil: The forgotten piece of the water, food, energy nexus. *advances in agronomy* **143**, 1-46.

Hayhoe, H. N., Topp, G. C., and Bailey, W. G. 1983. Measurement of soil water contents and frozen soil depth during a thaw using time-domain reflectometry. *Atmosphere-Ocean* **21**, 299-311.

He, H., and Dyck, M. 2013. Application of multiphase dielectric mixing models for understanding the effective dielectric permittivity of frozen soils. *Vadose Zone J.* **12**.

He, H., Dyck, M., Horton, R., Li, M., Jin, H., and Si, B. 2018a. Distributed temperature sensing for soil physical measurements and its similarity to heat pulse method. *In* "Advances in Agronomy" (D. L. Sparks, ed.), Vol. 148, pp. 173-230. Academic Press, Cambridge.

He, H., Dyck, M., Si, B., Zhang, T., Lv, J., and Wang, J. 2015a. Soil freezing–thawing characteristics and snowmelt infiltration in Cryalfs of Alberta, Canada. *Geoderma Regional* **5**, 198-208.

He, H., Dyck, M., Wang, J., and Lv, J. 2015b. Evaluation of TDR for quantifying heat-pulse-method-induced ice melting in frozen soils. *Soil Sci. Soc. Am. J.* **79**, 1275-1288.

He, H., Dyck, M., Zhao, Y., Si, B., Jin, H., Zhang, T., Lv, J., and Wang, J. 2016. Evaluation of five composite dielectric mixing models for understanding relationships between effective permittivity and unfrozen water content. *Cold Reg. Sci. Technol.* **130**, 33-42.

He, H., Dyck, M. F., Horton, R., Ren, T., Bristow, K. L., Lv, J., and Si, B. 2018b. Development and application of the heat pulse method for soil physical measurements. *Rev. Geophys.* **56**, 567-620.

He, H., Zhao, Y., Dyck, M. F., Si, B., Jin, H., Lv, J., and Wang, J. 2017. A modified normalized model for predicting effective soil thermal conductivity. *Acta Geotechnica* **12**, 1281-1300.

Heimovaara, T. J. 1993. Design of triple-wire time domain reflectometry probes in practice and theory. *Soil Sci. Soc. Am. J.* **57**, 1410-1417.

Heimovaara, T. J. 1994. Frequency domain analysis of time domain reflectometry waveforms, 1, Measurements of the complex dielectric permittivity of soils. *Water Resour. Res.* **30**, 189-199.

Heimovaara, T. J., and Bouten, W. 1990. A computer-controlled 36-channel time domain reflectometry system for monitoring soil water contents. *Water Resour. Res.* **26**, 2311-2316.

Heimovaara, T. J., Bouten, W., and Verstraten, J. M. 1994. Frequency domain analysis of time domain reflectometry waveforms: 2. A four-component complex dielectric mixing model for soils. *Water Resour. Res.* **30**, 201-209.

Heimovaara, T. J., Focke, A. G., Bouten, W., and Verstraten, J. M. 1995. Assessing temporal variations in soil water composition with time domain reflectometry. *Soil Sci. Soc. Am. J.* **59**, 689-698.

Heimovaara, T. J., Freijer, J. I., and Bouten, W. 1993. The application of TDR in laboratory column experiments. *Soil Technology* **6**, 261-272.

Heimovaara, T. J., Huisman, J. A., Vrugt, J. A., and Bouten, W. 2004. Obtaining the spatial distribution of water content along a TDR probe using the SCEM-UA Bayesian inverse modeling scheme. *Vadose Zone J.* **3**, 1128-1145.

Hendrayanto, Kosugi, K. i., and Mizuyama, T. 1998. Field determination of unsaturated hydraulic conductivity of forest soils. *Journal of Forest Research* **3**, 11-17.

Hendrickx, J. M. H., Wraith, J. M., Corwin, D. L., and Kachanoski, R. G. 2002. Solute content and concentration. *In* "Methods of Soil Analysis. Part 4. Physical Methods." (J. H. Dane and G. C. Topp, eds.), pp. 1253-1322, ASA, Madison, WI.

Herkelrath, W. N., Hamburg, S. P., and Murphy, F. 1991. Automatic, real-time monitoring of soil moisture in a remote field area with time domain reflectometry. *Water Resour. Res.* **27**, 857-864.

Hernández-Santana, V., and Martínez-Fernández, J. 2010. TDR measurement of stem and soil water content in two Mediterranean oak species. *Hydrol. Sci. J.* **53**, 921-931.

Hillel, D., and Gardner, W. R. 1970. Measurement of unsaturated conductivity and diffusivity by infiltration through an impeding layer. *Soil Sci.* **109**, 149-153.

Hirota, T., Iwata, Y., Hayashi, M., Suzuki, S., Hamasaki, T., Sameshima, R., and Takayabu, I. 2006. Decreasing soil-frost depth and its relation to climate change in Tokachi, Hokkaido, Japan. *Journal of the Meteorological Society of Japan* **84**, 821–833.

Hoekstra, P., and Delaney, A. 1974. Dielectric properties of soils at UHF and microwave frequencies. *Journal of Geophysical Research* **79**, 1699-1708.

Holbrook, N. M., Burns, M. J., and Sinclair, T. R. 1992. Frequency and time-domain dielectric measurements of stem water content in the arborescent palm,sabal palmetto. *J. Exp. Bot.* **43**, 111-119.

Holbrook, N. M., and Sinclair, T. R. 1992. Water balance in the arborescent palm, Sabal palmetto. II. Transpiration and stem water storage. *Plant, Cell Environ.* **15**, 401-409.

Hopmans, J. W., and Dane, J. H. 1986. Temperature dependence of soil water retention curves. *Soil Sci. Soc. Am. J.* **50**, 562-567.

Hudson, D. B., Wierenga, P. J., and Hills, R. G. 1996. Unsaturated hydraulic properties from upward flow into soil cores. *Soil Sci. Soc. Am. J.* **60**, 388-396.

Huebner, C., and Kupfer, K. 2007. Modelling of electromagnetic wave propagation along transmission lines in inhomogeneous media. *Measurement Science and Technology* **18**, 1147-1154.

Huisman, J. A., Weerts, A. H., Heimovaara, T. J., and Bouten, W. 2002. Comparison of travel time analysis and inverse modeling for soil water content determination with time domain reflectometry. *Water Resour. Res.* **38**, 13-1-13-8.

Huza, J., Teuling, A. J., Braud, I., Grazioli, J., Melsen, L. A., Nord, G., Raupach, T. H., and Uijlenhoet, R. 2014. Precipitation, soil moisture and runoff variability in a small river catchment (Ardèche, France) during HyMeX Special Observation Period 1. *J. Hydol.* **516**, 330-342.

Irvine, J., and Grace, J. 1997. Non-destructive measurement of stem water content by time domain reflectometry using short probes. *J. Exp. Bot.* **48**, 813-818.

Jackson, G. E., Irvine, J., and Grace, J. 1995. Xylem cavitation in two mature Scots pine forests growing in a wet and a dry area of Britain. *Plant, Cell Environ.* **18**, 1411-1418.

Jones, S. B., and Friedman, S. P. 2000. Particle shape effects on the effective permittivity of anisotropic or isotropic media consisting of aligned or randomly oriented ellipsoidal particles. *Water Resour. Res.* **36**, 2821-2833.

Jones, S. B., and Or, D. 2004. Frequency domain analysis for extending time domain reflectometry water content measurement in highly saline soils. *Soil Sci. Soc. Am. J.* **68**, 1568-1577.

Jones, S. B., Wraith, J. M., and Or, D. 2002. Time domain reflectometry measurement principles and applications. *Hydrol. Processes* **16**, 141-153.

Kaatze, U. 1989. Complex permittivity of water as a function of frequency and temperature. *Journal of Chemical & Engineering Data* **34**, 371-374.

Kachanoski, R. G., Pringle, E., and Ward, A. 1992. Field measurement of solute travel times using time domain reflectometry. *Soil Sci. Soc. Am. J.* **56**, 47-52.

Kafarski, M., Majcher, J., Wilczek, A., Szypłowska, A., Lewandowski, A., Zackiewicz, A., and Skierucha, W. 2019. Penetration depth of a soil moisture profile probe working in time-domain transmission mode. *Sensors* **19**.

Kane, W. F. 2000. Monitoring Slope Movement with Time Domain Reflectometry.

Kargas, G., Persson, M., Kanelis, G., Markopoulou, I., and Kerkides, P. 2017. Prediction of Soil Solution Electrical Conductivity by the Permittivity Corrected Linear Model Using a Dielectric Sensor. *Journal of Irrigation and Drainage Engineering* **143**.

Kato, T., Shibuya, K., Miyakawa, R., and Noborio, K. 2020. "Development of frost detecting sensor using time domain reflectometry [in Japanese with English abstract]." Bulletin of the Faculty of Agriculture, Meiji University.

Katsura, S. y., Kosugi, K. i., and Mizuyama, T. 2008. Application of a coil-type TDR probe for measuring the volumetric water content in weathered granitic bedrock. *Hydrol. Processes* **22**, 750-763.

Kennedy, I., and Sharratt, B. 1998. Model comparisons to simulate soil frost depth. *Soil Sci.* **163**, 636-645.

Klute, A. 1986. Water retention: laboratory methods. *Agronomy*, 635-662.

Knight, J. H. 1992. Sensitivity of time domain reflectometry measurements to lateral variations in soil water content. *Water Resources Research* **28**, 2345–2352.

Kobayashi, Y., and Tanaka, T. 2001. Measurement of stem water storage used by TDR (Time Domain Reflectometry) Method. *Journal of Japan Society of Hydrology And Water Resources* **14**, 207-216.

Kogure, T., and Okuda, Y. 2018. Monitoring the vertical distribution of rainfall-induced strain changes in a landslide measured by distributed fiber optic sensing (DFOS) with Rayleigh backscattering. *Geophysical Research Letters* **45**, 4033-4040.

Kojima, Y., Noborio, K., Mizoguchi, M., and Kawahara, Y. 2017. Matric potential sensor using dual probe heat pulse technique. *Agricultural Information Research* **26**, 77-85.

Kool, J. B., Parker, J. C., and Genuchten, M. T. V. 1985. Determining soil hydraulic properties from one-step outflow experiments by parameter estimation: I. *Soil Sci. Soc. Am. J.* **49**, 1348-1354.

Kraszewski, A. W., and Nelson, S. O. 2004. Microwave permittivity determination in agricultural products. *J Microw Power Electromagn Energy* **39**, 41-52.

Kumagai, T. o., Aoki, S., Otsuki, K., and Utsumi, Y. 2009. Impact of stem water storage on diurnal estimates of whole-tree transpiration and canopy conductance from sap flow measurements in Japanese cedar and Japanese cypress trees. *Hydrol. Processes* **23**, 2335-2344.

Laloy, E., Huisman, J. A., and Jacques, D. 2014. High-resolution moisture profiles from full-waveform probabilistic inversion of TDR signals. *J. Hydol.* **519**, 2121-2135.

Lathi, B. E. 1992. "Linear signal and systems analysis," Cambridge Press, Berkeley.

Lin, C.-P., Chung, C.-C., Huisman, J. A., and Tang, S.-H. 2008. Clarification and calibration of reflection coefficient for electrical conductivity measurement by time domain reflectometry. *Soil Sci. Soc. Am. J.* **72**, 1033-1040.

Lin, C.-P., Chung, C.-C., and Tang, S.-H. 2007. Accurate time domain reflectometry measurement of electrical conductivity accounting for cable resistance and recording time. *Soil Sci. Soc. Am. J.* **71**, 1278-1287.

Liu, H. H., and Dane, J. H. 1993. Reconciliation between measured and theoretical temperature effects on soil water retention curves. *Soil Sci. Soc. Am. J.* **57**, 1202-1207.

Loeb, H. W., Young, G. M., Quickenden, P. A., and Suggett, A. 1971. New methods for measurement of complex permittivity up to 13 GHz and their application to the study of dielectric relaxation of polar liquids including aqueous solutions. Vol. 75, pp. 1155-1165.

Lundberg, A. 1997. Laboratory calibration of TDR-probes for snow wetness measurements. *Cold Reg. Sci. Technol.* **25**, 197-205.

Lungal, M., and Si, B. 2008. Coiled time domain reflectometry matric potential sensor. *Soil Sci. Soc. Am. J.* **72**, 1422-1424.

Lv, L., Liao, K., Lai, X., Zhu, Q., and Zhou, S. 2016. Hillslope soil moisture temporal stability under two contrasting land use types during different time periods. *Environmental Earth Sciences* **75**, 560.

Lyu, D., Shi, X., Wang, X., and Dong, Y. 2016. Study on dynamic and non-destructive ultrasonic echo detection method of plant stem water content. *In* "2016 International Conference on Engineering and Technology Innovations". Atlantis Press.

Malavasi, U. C., Davis, A. S., and Malavasi, M. d. M. 2016. Estimating water in living woody stems-A review. *CERNE* **22**, 415-422.

Malicki, M. A., Plagge, R., and Roth, C. H. 1996. Improving the calibration of dielectric TDR soil moisture determination taking into account the solid soil. *Eur. J. Soil Sci.* **47**, 357-366.

Mallants, D., Vanclooster, M., Vanderborght, J., Feyen, J., Toride, N., and van Genuchten, M. T. 1996. Comparison of three methods to calibrate TDR for monitoring solute movement in undisturbed soil. *Soil Sci. Soc. Am. J.* **60**, 747-754.

Marchand, W. D., Bruland, O., and Killingtveit, Å. 2001. Improved measurements and analysis of spatial snow cover by combining a ground based radar system with a differential global positioning system receiver. *Hydrol. Res* **32**, 181-194.

Mboh, C. M., Huisman, J. A., and Vereecken, H. 2011. Feasibility of sequential and coupled inversion of time domain reflectometry data to infer soil hydraulic parameters under falling head infiltration. *Soil Sci. Soc. Am. J.* **75**, 775-786.

McGraw Jr, D. 2015. The measurement of the dielectric constant of three different shapes of concrete blocks. *IJRRAS* **25**, 82-102.

Mironov, V. L., Dobson, M. C., Kaupp, V. H., Komarov, S. A., and Kleshchenko, V. N. 2004. Generalized refractive mixing dielectric model for moist soils. *ITGRS* **42**, 773-785.

Miyamoto, T., Annaka, T., and Chikushi, J. 2005. Extended dual composite sphere model for determining dielectric permittivity of Andisols. *Soil Sci. Soc. Am. J.* **69**, 23-29.

Moret-Fernández, D., Arrúe, J. L., Pérez, V., and López, M. V. 2008. A TDR-pressure cell design for measuring the soil-water retention curve. *Soil Tillage Res.* **100**, 114-119.

Moret-Fernández, D., Vicente, J., Aragüés, R., Peña, C., and López, M. V. 2012. A new TDR probe for measurements of soil solution electrical conductivity. *Journal of Hydrology* **448-449**, 73-79.

Moret-Fernández, D., Vicente, J., Lera, F., Latorre, B., López, M., Blanco, N., González-Cebollada, C., Arrúe, J., Gracia, R., Salvador, M., and Bielsa, A. 2010. TDR-Lab Version 1.0 users guide (http://digital.csic.es/handle/10261/35790).

Moret, D., López, M. V., and Arrúe, J. L. 2004. TDR application for automated water level measurement from Mariotte reservoirs in tension disc infiltrometers. *J. Hydol.* **297**, 229-235.

Nadler, A. 2004. Relations between soil and tree stem water content and bulk electrical conductivity under salinizing irrigation. *Soil Sci. Soc. Am. J.* **68**, 779-783.

Nadler, A. 2005. Methodologies and the practical aspects of the bulk soil ec (σa)—soil solution ec (σw) relations. *In* "Advances in Agronomy", Vol. 88, pp. 273-312. Academic Press.

Nadler, A., Raveh, E., Yermiyahu, U., and Green, S. R. 2003. Evaluation of TDR use to monitor water content in stem of lemon trees and soil and their response to water stress. *Soil Sci. Soc. Am. J.* **67**, 437-448.

Nanda, A., Sen, S., Nath Sharma, A., and Sudheer, K. 2020. Soil temperature dynamics at hillslope scale-field observation and machine learning-based approach. *Water* **12**.

Nelson, S., and Trabelsi, S. 2008. Dielectric spectroscopy measurements on fruit, meat, and grain. *Transactions of the ASABE* **51**, 1829-1834.

Nissen, H. H., Moldrup, P., and Kachanoski, R. G. 2000. Time domain reflectometry measurements of solute transport across a soil layer boundary. *Soil Sci. Soc. Am. J.* **64**, 62-74.

Noborio, K. 2001. Measurement of soil water content and electrical conductivity by time domain reflectometry: a review. *Comput. Electron. Agric.* **31**, 213-237.

Noborio, K., Horton, R., and Tan, C. S. 1999. Time domain reflectometry probe for simultaneous measurement of soil matric potential and water content. *Soil Sci. Soc. Am. J.* **63**, 1500-1505.

Noborio, K., Kachanoski, R. G., and Tan, C. S. 2006. Solute transport measurement under transient field conditions using time domain reflectometry. *Vadose Zone J.* **5**, 412-418.

Noborio, K., McInnes, K. J., and Heilman, J. L. 1996a. Measurements of cumulative infiltration and wetting front location by time domain reflectometry. *Soil Sci.* **161**, 480-483.

Noborio, K., Mcinnes, K. J., and Heilman, J. L. 1996b. Measurements of soil water content, heat capacity, and thermal conductivity with a single TDR probe1. *Soil Sci.* **161**, 22-28.

O'Connor, K., and O'Connor, D. 1999. GeoMeasurements by pulsing TDR cables and probes. 420pp.

Or, D., Jones, S. B., Van Shaar, J. R., Humphries, S., and Koberstein, L. 2004. "WinTDR, Users guide, Version 6.1. Soil Physics Group, Utah State University, Logan, Utah. https://psc.usu.edu/soilphysics/win-tdr."

Or, D., and Wraith, J. M. 1999. A new soil metric potential sensor based on time domain reflectometry. *Water Resour. Res.* **35**, 3399-3407.

Oswald, B., Benedickter, H. R., Bächtold, W., and Flühler, H. 2003. Spatially resolved water content profiles from inverted time domain reflectometry signals. *Water Resources Research* **39**.

Overduin, P. P., Kane, D. L., and van Loon, W. K. P. 2006. Measuring thermal conductivity in freezing and thawing soil using the soil temperature response to heating. *Cold Reg. Sci. Technol.* **45**, 8-22.

Paolo, F. D., Cosciotti, B., Lauro, S., Mattei, E., Callegari, M., Carturan, L., Seppi, R., Zucca, F., and Pettinelli, E. 2015. Combined GPR and TDR measurements for snow thickness and density estimation. *In* "International Workshop on Advanced Ground Penetrating Radar".

Parkin, G. W., Elrick, D. E., and Kachanoski, R. G. 1992. Cumulative storage of water under constant flux infiltration: analytical solution. *Water Resour. Res.* **28**, 2811-2818.

Parkin, G. W., Kachanoski, R. G., Elrick, D. E., and Gibson, R. G. 1995. Unsaturated hydraulic conductivity measured by time domain reflectometry under a rainfall simulator. *Water Resour. Res.* **31**, 447-454.

Patterson, D. E., and Smith, M. W. 1980. The use of time domain reflectometry for the measurement of unfrozen water content in frozen soils. *Cold Reg. Sci. Technol.* **3**, 205-210.

Patterson, D. E., and Smith, M. W. 1981. The measurement of unfrozen water content by time domain reflectometry: results from laboratory tests. *Can. Geotech. J.* **18**, 131.

Patterson, D. E., and Smith, M. W. 1985. Unfrozen water content in saline soils: results using time-domain reflectometry. *Can. Geotech. J.* **22**, 95-101.

Pavlik, Z., Fiala, L., and Černý, R. 2008. Determination of moisture content of hygroscopic building materials using time domain reflectometry. *Journal of Applied Sciences* **8**, 1732-1737.

Payne, R. 1968. Application of the method of time-domain reflectometry to the study of electrode processes. *Journal of Electroanalytical Chemistry and Interfacial Electrochemistry* **19**, 1-14.

Persson, M., Berndtsson, R., Albergel, J., and Zante, P. 2000. Solute transport and water content measurements in clay soils using time domain reflectometry. *Hydrological Sciences Journal 2000 Vol. 45 No. 6 pp. 833-847* **45**, 833-847.

Persson, M., and Dahlin, T. 2010. A profiling TDR probe for water content and electrical conductivity measurements of soils. *Eur. J. Soil Sci.* **61**, 1106-1112.

Pettinelli, E., Cereti, A., Galli, A., and Bella, F. 2002. Time domain reflectrometry: Calibration techniques for accurate measurement of the dielectric properties of various materials. *Review of Scientific Instruments* **73**, 3553-3562.

Pilon, J. A., Annan, A. P., and Davis, J. L. 1985. Monitoring permafrost soil conditions near a buried oil pipeline using ground-probing radar and time-domain reflectometry techniques. *In* "SEG Technical Program Expanded Abstracts 1985", pp. 3-5.

Ponizovsky, A. A., Chudinova, S. M., and Pachepsky, Y. A. 1999. Performance of TDR calibration models as affected by soil texture. *J. Hydol.* **218**, 35-43.

Previati, M., Godio, A., and Ferraris, S. 2011. Validation of spatial variability of snowpack thickness and density obtained with GPR and TDR methods. *JAG* **75**, 284-293.

Puranik, S., Kumbharkhane, A., and Mehrotra, S. 1991. Dielectric properties of honey-water mixtures between 10 MHz to 10 GHz using time domain technique. *Journal of microwave power and electromagnetic energy* **26**, 196-201.

Ragni, L., Berardinelli, A., Cevoli, C., and Valli, E. 2012. Assessment of the water content in extra virgin olive oils by Time Domain Reflectometry (TDR) and Partial Least Squares (PLS) regression methods. *J. Food Eng.* **111**, 66-72.

Rajaei, P., and Baladi, G. Y. 2015. Frost depth: General prediction model. *Transportation Research Record: Journal of the Transportation Research Board* **2510**, 74-80.

Raschi, A., Tognetti, R., Ridder, H. W., and Beres, C. 1995. Water in the stems of sessile oak (*Quercus petraea)* assessed by computer tomography with concurrent measurements of sap velocity and ultrasound emission. *Plant, Cell Environ.* **18**, 545-554.

Reinders, J. E. A., As, H. V., Schaafsma, T. J., De Jager, P. A., and Sheriff, D. W. 1988a. Water balance in cucumis plants, measured by nuclear magnetic resonance, I. *J. Exp. Bot.* **39**, 1199-1210.

Reinders, J. E. A., As, H. V., Schaafsma, T. J., and Sheriff, D. W. 1988b. Water balance in cucumis plants, measured by nuclear magnetic resonance, II. *J. Exp. Bot.* **39**, 1211-1220.

Ren, T., Noborio, K., and Horton, R. 1999. Measuring soil water content, electrical conductivity, and thermal properties with a thermo-time domain reflectometry probe. *Soil Sci. Soc. Am. J.* **63**, 450-457.

Ren, T., Ochsner, T. E., and Horton, R. 2003. Development of thermo-time domain reflectometry for vadose zone measurements. *Vadose Zone J.* **2**, 544-551.

Reynolds, E. R. C. 1965. Transpiration as related to Internal Water Content. *Nature* **207**, 1001-1002.

Rizvi, Z., Zaidi, H., Shoarian Sattari, A., and Wuttke, F. 2019. Effective thermal conductivity of unsaturated sand using artificial neural network (ANN) and lattice element method (LEM). *Int. J. Therm. Sci.*

Roberson, R., and Siekmeier, J. 2000. Using a multisegment time domain reflectometry probe to determine frost depth in pavement systems. *Transportation Research Record: Journal of the Transportation Research Board* **1709**, 108-113.

Robinson, D., Schaap, M., Jones, S., Friedman, S., and Gardner, C. M. K. 2003a. Considerations for improving the accuracy of permittivity measurement using time domain reflectometry. *Soil Sci. Soc. Am. J.* **67**, 62.

Robinson, D. A. 2004. Measurement of the solid dielectric permittivity of clay minerals and granular samples using a time domain reflectometry immersion method. *Vadose Zone J.* **3**, 705-713.

Robinson, D. A., Campbell, C. S., Hopmans, J. W., Hornbuckle, B. K., Jones, S. B., Knight, R., Ogden, F., Selker, J., and Wendroth, O. 2008. Soil moisture measurement for ecological and hydrological watershed-scale observatories: A review. *Vadose Zone J.* **7**, 358-389.

Robinson, D. A., and Friedman, S. P. 2000. Parallel plates compared with conventional rods as TDR waveguides for sensing soil moisture. *Subsurface Sensing Technologies & Applications* **1**, 497-511.

Robinson, D. A., and Friedman, S. P. 2003. A method for measuring the solid particle permittivity or electrical conductivity of rocks, sediments, and granular materials. *J. Geophys. Res. Solid Earth* **108**, ECV5-1.

Robinson, D. A., Jones, S. B., Blonquist, J. M., and Friedman, S. P. 2005a. A physically derived water content/permittivity calibration model for coarse-textured, layered soils. *Soil Sci. Soc. Am. J.* **69**, 1372-1378.

Robinson, D. A., Jones, S. B., Wraith, J. M., Or, D., and Friedman, S. P. 2003b. A review of advances in dielectric and electrical conductivity measurement in soils using time domain reflectometry. *Vadose Zone J.* **2**, 444-475.

Robinson, D. A., Schaap, M. G., Or, D., and Jones, S. B. 2005b. On the effective measurement frequency of time domain reflectometry in dispersive and nonconductive dielectric materials. *Water Resour. Res.* **41**, p.W02007.1-W02007.9.

Romano, N., and Santini, A. 2002. 3.3.3 Field. *In* "Methods of Soil Analysis: Part 4 Physical Methods" (J. H. Dane and C. G. Topp, eds.), pp. 721-738. Soil Science Society of America, Madison, WI.

Roth, K., Schulin, R., Flühler, H., and Attinger, W. 1990. Calibration of time domain reflectometry for water content measurement using a composite dielectric approach. *Water Resour. Res.* **26**, 2267-2273.

Rousseva, S., Kercheva, M., Shishkov, T., Lair, G. J., Nikolaidis, N. P., Moraetis, D., Krám, P., Bernasconi, S. M., Blum, W. E. H., Menon, M., and Banwart, S. A. 2017. Soil water characteristics of European SoilTrEC critical zone observatories. *advances in agronomy* **142**, 29-72.

Rubio, M., Fulladosa, E., Claret, A., Guàrdia, M., and García-Gil, N. 2013. Detection of pastiness in dry-cured ham using dielectric time domain reflectometry. *In* "59th International Congress of Meat Science and Technology–ICoMST".

Saha, S., Roy, J., Arabameri, A., Blaschke, T., and Tien Bui, D. 2020. Machine learning-based gully erosion susceptibility mapping: A case study of Eastern India. *Sensors* **20**, 1313.

Sargand, S. M., Sargent, L., and Farrington, S. P. 2004. Inclinometer-time domain reflectometry comparative study. Ohio Research Institute for Transportation and the Environment.

Scanlon, B. R., Andraski, B. J., and Bilskie, J. 2002. 3.2.4 Miscellaneous methods for measuring matric or water potential. *In* "Methods of Soil Analysis: Part 4 Physical Methods" (J. H. Dane and C. G. Topp, eds.), pp. 643-670. Soil Science Society of America, Madison, WI.

Schaap, M. G., and Bouten, W. 1996. Modeling water retention curves of sandy soils using neural networks. *Water Resour. Res.* **32**, 3033-3040.

Schaap, M. G., de Lange, L., and Heimovaara, T. J. 1997. TDR calibration of organic forest floor media. *Soil Technology* **11**, 205-217.

Scheuermann, A., and Hübner, C. 2009. On the feasibility of pressure profile measurements with time-domain reflectometry. *Instrumentation and Measurement, IEEE Transactions on* **58**, 467-474.

Seyfried, M. S., and Murdock, M. D. 1996. Calibration of time domain reflectometry for measurement of liquid water in frozen soils. *Soil Sci.* **161**, 87-98.

Sheng, W., Zhou, R., Sadeghi, M., Babaeian, E., Robinson, D. A., Tuller, M., and Jones, S. B. 2017. A TDR array probe for monitoring near-surface soil moisture distribution. *Vadose Zone J.* **16**, 1-8.

Shibuya, K., Miyakawa, R., Nishiwaki, J., Komatsuzaki, M., and Noborio, K. 2020. "Frost detection sensitivity of time domain reflectometry (TDR) frost sensors with different thicknesses [in Japanese with English abstract]." Bulletin of the Faculty of Agriculture, Meiji University.

Shibuya, K., Noji, H., and Noborio, K. 2021. Differentiating frost forms with a time domain reflectometry probe operated by a novel electronic circuit. *Journal of Agricultural Meteorology*.

Si, B., Kachanoski, R. G., Zhang, F., Parkin, G. W., and Elrick, D. E. 1999. Measurement of hydraulic properties during constant flux infiltration field average. *Soil Sci. Soc. Am. J.* **63**, 793-799.

Si, B. C., and Kachanoski, R. G. 2000a. Estimating soil hydraulic properties during constant flux infiltration: Inverse procedures. *Soil Sci. Soc. Am. J.* **64**, 439-449.

Si, B. C., and Kachanoski, R. G. 2000b. Unified solution for infiltration and drainage with hysteresis: Theory and field test. *Soil Sci. Soc. Am. J.* **64**, 30-36.

Si, B. C., and Kachanoski, R. G. 2003. Measurement of local soil water flux during field solute transport experiments. *Soil Sci. Soc. Am. J.* **67**, 730-736.

Siddiqui, S. I., Drnevich, V. P., and Deschamps, R. J. 2000. Time domain reflectometry development for use in geotechnical engineering. *Geotechnical Testing Journal* **23**, 9-20.

Sihvola, A. 2000. Mixing rules with complex dielectric coefficients. *Subsurface Sensing Technologies and Applications* **1**, 393-415.

Sihvola, A. H., and Lindell, I. V. 1990. Polarizability and effective permittivity of layered and continuously inhomogeneous dielectric ellipsoids. *JEWA* **4**, 1-26.

Sipahioglu, O., Barringer, S. A., and Bircan, C. 2003. The dielectric properties of meats as a function of temperature and composition. *Journal of Microwave Power and Electromagnetic Energy* **38**, 161-169.

Skierucha, W., Walczak, R., and Wilczek, A. 2004. Comparison of open-ended coax and TDR sensors for the measurement of soil dielectric permittivity in microwave frequencies. *Int. Agrophys.* **18**.

Skierucha, W., Wilczek, A., and Alokhina, O. 2008. Calibration of a TDR probe for low soil water content measurements. *Sensors and Actuators A: Physical* **147**, 544-552.

Smith, M. W., and Tice, A. R. 1988. "Measurement of the unfrozen water content of soils: a comparison of NMR and TDR methods," Rep. No. 88-18.

Souza, C., Or, D., and Matsura, E. 2004. A variable-volume TDR probe for measuring water content in large soil volumes. *Soil Sci. Soc. Am. J.* **68**.

Spaans, E. J. A., and Baker, J. M. 1993. Simple baluns in parallel probes for time domain feflectometry. *Soil Science Society of America.Soil Science Society of America journal* **57**, 668-673.

Spaans, E. J. A., and Baker, J. M. 1995. Examining the use of time domain reflectometry for measuring liquid water content in frozen soil. *Water Resour. Res.* **31**, 2917-2925.

Sparks, J. P., Campbell, G. S., and Black, A. R. 2001. Water content, hydraulic conductivity, and ice formation in winter stems of Pinus contorta: a TDR case study. *Oecologia* **127**, 468-475.

Stahli, M., and Stadler, D. 1997. Measurement of water and solute dynamics in freezing soil columns with time domain reflectometry. *Journal of Hydrology* **195**, 352-369.

Stein, J., and Kane, D. L. 1983. Monitoring the unfrozen water content of soil and snow using time domain reflectometry. *Water Resour. Res.*, 1573-1584.

Stein, J., Laberge, G., and Lévesque, D. 1997. Monitoring the dry density and the liquid water content of snow using time domain reflectometry (TDR). *Cold Regions Science & Technology* **25**, 123-136.

Sturm, M., and Holmgren, J. 2018. An automatic snow depth probe for field validation campaigns. *Water Resour. Res.* **54**, 9695-9701.

Suchorab, Z., Widomski, M. K., Łagód, G., Barnat-Hunek, D., and Majerek, D. 2018. A noninvasive TDR sensor to measure the moisture content of rigid porous materials. *Sensors* **18**, 3935.

Sun, Y., Zhou, H., Shan, G., Grantz, D. A., Schulze Lammers, P., Xue, X., Damerow, L., and Burkhardt, J. 2019. Diurnal and seasonal transitions of water and ice content in apple stems: Field tracking the radial location of the freezing- and thawing-fronts using a noninvasive smart sensor. *Agric. For. Meteorol.* **274**, 75-84.

Szerement, J., Woszczyk, A., Szypłowska, A., Kafarski, M., Lewandowski, A., Wilczek, A., and Skierucha, W. 2019. A seven-rod dielectric sensor for determination of soil moisture in well-defined sample volumes. *Sensors* **19**, 1646.

Tan, E., Fredlund, D. G., and Marjerison, B. 2007. Installation procedure for thermal conductivity matric suction sensors and analysis of their long-term readings. *Can. Geotech. J.* **44**, 113-125.

Tanaka, F., Mallikarjunan, P., Kim, C., and Hung, Y.-C. 2000. Measurement of dielectric properties of chicken breast meat. *Journal of the Japanese Society of Agricultural Machinery* **62**, 109-119.

Thomsen, A. 1994. "Program AUTOTDR for making automated TDR measurements of soil water content. User's Guide.." Danish Institute of Agricultural Sciences, Tjele, Denmark.

Thomsen, A., Hansen, B., and Schelde, K. 2000. Application of TDR to water level measurement. *J. Hydol.* **236**, 252-258.

Thomsen, A., and Thomsen, H. 1994. "Automated TDR measurements: control box for Tektronix TSS 45 relay scanners." Danish Institute of Agricultural Sciences, Tjele, Denmark.

Thuro, K., Singer, J., Festl, J., Wunderlich, T., Wasmeier, P., Reith, C., Heunecke, O., and Schuhbäck, S. 2010. New landslide monitoring techniques-developments and experiences of the alpEWAS project. *Journal of Applied Geodesy* **4**, 69-90.

Topp, G. C., Annan, A. P., and Davis, J. L. 1980. Electromagnetic determination of soil water content: measurements in coaxial transmission lines. *Water Resour. Res.* **16**, 574-582.

Topp, G. C., Annan, A. P., and Davis, J. L. 1982a. Electromagnetic determination of soil water content using TDR. I. Applications to wetting fronts and steep gradients. *Journal - Soil Science Society of America* **46**, 672-678.

Topp, G. C., Annan, A. P., and Davis, J. L. 1982b. Electromagnetic determination of soil water content using TDR. II. Evaluation of installation and configuration of parallel transmission lines. *Journal - Soil Science Society of America* **46**, 678-684.

Topp, G. C., Annan, A. P., and Davis, J. L. 2003. The early development of TDR for soil measurements. *Vadose Zone J.* **2**, 492-499.

Topp, G. C., and Davis, J. L. 1981. Detecting infiltration of water through soil cracks by time-domain reflectometry. *Geoderma* **26**, 13-23.

Topp, G. C., and Davis, J. L. 1985. Time-domain reflectometry (TDR) and its application to irrigation scheduling. *In* "Advances in Irrigation" (D. Hillel, ed.), Vol. 3, pp. 107-127. Elsevier.

Topp, G. C., Zebchuk, W. D., Davis, J. L., and Bailey, W. G. 1984. The measurement of soil water content using a portable TDR hand probe. *Can. J. Soil Sci.* **64**, 313-321.

Trcala, M., Čermák, J., and Nadezhdina, N. 2015. Water content measurement in tree wood using a continuous linear heating technique. *Int. J. Therm. Sci.* **88**, 164-169.

Turcotte, A., Rossi, S., Deslauriers, A., Krause, C., and Morin, H. 2011. Dynamics of depletion and replenishment of water storage in stem and roots of black spruce measured by dendrometers. *Frontiers in Plant Science* **2**, 21.

van Genuchten, M. T. 1980. A closed-form equation for predicting the hydraulic conductivity of unsaturated soils. *Soil Sci. Soc. Am. J.* **44**, 892-898.

Vaz, C. M. P., and Hopmans, J. W. 2001. Simultaneous measurement of soil penetration resistance and water content with a combined penetrometer-TDR moisture probe. *Soil Sci. Soc. Am. J.* **65**, 4-12.

Vaz, C. M. P., Hopmans, J. W., Macedo, A., Bassoi, L. H., and Wildenschild, D. 2002. Soil water retention measurements using a combined tensiometer-coiled time domain reflectometry probe. *Soil Sci. Soc. Am. J.* **66**, 1752-1759.

Vaz, C. M. P., Jones, S., Meding, M., and Tuller, M. 2013. Evaluation of standard calibration functions for eight electromagnetic soil moisture sensors. *Vadose Zone J.* **12**.

Wang, Z., Lu, Y., Kojima, Y., Lu, S., Zhang, M., Chen, Y., and Horton, R. 2016. Tangent line/second-order bounded mean oscillation waveform analysis for short TDR probe. *Vadose Zone J.* **15**.

Waring, R. H., and Running, S. W. 1978. Sapwood water storage: its contribution to transpiration and effect upon water conductance through the stems of old-growth Douglas-fir. *Plant, Cell Environ.* **1**, 131-140.

Waring, R. H., Whitehead, D., and Jarvis, P. G. 1979. The contribution of stored water to transpiration in Scots pine. *Plant, Cell Environ.* **2**, 309-317.

Watanabe, K., and Wake, T. 2009. Measurement of unfrozen water content and relative permittivity of frozen unsaturated soil using NMR and TDR. *Cold Reg. Sci. Technol.* **59**, 34-41.

Whalley, W. R. 1993. Considerations on the use of time-domain reflectometry (TDR) for measuring soil water content. *J. Soil Sci.* **44**, 1-9.

Whalley, W. R., Leeds-Harrison, P. B., Joy, P., and Hoefsloot, P. 1994. Time Domain Reflectometry and Tensiometry Combined in an Integrated Soil Water Monitoring System. *Journal of Agricultural Engineering Research* **59**, 141-144.

White, I., and Broadbridge, P. 1988. Constant rate rainfall infiltration: A versatile nonlinear model: 2. Applications of solutions. *Water Resour. Res.* **24**, 155-162.

White, I., Zegelin, S. J., and Wilson, L. G. 1995. Electric and dielectric methods for monitoring soil-water content. *In* "Handbook of vadose zone characterization and monitoring", pp. 343-385.

Windt, C. W., Gerkema, E., and Van As, H. 2009. Most water in the tomato truss is imported through the xylem, not the phloem: a nuclear magnetic resonance flow imaging study. *Plant Physiol.* **151**, 830-42.

Wraith, J. M. 2003. Measuring solutes and salinity using time domain reflectometry. *In* "Encyclopedia of Water Science" (B. A. Stewart and T. A. Howell, eds.), pp. 832-835. Dekker Publications, New York, NY.

Wraith, J. M., and Or, D. 2001. Soil water characteristic determination from concurrent water content measurements in reference porous media. *Soil Sci. Soc. Am. J.* **65**, 1659-1666.

Wraith, J. M., Robinson, D. A., Jones, S. B., and Long, D. 2005. Spatially characterizing apparent electrical conductivity and water content of surface soils with time domain reflectormetry. *Comp. Electron. Agric.* **1**, 239–261.

Wraith, J. M., Woodbury, B. L., Inskeep, W. P., and Comfort, S. D. 1993. A simplified waveform analysis approach for monitoring solute transport using time-domain reflectometry. *Soilence Society of America Journal* **57**, 637-642.

Wullschleger, S. D., Hanson, P. J., and Todd, D. E. 1996. Measuring stem water content in four deciduous hardwoods with a time-domain reflectometer. *Tree Physiol.* **16**, 809-15.

Yadav, D., Karthik, G., Jayanthu, S., and Das, S. 2019. Design of real-time slope monitoring system using time-domain reflectometry with wireless sensor network. *IEEE Sens. J.* **PP**, 1-1.

Yami, E. R., Khalili, A., Rahimi, H., and Etemad, A. 2012. Investigation of effects of moisture on soil temperature regimes and frost depth in a laboratory model. *International Journal of Agriscience*, 717-732.

Yanai, Y., Iwata, Y., and Hirota, T. 2017. Optimum soil frost depth to alleviate climate change effects in cold region agriculture. *Scientific Reports* **7**, 44860.

Yasunaga, E., Miyamoto, H., Yoshida, S., and Chikushi, J. 2009. Response of ECH_2O probe and TDR probe in the determination of dielectric characteristics of rough rice during drying process. *In* "Asia Pacific Symposium on Assuring Quality and Safety of Agri-Foods" (S. Kanlayanarat, Y. Desjardins and V. Srilaong, eds.), Vol. 837, pp. 371-376. Int Soc Horticultural Science, Leuven 1.

Yazaki, T., Shoji, Y., and Noborio, K. 2008. Measuring temporal changes in flooding depths in a rice paddy field using time domain reflectometry [in Japanese with English abstract]. *Journal of Japanese Society of Soil Physics* **109**, 57-65.

Zegelin, S. J., White, I., and Jenkins, D. R. 1989. Improved field probes for soil water content and electrical conductivity measurement using time domain reflectometry. *Water Resour. Res.* **25**, 2367-2376.

Zhang, M., and Shi, W. 2020. "Systematic comparison of five machine-learning methods in classification and interpolation of soil particle size fractions using different transformed data."

Zhang, Z. F., Kachanoski, R. G., Parkin, G. W., and Si, B. 2000a. Measuring hydraulic properties using a line source. I. Analytical expressions. *Soil Sci. Soc. Am. J.* **64**, 1554-1562.

Zhang, Z. F., Kachanoski, R. G., Parkin, G. W., and Si, B. 2000b. Measuring hydraulic properties using a line source. II. Field test. *Soil Sci. Soc. Am. J.* **64**, 1563-1569.

Zhou, H., Sun, Y., Shan, G., Grantz, D. A., Cheng, Q., Schulze Lammers, P., Damerow, L., Wen, B., Xue, X., and Chen, B. 2018. In situ measurement of stem water content and diurnal storage of an apricot tree with a high frequency inner fringing dielectric sensor. *Agric. For. Meteorol.* **250-251**, 35-46.

Zhou, H., Sun, Y., Tyree, M. T., Sheng, W., Cheng, Q., Xue, X., Schumann, H., and Schulze Lammers, P. 2015. An improved sensor for precision detection of in situ stem water content using a frequency domain fringing capacitor. *New Phytol.* **206**, 471-481.

Zhou, Q., Fellows, A., Flerchinger, G., and N. Flores, A. 2019. Examining interactions between and among predictors of net ecosystem exchange: A machine learning approach in a semi-arid landscape. *Scientific Reports* **9**, 2222.